Evaluating the therapeutic use of Indoleamine 2,3-dioxygenase (IDO) expressing allogenic dermal fibroblast populated within an acellular skin substitute as a wound coverage

by

Ali Farrokhi

M.Sc., The University of Tehran, 2007

A THESIS SUBMITTED IN PARTIAL FULFILLMENT OF

THE REQUIREMENTS FOR THE DEGREE OF

DOCTOR OF PHILOSOPHY

in

THE FACULTY OF GRADUATE AND POSTDOCTORAL STUDIES

(Experimental Medicine)

THE UNIVERSITY OF BRITISH COLUMBIA

(Vancouver)

November 2017

Abstract

Acute and chronic wounds contribute to increased morbidity and mortality in affected people and impose significant financial burdens on healthcare systems. Allogeneic cell-based skin substitutes have been proposed as ready-to-use wound coverage as an alternative to conventional split-thickness skin grafts, but the survival and usefulness of such cells after transplantation into an immunocompetent host remain controversial.

We hypothesize that the application of an indoleamine 2,3-dioxygenase (IDO) expressing allogenic dermal fibroblast populated within an acellular dermal matrix (ADM) is sufficient to create an immune-privileged area within the wound to protect fibroblasts from rejection. Fibroblasts in the skin substitute can potentially assist the graft to restore its function by synthesizing extracellular matrix components and growth factors.

In this study, ADMs were prepared using a novel detergent–free method, recellularized with IDO-expressing or control fibroblasts from C57/B6 mice, and were transplanted on splinted full-thickness skin wounds in Balb/c mice.

Transplantation studies demonstrated that ADM significantly enhanced the wound-healing process but there was no demonstrable benefit when the ADM was recellularized with fibroblasts. Investigating the transplanted cells' fate by bioluminescence *in vivo* imaging after intra-hypo-dermal injection of fibroblasts in to mouse skin revealed that both type of fibroblasts were rejected in allogeneic recipients while in immunodeficient NOD-SCID-Il2r gamma null (NSG) mice they were not. Allogeneic fibroblasts transplanted in natural killer T cell and gamma delta T (NKT) cell deficient mice were rejected as well. Depleting natural killer (NK) cells or CD4+

T cells could delay the rejection but not prevent it. Double depletion of CD4+ and CD8+ cells could partially prevent the rejection. Analyzing the infiltrated immune cells to graft region in time of cell rejection revealed the presence of high number of monocytes, macrophage and neutrophils. Our data indicate a clear immune response to allogeneic fibroblasts in which both innate and T-cell immune response are involved in targeting cells. Although it has been reported by other researchers that IDO-expressing cells exhibit strong immunosuppressive activity *in vitro* and *in vivo*, we documented rejection of these cells in our study, suggesting that the application of these cells in wound sites requires further improvements.

Lay Summary

Burn injuries and chronic wounds such as bedsores and diabetic foot ulcers affect millions of patients worldwide. Covering the wound is essential to prevent infection and loss of fluid and heat.

Here we have prepared a skin substitute by a novel method for removing cells from skin while keeping structural components in the skin scaffold relatively intact. Then we used this scaffold as non-rejectable wound coverage. Further, we investigated the transplantation of fibroblasts cells in combination with our skin substitute to help the wound heal faster.

In the animal model, we showed that this skin substitute promotes wound healing without scar formation. We showed that transplantation of fibroblast can induce immune rejection and proposed a method to prevent this.

We believe that the outcome of this study can allow us to design a novel strategy to use a non-rejectable skin substitute for treatment of many different types of wounds.

Preface

This thesis was compiled under the guidance of Dr. Aziz Ghahary who devised the original concept for the research.

Chapters 2 is based on work conducted in the BC Professional Fire Fighters' (BCPFF) Burn and Wound Healing Research Laboratory. I was responsible for running experiments, analyzing the data, and writing the draft of papers. Chapters 3 is based on work conducted in BCPFF Burn and Wound Healing Research Laboratory and Michael Cuccione Childhood Cancer Research Program in BC Children's Hospital under supervision of Dr. Gregor Reid.

A version of Chapter 2 has been submitted for publication. **Biofunctional Evaluation of Detergent- free Decellularization of Murine Skin in In Vitro and In Vivo Models.** Ali Farrokhi, MSc, Mohammadreza Pakyari, MD, Layla Nabai, MD, Ryan Hartwell, PhD, Reza Jalili, MD/PhD, and Aziz Ghahary, PhD. A version of Chapter 3 has been prepared for submission. Check the first pages of these chapters to see footnotes for similar information.

I conducted and analyzed most of the data and wrote the first draft of manuscripts. These were critically reviewed by Dr. A. Ghahary.

The work described in this thesis has been conducted with the approval of the University of British Columbia Biohazards Committee under the certificate number B15-0002. All animal studies have been conducted under the close supervision of the University of British Columbia Animal Care Committee and under the protocol number A14-0309.

Table of Contents

List of Figures

List of Abbreviations

ANOVA	Analysis of Variance
APC	Allophycocyanin
APC	Antigen Presenting Cell
B6	C57BL/6 mice
wt-Balbc	wild type Balbc mice
CFSE	Carboxyfluorescein Diacetate Succinimnidyl Ester
ddH_2O	De-ionised distilled water
DMEM	Dulbecco's Modified Eagle Medium
DNA	Deoxyribonucleic Acid
ELISA	Enzyme-linked Immunosorbent Assay
FACS	Fluorescence Activated Cell Sorting
FBS	Fetal Bovine Serum
Fib	Fibroblasts
FITC	Fluorescein Isothiocyanate
Foxp3	Forkhead box P3
GCN-2	General Control Non-derepressible 2
IDO	Indoleamine 2,3-dioxygenase
IFN-γ	Interferon-gamma
IL	Interleukin
LDH	Lactate Dehydrogenase

MHC	Major Histocompatibility Complex
MLR	Mixed Lymphocyte Reaction
m-RNA	Messenger Ribonucleic Acid
NK	Natural killer cells
NKT	Natural killer T cells
NLS	*N*-Lauroyl sarcosinate
NSG	NOD-SCID-Il2r gamma null mice
PBS	Phosphate Buffered Saline
PE	Phycoerythrin
PI	Propidium Iodide
RBC	Red Blood Cell
RNA	Ribonucleic Acid
RPMI	Roswell Park Memorial Institute medium
SD	Standard deviation
SDS	Sodium Dodecyl Sulfate
sGAG	sulfated glycosaminoglycans
SPSS	Statistical Package for the Social Sciences

Acknowledgements

First and foremost, I must express my unending praise and gratitude to the Almighty God, the Creator and the Guardian, and to whom I owe my very existence, for giving me wisdom and guidance throughout my life and for it is under his grace that we live, learn and flourish.

Next, I would like to express my heartfelt gratitude to my supervisor, Dr. Aziz Ghahary for providing me with the exceptional opportunity to work and study as a member of his wonderful research group and for his endless patience, guidance and support.

I am also deeply and truly appreciative of the members of my doctoral advisory committee at the University of British Columbia; Dr. Erin Brown, Dr. David Granville, and Dr. Anthony Papp for their unending willingness to share their invaluable time, exceptional scientific expertise and helpful advice.

I am also indebted to my colleague Dr. Reza Jalili who has been a great support throughout my research. I am also deeply appreciative to Dr. Gregor Reid for opening up a new world in immunology research for me. He trusted and supported me in the toughest time of my research.

My thanks also to my wonderful laboratory colleagues who made it a pleasure to come into work today and were always on hand to offer expertise and encouragement; Dr. Ruhangiz Kilani, Dr. Yunyuan Li, Dr. Azadeh Taba, Dr. Layla Nabai, Dr. Ryan Hartwell, Dr. Yun Zhang, Dr. Mohammadreza Pakyari, Dr. Mohsen Khosravi, Dr. Malihe Meibod and Dr. Sanam Salimi.

I am very grateful to the Skin Research Training Program and WorkSafe BC for recognizing the importance of my research and the potential benefits of this research for burn victims and patients with chronic wounds in Canada and across the globe. Thank you for your financial assistance.

Finally, the accomplishment of this thesis would not have been possible without the love and support of my family. I would like to convey my heartfelt thanks to my parents who have endured the most difficult times to provide an exceptional life for their children, to my sisters and brother who always stood by me and to my beloved daughters Zeinab and Zoha, who brought hope and joy to our family.

My deepest love and thanks go to my wife, Tahereh, who has always been my best friend, soul mate and inspiration all these years.

Dedication

This work is dedicated to:

All my teachers and mentors in my life.

My mother and father who have given their unending love and exceptional support throughout my life and taught me the right way to live.

My wife, Tahereh, for her support and patience.

And my daughters, Zeinab and Zoha, for making life lovely for me.

Chapter 1: Introduction, Specific Aims and Research Plans

1.1 Overview

Acute and chronic wounds affect millions of people around the world. Approximately 11 million people are affected by acute wounds with 300,000 hospitalizations each year in the United States. Additionally, the anticipated risks of non-healing chronic wounds such as diabetic, pressure, and venous ulcers continue to increase dramatically. The annual cost of chronic wound care now exceeds $1 billion in the United States alone and in the European Community it is about 2% of total health care costs [1].

The ideal treatment for wounds should stimulate regeneration rather than repair in the involved area. During wound repair in the skin, the tissue tries to restore normal function by the formation of an epidermal layer as a barrier to fluid loss and further infection. It also attempts to restore normal vascular anatomy, and to reestablish mechanical integrity. Because of the high demand for the restoration of adequate function, the perfect reorganization of tissue's structure which might needs longer time to proceed is ignored. Consequently, this leads to scar formation and the absence of some cellular elements. On the other hand, regeneration leads to the complete restoration of original tissue without any problem. Although regeneration is an optimal outcome for wound healing, it is mainly found in embryonic development and not in adult tissue [2].

The ultimate objective for the application of skin substitutes in treatment of wounds is restoration of fully functional skin rather than repaired or scarred skin. At present, only autologous full-thickness skin grafts and free flaps can restore the normal architecture and functions of skin. However, in large wounds and i1n areas with low vascularity these methods are not applicable. Moreover, the harvest of full thickness skin grafts or skin flaps is associated

with donor site morbidity. These challenges necessitate the production of skin substitutes that contain extracellular matrices and cultured cells to provide large quantities of grafts for transplantation [3].

Numerous strategies for skin replacement or reconstruction have been investigated. Among these, the extracellular matrix-based biomaterials have appropriate mechanical strength and retain biological activity [4]. The acellular dermal matrix (ADM) has been used as a temporary or permanent wound covering for partial- and full-thickness wounds [5] [6] [7] [8]. ADM is non-immunogenic and mechanically similar to skin. Because of the better preserved physiological structures of the dermis in ADM, with papillary and reticular dermis structure, it offers an ideal template for the growth of angiogenic cells and the promotion of vascularization [9] **.**

Ideal skin substitutes should possess an appropriate physical structure or scaffold, biologically relevant growth and differentiation factors, and living cells to be able to facilitate the restoration of functional skin. ADM acts as a scaffold as well as a source of growth and chemotactic factors, but living functional cells are absent. It has been demonstrated that normal dermal fibroblasts synthesize essential extracellular matrix components, as well as secrete key growth factors and cytokines that are important for wound healing [10] [11].

It is not feasible to use autologous dermal fibroblasts in ready-to-use skin substitute harbouring live fibroblasts, because of the long *in vitro* culture period required to obtain enough fibroblasts for transplantation, especially in patients with a large burn area. On the other hand, using allogenic fibroblasts can potentially overcome this limitation but would be associated with rejection.

Studies show that an immunologic response to an allogenic skin graft requires T cell activation and proliferation. Thus, to prevent acute rejection, suppression of infiltrated immune

cells at early time points of engraftment is necessary [12]. Although systemic immunosuppressive drugs are widely used for prevention of allorejection, side-effects associated with these medications precludes their use in the management of skin defects or wounds.

Pregnancy is a good example of the body's natural tolerance cells at work. For instance, the mother releases interferon-gamma, which then induces expression of the enzyme indoleamine 2,3-dioxygenase (IDO) from the trophoblast cells. IDO metabolizes the Tryptophan in the environment. The deficiency of this essential amino acid and the toxic metabolites induce T cell anergy and apoptosis [13].

The present thesis evolved from our previous studies that showed that adeno and lentiviral vectors are efficient to transduce skin cells to express IDO, and the use of these IDO-expressing fibroblasts protects allogenic skin substitutes [14].

As such, we hypothesized that the application of an IDO-expressing allogenic dermal fibroblast populated within an ADM is sufficient to create an immune-privileged area within the wound to protect fibroblasts from rejection and help the graft to restore its function by synthesizing extracellular matrix components and growth factors by these cells.

1.2 Acellular dermal matrix (ADM) as a biological wound coverage

Covering skin defects is essential for healing of chronic wounds and large acute wounds such as burn. Any delay in coverage can lead to hypothermia, electrolyte imbalance, fibrotic scarring, and sepsis. As such, the main goals of wound treatment strategies are to achieve a rapid closure of the defect and a functional aesthetic scar. Autologous full-thickness skin graft (FTSG) is an ideal wound coverage, but in large wounds and in areas with low vascularity it is not applicable. Split-thickness skin grafts (STSG) including varying amounts of dermis covered by an

epidermal layer have been recognized as the gold-standard treatment for skin wound coverage. Despite the advantages of skin grafts, they come with short-comings such as morbidity of donor sites, secondary contracture, lack of sweating and natural lubrication, loss of elasticity, sensory impairment, and undesirable cosmetic results, including hypo- or hyper-pigmentation [15],[16].

Because of these limitations there has been an emergence of tissue-engineered alternatives. Among those alternatives, biological scaffold materials composed of an extracellular matrix (ECM) have been reported to facilitate the constructive remodeling of different tissues in both preclinical animal studies and in human clinical applications. The structural, biomechanical, and biochemical properties of ECM scaffolds are inherently determined by the material properties of original tissue [4]. It is well known that ECM is not only a scaffold but also a reservoir of molecules secreted by tissue resident cells like growth factor and cytokines and facilitate signal transfer between cells [17]. Studies support the idea of the direct binding of specific growth factors and morphogens to the specific ECM proteins in extracellular microenvironments, suggesting the possible role of ECM in regulating soluble factor spatially, facilitating signal transduction through integrin/transmembrane receptors. These interactions are important in regulating several cell biological activities such as proliferation, survival, and differentiation. [18].

To get the benefit of natural ECM components, including the structural and functional molecules, removing cells from tissue can leave such an ECM. This process is called decellularization and has been applied to several tissues including skin [4]. Decellularized skin is commonly called an acellular dermal matrix (ADM), representing the fact that during decellularization the epidermal layer has been removed and the dermis, which is the major part and contains the ECM, remains.

The ideal decellularization process would remove cellular components but keep the original tissue architecture and ECM components intact without any adverse effect on biomechanical properties of the natural ECM [19]. The ideal bioscaffold resulting from the decellularization of skin lacks cellular components to avoid any immune response or cause inflammation. It supports rapid and directed proliferation of infiltrated host cells, has the capacity for rapid vascularization and stability as a dermal template, be slowly bio-degradable to support the reconstruction and remodelling of normal skin, and has similar biomechanical properties to the skin it replaces with essentially no risk of disease transmission. Practically, the capability of being stored with a long shelf life and readily prepared for transplantation are important features as well [20].

In addition to the above mentioned advantages of ADMs, because of the better preserved physiological structures of the dermis in ADMs, with papillary and reticular dermis structure, they offer an ideal template for the growth of angiogenic cells and promotion of vascularization [9] .

Clinical application of ADMs have been reported for different purposes, including treatment of abdominal wall defects [21], partial- and full-thickness wounds [5] [6] [7] [8], prevention of post-parotidectomy gustatory sweating [22], cleft palate repair [23], resurfacing of intraoral defects [24], lip augmentation [25], reconstructive breast surgery [26], and chronic wound repair [27].

A number of different decellularization methods have been reported, and products from human or xenogeneic sources have been commercialized.

However, decellularization would have a negative effect on the graft function if it altered the biochemical composition, structure, and biomechanical properties of tissue. Therefore,

decellularization methods that leads to preservation of these molecules would be beneficial for graft function after transplantation.

It is essentially impossible to remove all cellular components without adverse effect on the ECM. Even though the use of harsh reagents in the decellularization process can help to efficiently remove cells, it can disrupt the ECM molecules. Therefore, a balanced methodology that removes cell components yet keeps the native ECM molecules as intact as possible is highly desirable.

According to "International Consensus. Acellular Matrices for the Treatment of Wounds", there is no definitive guideline on the application of acellular matrices in acute and chronic wounds [28]. Therefore, regulatory standards for decellularization of skin and application of their products are needed. However, such standards must be based on reliable data that identify quantifiable thresholds for different aspects of ADMs upon implantation.

In this thesis one of the objectives was to develop a detergent-free method of decellularization to minimize any potential damage on matrix molecules and compare this method with non-ionic and anionic detergent methods of ADM preparation.

1.3 Revitalization of biostatic acellular dermal matrix by fibroblasts

The acellular dermal matrix as a biostatic (nonvital) tissue allograft has been used for temporary and permanent wound coverage, as well as to stimulate regeneration of a recipient's own tissues. This matrix which lacks the cells does not require immunosuppressive treatment and can be sterilized and stored on shelf for long periods of time.

To induce tissue regeneration, three elements are required: a scaffold, growth and differentiation factors, and living cells capable of remodeling the extracellular matrix and restoring normal tissue function. Biostatic grafts act as a scaffold as well as a potential source of

growth and chemotactic factors, but the third necessary element of living functional cells is missing. It is expected that after implantation, in response to chemotactic factors released from the graft, host cells migrate onto the graft and start regenerating the structure of the damaged tissue, however this desired process is not always effective. There is a growing body of evidence in different fields of regenerative medicine that shows that seeding a recipient's cells into the graft prior to implantation has positive effects on graft remodeling. The process of introducing cells into the biostatic graft is described as "revitalization" as the graft becomes revived [29].

In the case of application of skin substitutes for the treatment of wounds, experimental and clinical results show promising positive effects upon revitalization of grafts with fibroblasts.

The fibroblast traditionally has been described as a provider of maintenance and support for tissues. Recently, it has become evident that these cells contribute much more than a supportive effect for tissue integrity. Fibroblasts are dynamic cells and have functionally and morphologically heterogeneous subtypes. They are actively involved in wound healing and skin regeneration [30].

1.3.1 Fibroblast in the skin

In practice, spindle-shaped morphology and adherence to plastic culture dishes are important characteristics of fibroblasts. Although fibroblasts are one of the widely-used mammalian cell types in in vitro culture, they remain poorly defined in molecular level [31]. Despite considerable progress in lineage tracing tools, characterisation of fibroblasts is underdeveloped. One of the reasons is the lack of specific markers to distinguish different In practice, spindle-shaped morphology and adherence to plastic culture dishes are important characteristics of fibroblasts. Although fibroblasts are one of the widely-used mammalian cell

types in *in vitro* culture, they remain poorly defined in molecular level [31]. Despite considerable progress in lineage tracing tools, there is limited characterisation of fibroblasts. One of the reasons is the lack of specific markers to distinguish different fibroblast subtypes [32].

Fibroblasts are mesenchymal cells, and in the skin from different body sites, they have different embryonic origins. In facial skin, they come from the neural crest. In ventral body skin, they derive from the lateral plate mesoderm. And in back skin, they come from the dermomyotome [32].

cDNA-microarray studies have demonstrated that cultured fetal and adult human fibroblasts from different anatomical sites have their own gene-expression profile, suggesting that fibroblasts at different locations should be considered distinct populations of differentiated cells [31].

We can see fibroblast diversity even in one single body site and at a single developmental stage in the skin dermis. Fibroblasts are different in papillary dermis, reticular dermis, dermal papilla (DP), and hypodermis [33] [32].

In the study by Driskell at al., using transplantation assays and lineage tracing, they showed the presence of a common fibroblasts progenitors in mouse dermis at embryonic day (E) 12.5 which are expressing pan-fibroblast marker platelet-derived growth factor receptor (Pdgfr-α), Delta-like homologue 1 (Dlk1), and leucine-rich repeats and immunoglobulin-like domains protein 1 (Lrig1) markers. By E16.5 two distinct subpopulations derived from common progenitors can be identified. One (Pdgfr-α+, Dlk1-, Lrig1+, and Blimp1+ (B-lymphocyte-induced maturation protein 1)) forms the upper dermis, including the papillary dermis, dermal papilla, and the arrector pili muscle (APM). The second (Pdgfr-α+, Dlk1+, and Blimp1-) forms the lower dermis, including the reticular fibroblasts and the preadipocytes of the hypodermis.

Later, at E18.5 and postnatal day (P) 2, further differentiation and fate restriction of these two main fibroblasts progenitors led to the formation of specific fibroblasts lineages in skin [34]. It has been shown by lineage-tracing experiments that epidermal cells and haematopoietic stem cells or bone marrow derived mesenchymal cells cannot be the origin of dermal cells [35] [36] [34].

Understanding the origin and molecular regulation of different fibroblasts sub-populations in our body, specifically in skin, will help us in designing appropriate therapeutic approach such as developing a skin substitute for promoting wound healing and regeneration of damaged skin.

1.3.2. Fibroblast in the skin substitute

Since the development of the first human skin substitute in the early 1980s by Bell et al. [37], reconstruction of different types of human skin equivalents has been reported. The common feature of these skin substitutes is the use of a combination of ECM components with Keratinocytes and/or fibroblasts.

Fibroblasts used in skin substitutes are allogeneic or autologous. The advantage of using autologous fibroblasts is that there is no risk of rejection or infection transmission. However, there is a delay in culturing autologous cells, which can take two to three weeks to obtain sufficient cell numbers, whereas allogeneic cells are readily available [38]. Also, the production of autologous cells is more expensive than the allogeneic cells [20]

Regardless of the source of fibroblasts used in skin substitutes, the improved outcome of grafting has been supported in several experimental and clinical studies. In clinical studies, the application of this living skin substitute has been investigated in treatments of burn [39] and chronic wounds [40] [41].

Coulomb et al. have shown that irrespective of the epidermalization technique they used, the presence of dermal fibroblasts seeded into the collagen matrix as a graft bed was found to reduce pain, to promote keratinocytes growth and dermal-epidermal organization, and to improve the mechanical (e.g., elasticity) and cosmetic properties of the graft [42]. In another study, the dermal matrix was prepared by plating allogeneic fibroblasts on a spongy collagen and used to treat 145 clinical cases of various wounds including dermal burns, partial-thickness donor wounds, traumatic skin defects, chronic skin ulcers, and coverage for autologous meshed graft. The study showed 95% of the treatments (138/145) achieved good or excellent results in terms of graft take and wound healing outcome [43].

Fibroblasts play a central role in wound healing. Wound healing is a complex biologic process and an orchestrated progression of events that is regulated through different types of cells, including fibroblasts. Fibroblasts migrate in to the injury site after the inflammatory stage and play a key role in granulation tissue formation [2]. By producing extracellular matrix components such as type I and type IV collagen, elastin, laminin, and synthesizing matrix metalloproteinase enzymes (MMPs), fibroblasts accelerate matrix remodelling and dermal regeneration [11]. Fibroblasts release cytokines and growth factors that have autocrine and paracrine effects. Paracrine activity has a regulatory effect on other cells including epidermal, vascular, and lymphatic endothelial cells. The growth factors produced by fibroblasts that have been shown to regulate many of these processes are acidic FGF (aFGF), basic FGF (bFGF), keratinocyte growth factor (KGF), insulin-like growth factor (IGF-I), platelet derived growth factor (PDGF), transforming growth factor-β (TGF-b) [44], [11]., and the vascular endothelial growth factor (VEGF) family members include VEGF-A, B, -C and -D, which are involved in vascular and lymphatic vessel development [45].

In order to make a decision about including fibroblasts in skin substitutes, it is important to evaluate its possible functions in promoting wound healing. Several studies have addressed this question by analysing the secretion of growth factors and wound-healing mediators in skin substitutes in vitro. Spiekstra et al. have shown that skin substitutes with cultured fibroblasts and keratinocytes (bi-layer skin substitutes) produce high amounts of inflammatory / angiogenic mediators, including IL-6, CCL2, CXCL1, CXCL8, and sST2, but single-layer skin substitutes of keratinocytes or fibroblasts produced less of these proteins, which highlights the importance of keratinocyte–fibroblast interactions in the production of these factors [46]. In another study, Maarof et al. quantified the secretion of wound-healing mediators and compared single and bi-layer skin substitutes in vitro. They have found that all three skin substitutes secreted CCL2, CCL5, CCL11, GM- CSF, IL8, IL-1a, TNF-a, ICAM-1, FGF-b, TGF-b, HGF, VEGF-a, and PDGF-BB factors, without any significant difference between groups [47].

It has been shown that the presence of fibroblasts in skin substitutes can induce the proliferation and differentiation of cultured keratinocytes to stratify more and to form rete ridges more effectively than those on skin substitutes without fibroblasts [48] [49]**.**

The transplantation of skin substitutes with fibroblasts onto animal models demonstrated that the addition of fibroblasts to keratinocyte based skin substitutes improves epidermis formation, induces vascularization, and reduces wound contraction and myofibroblast formation in granulation tissue [11] [8] [50]. One of the reasons for wound contraction is the differentiation of fibroblasts in to myofibroblasts. It is believed that wound contraction is very potent in the early wound-healing phase and reducing healing times at early stages has a positive impact on the prevention of contraction and scar formation. The early presence of fibroblasts in the skin

substitutes accelerate the healing process by reducing the time needed for migration or proliferation of host fibroblasts in the wound [10] [50].

As reviewed above, many studies have shown the benefits of in vitro recellularizing of skin substitutes with autologous and allogeneic fibroblasts. There are several advantages to using allogenic fibroblasts over autologous ones, including reduced morbidity in patient donor sites and avoiding of a delay in treatment because of the time needed for autologous cell isolation and culture. However, the viability and distribution of such cells after transplantation into an immunocompetent host have been controversial and the usefulness of the seeded fibroblasts is still unclear, questioning whether we need to repopulate ADMs with allogenic fibroblasts or we should use only autologous fibroblasts.

In an early work by Sher et al. in a rat model, they evaluated the survival of allogeneic female rat fibroblasts or xenogeneic rabbit or human fibroblasts in their skin substitute after transplantation in male rats. After taking biopsies of the grafts and culturing fibroblasts from them, cells were karyotyped to determine the percentage of donor fibroblasts present in the graft. They found that xenogeneic cell did not survive one month after grafting but allogenic cells could survive in the graft as late as 210 days [51].

In human cases of full-thickness excision of tattoos, following grafting by skin substitutes with sex-mismatched human fibroblasts, Otto et al. have demonstrated allografts could survive in the hosts as late as 2.5 years, as evident by in situ hybridization of the PHY2.1 repetitive Y chromosome sequence [52].

In a study carried out with a porcine full-thickness wound model, it was shown that in all wounds treated with allogeneic fibroblast populated in dermal substitute in comparison to autologous fibroblasts, there were more inflammatory cells, and the presence of mixed

granulomatous and lymphocytic inflammatory foci were detectable. Also, myofibroblasts were present in allogeneic fibroblast-treated wounds. These cells colocalized with inflammation foci. Accordingly, allogenic fibroblasts induced more wound contraction compared with treatments with the dermal substitute seeded with control fibroblasts and the overall cosmetic result was worse [53].

In another study by Price et al. in a porcine wound model, seven days after transplantation, no cells were detectable by polymerase chain reaction, and histologic results showed little difference in wound-healing outcome [54].

Morimoto et al. have examined the application of an acellular collagen sponge and a collagen sponge seeded with either autologous fibroblasts or with allogeneic fibroblasts on full-thickness wounds on the backs of guinea pigs. They labelled cells with PKH26 before transplantation. They found viable autologous and allogenic fibroblasts in the grafts after three weeks but allogenic fibroblasts not only did not accelerate wound healing but also induced inflammation and showed a decreased number of allogeneic fibroblasts, which might have been the result of rejection [55].

A literature review was inconclusive about immunogenicity of allogeneic fibroblast when it is transplanted within skin substitutes. In most experimental and clinical studies, the aspect of immunogenicity of these cells has not been studied in detail. Therefore, we used IDO-expressing allogenic fibroblasts along with normal allogenic fibroblasts in our study. IDO-expressing fibroblasts exhibit strong immunosuppressive activity in vitro and in vivo.

1.4. Local immunosuppression effect of IDO

Tryptophan is an essential amino acid used in the biosynthesis of proteins. It is essential because it cannot be made in our body and therefore it must be obtained from the food. IDO is a 42 kDa monomeric protein and has high affinity for L-tryptophan. It can rapidly catalyze the first and rate-limiting step in the breakdown of this amino acid along the kynurenine pathway [56]. Cells that produce this enzyme can create a local microenvironment devoid of this essential amino acid.

It has been shown that IDO could be expressed in a variety of different cell types, including placenta, macrophages, endothelial cells, smooth muscle cells, fibroblasts, astrocytes, or dendritic cells. IDO expression can be induced by variety of inflammatory cytokines such as IFN-γ (one of its strongest activators), IFN-α, IFN-β, TNF-α , TLR-ligands , glucocorticoid-induced tumour necrosis factor receptor (GITR) ligand, or histone deacetylase inhibitors (HDACS) [56].

It is worth noting that cellular expression of IDO protein does not necessarily means it is an active enzyme. The IDO protein needs extra factors such as superoxide anion to be activated, and its activity is dependent on the presence of redox active compounds [57]. IDO in its inactive form contains a heme-prostetic group with ferric (Fe3+) iron bound and redox active compounds (e.g., superoxide) being required to generate the active Fe2+ form. These compounds are produced in large amounts at the site of inflammation by activated leukocytes, suggesting that IDO activity would be restricted to sites of infection or inflammation [56] [58].

In 1998, Munn and Mellor showed that IDO expression by trophoblast cells during pregnancy at the maternal-fetal interface suppress maternal T cell responses and that it is necessary to prevent immunological rejection of allogeneic conceptus. They demonstrated that

the inhibition of the enzyme by 1-methyl-tryptophan (1MT), resulted in spontaneous abortion in a pregnant mouse model [13].

Two major mechanisms of immune regulation by the IDO pathway have been proposed. One through the regulation of metabolic pathways and the other as a local effect of IDO on T cells and Tregs [59]. KYN-pathway metabolites generated during Tryptophan catabolism by IDO enzymes are biologically active, both as natural immunologic ligands for aryl hydrocarbon receptor (AhR) and as excitatory neurotoxins. The effect of KYN-pathway metabolites on AhR is immunosuppressive and promoting differentiation of forkhead box (Fox)p3+ T regulatory cells. Another metabolic pathway regulatory effect of IDO is the rapid consumption of TRP from the local microenvironment. TRP depletion can activate molecular stress-response pathways in T cells, such as the general control non-derepressible- 2 (GCN-2) kinase and the mammalian target of rapamycin (mTOR) that responds to the amino-acid withdrawal stress pathway [59]. GCN-2 activation finally inhibits the ribosomal translation of most mRNA species, though it induces the translation of a small number of genes resulting in an induction of anergic state and apoptosis. As a local effect of IDO on T cells and Tregs, activation of GCN2 in CD8+ T cells leads to cell-cycle arrest and anergy. In CD4+T cells, it inhibits T helper (TH)17 differentiation and induces de novo Treg differentiation and their suppressor activity. Thus, IDO creates an immune-privileged microenvironment where Foxp3+ Treg are promoted but effector T cells become anergic or apoptotic.

In the context of skin biology, fibroblasts and keratinocytes can also produce IDO in response to stimulation with the proinflammatory cytokines such as interferon-gamma (IFN-γ). IDO expression in these cells contributes to the barrier defence property against the external

pathogens in skin. It has been shown that the local tryptophan depletion by IDO leads to potent inhibition of proliferation in some gram positive and negative bacteria.

It has been suggested that fibroblasts can act as non-professional antigen presenting cells (APCs) [60] [61]. The ability of APCs to present antigens to $CD4^+$ T cells is dependent on the expression of class II MHC molecules by the APCs. It has been shown that fibroblasts express MHC class II in response to IFN-γ [62] [63] [64]. This allows fibroblasts to present antigens to CD4 T- cells to initiate an immune response. On the other hand, the capability of IDO to induce Treg cells, brings this idea that fibroblasts expressing MHC class II can activate Treg cell proliferation in the presence of IDO.

The present thesis was evolved from our previous studies that demonstrated that dermal fibroblasts expressing IDO can expand a suppressive antigen specific Treg cells [65] and the studies that showed IDO can act as a local immunosuppressive factor in a non-rejectable skin substitute.

1.5. Hypothesis and objectives:

Hypothesis:

The application of an IDO-expressing allogenic dermal fibroblast populated within an acellularized dermis is sufficient to create an immune-privileged area within the wound to prevent rejection, while providing a rich source of nutrients and growth factors, in addition to serving as wound coverage for burns.

Objective one: The primary objective of this study was to characterize the ADMs prepared by three methods of decellularization to determine which one would be most effective for

removing all cellular components without significantly affecting the composition, mechanical integrity, and biological activity of the remaining extracellular matrix (ECM) components.

Specific aim 1: Developing a detergent-free decellularization method that maintains the mechanical and structural integrity of dermal tissue with minimal disruption to the ECM in comparison with ionic and non-ionic detergent decellularization methods to determine the most effective method, i.e., the treatment that removes all cellular components without significantly affecting the composition, mechanical integrity, and biological activity of the remaining ECM molecules.

Specific aim 2: Although there are several methods published for the decellularization of skin, those studies have typically focused on *in vitro* cytocompatibility and scaffold characterization, with minimal *in vivo* evidence to assess biofunctionality. Consequently, there is relatively little clinically relevant information with which to make decisions regarding the selection of ADMs for various applications. Thus, as a second specific aim, we evaluated the outcome of using these ADMs for transplantation in a full-thickness skin wound in a mouse model.

Objective two: To evaluate the outcome of the presence of normal and IDO-expressing fibroblasts within ADMs for wound treatment, ADMs were prepared using a new detergent-free method, recellularized with IDO-expressing, or control, fibroblasts, and were transplanted on splinted full-thickness murine skin wounds.

Specific aim 1: Comparing the outcome of transplanting ADM with or without normal and IDO-expressing fibroblasts for wound healing

Specific aim 2: studying the allogeneic response to fibroblasts and possible protective role of IDO

1.6. Research plans:

In this study, we used ionic detergent, non-ionic detergent, and detergent-free methods for decellularization of mouse skin. In a series of *in vitro* and *in vivo* studies, skin samples were evaluated for efficacy of removal of cellular content and the effect on maintenance of several ECM components, including basement membrane proteins. For each method, allogenic skin transplantation on a full-thickness wound mouse model was performed. Immunogenic response to ADM, neovascularization, and migration of host cells to scaffold were investigated at different time points (Fig. 1). In the second step, we used our new detergent-free method for preparation of ADM, then recellularized it with IDO-expressing fibroblast or normal dermal fibroblast as a control. Then, recellularized ADMs were transplanted on splinted full-thickness skin wounds generated on the dorsal side of mice. The outcome of wound healing was evaluated by checking a list of criteria for graft take, clinical appearance, tissue cellularity, infiltrated immune cells, angiogenesis, and reepithelialisation (Fig. 2). To further investigate the transplanted cells' fate, we intradermally injected luciferase-labeled fibroblasts in wild type Balbc and immunodeficient NOD-SCID-Il2r gamma null (NSG) mice and tracked the cells by bioluminescence in vivo imaging.

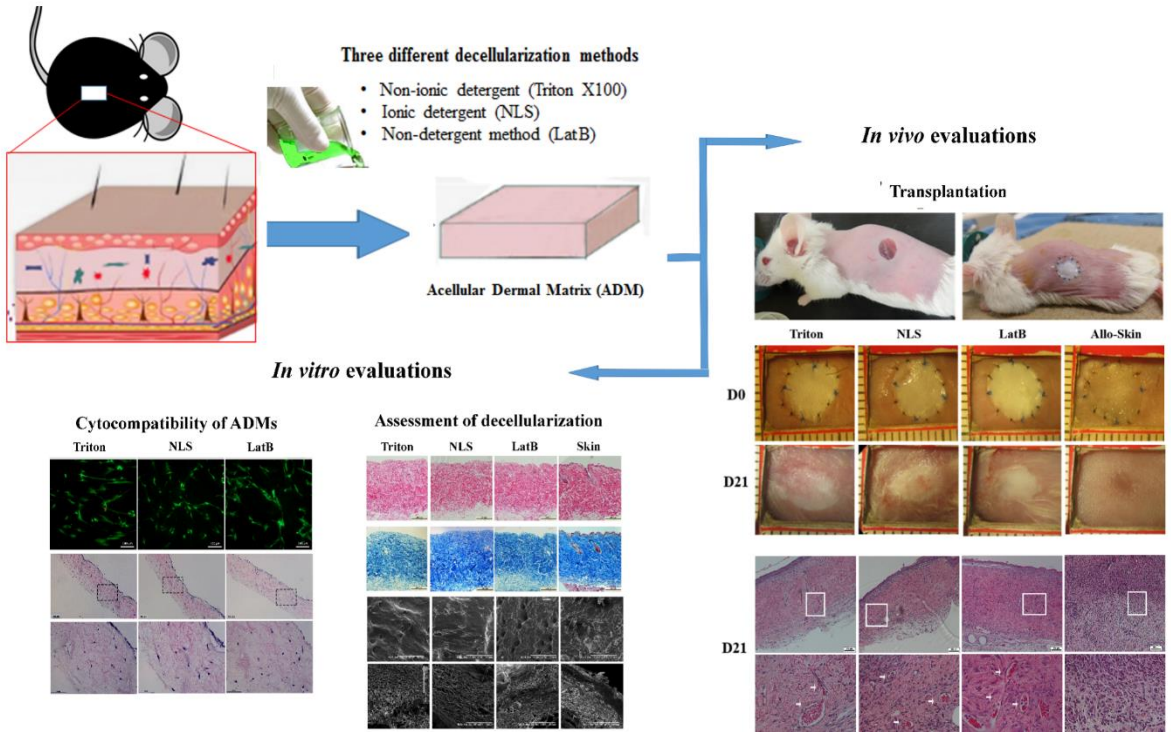

Figure 1: Method for first objective: characterizing the ADMs prepared by three methods of decellularization.

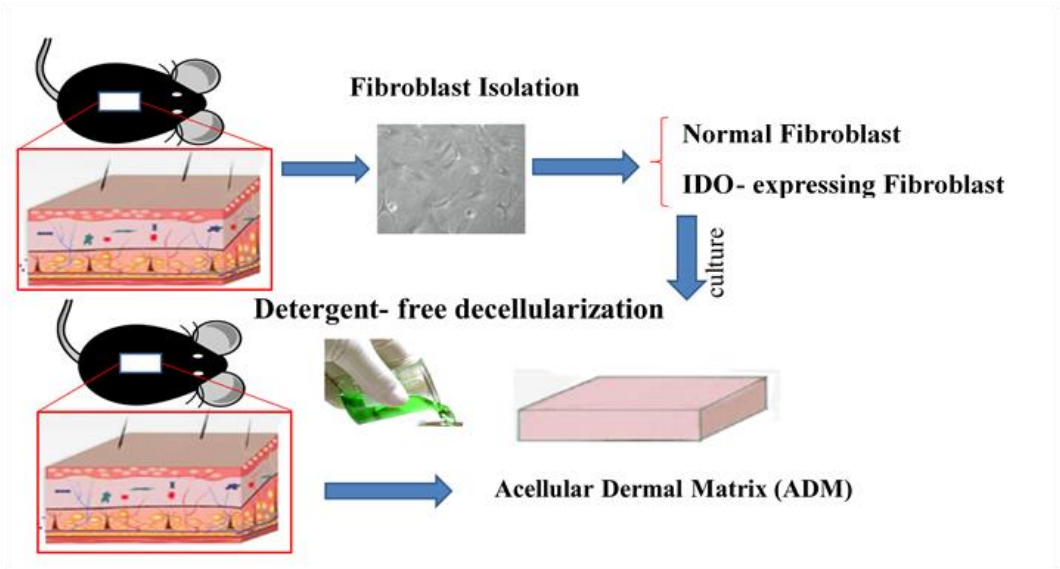

Chapter 2: Biofunctional Evaluation of Detergent- free Decellularization of Murine Skin in *In Vitro* and *In Vivo* Models [1]

2.1 Introduction:

Acute and chronic wounds affect millions of people worldwide. It is estimated that there are 37 million people with ulcers worldwide and roughly 500,000 burn patients within the United States, all of whom would benefit from rapid, biological wound coverage [66]. Additionally, at least 1% of the population in developed countries will experience non-healing chronic wounds such as diabetic, pressure, and venous ulcers in their lifetimes [67].

Adequate coverage of the wound is essential for healing regardless of the type of wound. The primary purpose of a wound dressing is to achieve a rapid closure of the lesion and reduce further insult during the wound repair process. Prolongation of wound repair due to inflammation, infection, and severity of injury can increase the risk of complications and aberrant healing, such as hypertrophic scarring. Chronic and large surface area wounds share a common characteristic of delayed wound repair, which may be mitigated through the application of skin grafts and skin substitutes. Despite the advantages of full-thickness skin grafts (FTSGs) and split-thickness skin grafts (STSGs), problems such as morbidity of donor site, low vascularity, contracture, decreased elasticity, sensory loss, and undesirable cosmetic results remain problematic [15,16].

To overcome these drawbacks tissue-engineered alternatives have been developed. Among those alternatives, biological scaffold materials composed of an extracellular matrix (ECM) have been reported to facilitate the constructive remodelling of different tissues in both preclinical animal studies and in human clinical applications. The structural, biomechanical, and biochemical properties of ECM scaffolds are inherently determined by the material properties of the original

[1] A version of this chapter has been submitted for publication. Ali Farrokhi, MSc, Mohammadreza Pakyari, MD, Layla Nabai, MD, Ryan Hartwell, PhD, Reza Jalili, MD/PhD, and Aziz Ghahary, PhD. Tissue Engineering (May 2016).

tissue, because ECM consists of the structural and functional molecules secreted by the resident cells of each tissue and organ [4]. Thus, *de novo* engineered skin substitutes, using biopolymers, lack the addition of the mosaic heterogeneity of cell-derived molecules that are found in normal skin. In order to fabricate a skin substitute with the molecular heterogeneity and biochemical and mechanical properties of normal skin, a decellularization process is desirable.

Acellular Dermal Matrices (ADMs) are decellularized allogeneic skin and have been used clinically for different purposes, including the treatment of abdominal wall defects [21] and full-thickness burns [5], the prevention of post-parotidectomy gustatory sweating [22], cleft palate repair [23], resurfacing of intraoral defects [24], lip augmentation [25], reconstructive breast surgery [26], and chronic wound repair [27].

The ideal bioscaffold resulting from decellularization of skin should preserve the original ECM materials with similar biomechanical properties to the skin and not induce an immune response. It should support rapid and directed proliferation of infiltrated cells, be easily revascularized, and exude stability throughout the repair process while being able to be remodelled over time, just as any other tissue. Practically, the ADM should be easy to apply by the end-user and have a commercially viable shelf-life [20].

A number of different decellularization methods have been reported and employed to produce commercially available human- and xenogenic-derived products. However, decellularization would have a negative effect on the graft function if it altered the biochemical composition, structure, and biomechanical properties of tissue. It is well known that ECM is not only a scaffold but also a reservoir of all molecules, such as growth factors and cytokines secreted by tissue resident cells [68]. Any decellularization method that leads to the preservation of these molecules should therefore ideally improve wound healing.

Conventional decellularization processes require the use of harsh reagents that cause unavoidable adverse effects on the ECM components and molecules contained within. Any process improvements that seek to mitigate ECM damage are highly desirable.

In this study the primary objective was to develop a detergent-free method of decellularization to minimize any potential damage on matrix molecules and compare this method with Triton X-100 and *N*-Lauroyl sarcosinate (NLS) as non-ionic and anionic detergent methods of ADM preparation, respectively, against specific design criteria. Triton X-100 is one of the most widely used non-ionic detergents for decellularization of tissues [69–71]. NLS, also known as sarkosyl, is a non-denaturing anionic detergent derived from sarcosine. This surfactant is amphiphilic and is believed to be milder than other ionic detergents like Sodium dodecyl sulfate (SDS). It has been used for the decellularization of skin and artery tissues [72,73].

Our criteria comprised indicators and measures of mechanical performance, removal of cellular components, product biocompatibility, and preservation of ECM molecules. Although there are several methods published for the decellularization of the skin, those studies have typically focused on *in vitro* cytocompatibility and scaffold characterization, with minimal *in vivo* evidence to assess biofunctionality. Consequently, there is relatively little clinically relevant information with which to make decisions regarding the selection of ADMs for various applications. Thus, as a secondary objective, we evaluated the wound-healing outcome of using these ADMs for transplantation in a full-thickness skin wound in a mouse model. The results of this comparable head-to-head study of decellularization methods demonstrated that a detergent-free process preserves matrix composition and mechanical properties significantly better than detergent-based methods.

2.2 Materials and methods:

2.2.1 Ethics statement

All methods and procedures, as well as the use of animals and tissue specimens derived from animals and humans, are approved by the Ethics Committees of the University of British Columbia.

2.2.2 Animals and skin preparation

Male C57/B6 mice (Jackson Lab, USA) aged 3 to 4 months were used as skin donors, and BALB/c female mice aged 2 to 3 months were used as recipients of ADMs grafts. Donor C57/B6 mice were anaesthetized with CO2 and euthanized by cervical dislocation. The mouse dorsum was depilated using a shaver and hair removal cream. Skin was then scrubbed with povidone-iodine solution (Triadine, H&P Industries Inc., Franklin, WI, USA). Full-thickness donor skin was removed from the mouse dorsum. The removed skin was washed three times in phosphate buffered saline (PBS), and panniculus carnosus and hypodermis tissues were removed manually using a surgical blade. After washing with PBS, the remaining part of skin tissue was processed for decellularization as described below.

2.2.3 Cell Isolation and culture

Mouse dermal fibroblasts were explanted from B6 mice skin as previously described [74]. Human primary fibroblasts were isolated from the discarded foreskins of consenting donors. Skin specimens were briefly washed several times with 1x PBS (pH 7), containing 1% antibiotic, minced into small pieces, then fixated with Fetal Bovine Serum (FBS) for 4 hours on a tissue culture plate. After 4 hours, one drop of 1x Dulbecco's Modified Essential Medium (DMEM) containing 10% FBS and 1% antibiotic was added to FBS drops overnight. The next day DMEM was used to cover the fixated skin section in the dish. Skin pieces were maintained in culture until fibroblasts reached 60% confluency, after which cells were trypsinized and passaged.

2.2.4 Decellularization methods

In this study, we used three different methods based on effective agents for decellularization that have been reported previously: Triton (non-ionic detergent), NLS (non-denaturing anionic detergent), and latrunculin B (LatB) treatment followed by hyper- and hypotonic solutions as a detergent-free method. Triton and NLS have previously been reported for preparation of ADMs, whereas LatB, to the best of our knowledge, has only been reported for preparation of decellularized muscle. The LatB method, described herein, was modified for the preparation of ADMs.

All donor skin was treated with 2 units/mL Dispase II (Invitrogen/Gibco, cat. no. 17105-041) in high-glucose DMEM at 37 °C for 90 min to remove the epidermis and disrupt cell attachment to the dermal matrix prior to preparation of the ADMs using one of the following methods:

(A) Triton method: This was based on a previously described decellularization method by Takami et al. with some modifications [69]. After Dispase treatment and washing 3 times with PBS, the dermal matrix was incubated in 0.5 % Triton X-100 (Fisher Scientific, ON, Canada) for 24 h at room temperature with continuous shaking and renewing the solution after the first 12 h. Subsequently, ADM was extensively washed with PBS for 12 h.

***(B) N*-Lauroylsarcosinate (NLS) method:** Samples in this treatment group were subjected to a modified, previously described decellularization method that has led to developing a commercial product named Matracell® [72]. Following Dispase II treatment and washing 3 times with PBS, the dermal matrix was incubated in 1 % NLS (Sigma-Aldrich) for 24 h at room temperature with continuous shaking and renewing the solution after the first 12 h. Subsequently, ADMs were extensively washed with PBS for 12 h.

(C) LatB method: A non-detergent protocol was used according to the method of Gillies et al. with some modifications [75]. Briefly, after Dispase II treatment and washing 3 times with PBS (this step was not in the original protocol), skin samples were incubated in 50 nM LatB (Enzo

Life science, BML-T110) in high-glucose DMEM (Gibco) for 2 h at 37 °C to depolymerize actin filaments. Then samples were washed with distilled water twice for 15 min and subsequently were incubated in 0.6 mol/L potassium chloride (Sigma-Aldrich) for 90 min, followed by 1.0 M potassium iodide (Sigma-Aldrich) for 90 min. Following the high ionic solution incubations, skin samples were washed in distilled water overnight. The potassium chloride and potassium iodide incubations and overnight distilled-water incubation were then repeated. Samples were washed with distilled water twice for 15 min between incubation steps. All steps were performed at room temperature with continuous shaking.

At the final step, all of the ADMs prepared with the three methods were treated with 50 units/mL Benzonase® Nuclease (Santa Cruz, sc-202391) for 12 h at 37 °C, then washed with PBS for another 12 h. All solutions used for ADM preparation were filter-sterilized, and all procedures were performed aseptically. Solutions contained Sodium azide (0.02% w/v) at all times, except during the last PBS washing step, to prevent microbial growth.

2.2.5 Histological examination of ADMs

For histological evaluation of the ADM structures, conventional H&E as well as Masson trichrome staining were done on paraffin sections. Paraffin-embedded ADMs were sectioned at a thickness of 5 µm. After removing the paraffin, sections were first rehydrated with a decreasing series of alcohol concentrations to water, and then standard protocol was followed for hematoxylin and eosin staining or Masson trichrome staining. After sealing, samples were examined by light microscopy at a different magnification to inspect for the presence of cells (stained by hematoxylin to a bluish-purple color) and collagen fibres (stained by eosin to a pink color or blue with aniline-blue in Masson trichrome).

2.2.6 DNA Quantification and Fragment Length Analysis

To assess presence of residual cells or debris within the ADMs after decellaularization, total DNA content of the ADMs and native skin was measured as described previously [76]. Briefly, Samples were freeze-dried and cut into thin strips and then small pieces. Then digested with 50 μg/mL protease K in 0.5 mL of a lysis buffer. The DNA was extracted with phenol/chloroform method and purified by 2M NaCl- Isopropanol precipitation and 70% ethanol washing. Precipitated DNA samples were dehydrated to remove residual ethanol and then rehydrated in 1X TE buffer. The residual DNA content was measured at 260 nm using a nanodrop spectrophotometer. To determine DNA fragment size, samples were separated by electrophoresis on a 1% LMP agarose gel stained with SYBR-safe dye at 80 V for 75 minutes and visualized with the Gel Doc EZ system (Bio-Rad Inc.)

2.2.7 Sodium dodecyl sulfate (SDS)-polyacrylamide gel electrophoresis and western blot analysis

Skin and ADMs were freeze-dried, minced, and homogenized in the presence of protease inhibitor. Total protein content was measured using the BCA method (ThermoFisher Scientific, Cat # 23225). Due to the discrepancy between protein content of skin and ADM, protein amount equal to 1 mg from each sample was loaded into wells of 10% gradient polyacrylamide gels (Bio-Rad, Hercules, CA). Proteins were transferred to polyvinylidene difluoride (PVDF) membranes (MilliporeSigma, IPVH00010), and subsequently blocked in 5% skim milk in Phosphate buffered saline with 0.1% Tween-20. The blots were probed with Anti-ß-actin Mouse Monoclonal Antibody (Sigma-Aldrich, Cat # A5441) for 2 hours, and detected using Goat anti-Mouse IgG (H+L) Cross Adsorbed Secondary Antibody, DyLight 800 (Catalog # SA5-

10176) at dilutions 1: 30,000 and 1:10,000, respectively. Blots were scanned with LI-COR Odyssey Classic imaging system. Molecular weight was determined using PageRuler Plus Prestained Protein Ladder (ThermoFisher Scientific, Cat # 26619).

2.2.8 Scanning electron microscopy (SEM)

Lyophilized ADMs were cross-sectioned using a surgical blade. Samples were first gold-coated, then scanned with the Hitachi S-3000N scanning electron microscope (Hitachi, Tokyo, Japan). Comparisons between ADMs and normal skin were made for morphological changes to collagen fibres in cross sections and surface topography of epidermal and hypodermal sides.

2.2.9 Hydroxyproline content

Lyophilized ADMs or fresh tissues were collected from five independent experiments and digested with proteinase K (in Tris-HCl buffer) (Thermo Scientific) at 54 °C while shaking for 5 to 6 h, and then homogenates were incubated with an equal volume of 12N HCl at 105 °C overnight to hydrolyze the collagen (1 mg tissue/1 mL HCl 6N). After evaporation of the acid under a nitrogen flow, the dried samples were suspended in 40 µL of ethanol:dH2O:TEA (2:2:1) and re-dried. Derivatization to phenylthiocarbamyl was achieved by adding 40 µL of ethanol:dH2O:TEA:PITC (Edman's reagent, Pierce Biotechnology) (7:1:1:1) to each sample and incubating at room temperature for 20 min before drying. The samples were then resuspended in 1 mL of analysis solution (dH2O: Acetonitril, 7:2) and cleared before high-performance liquid chromatography (HPLC) analysis. In addition, and using the same procedure, 1 mg of purified type I bovine collagen was hydrolyzed and derivatized as a control. For the calibration curve, different amounts of hydroxyprolin (1–320 µg) were dried from freshly prepared stock solution of trans-4-hydroxy-L-proline (Sigma) in dH2O and derivatized before analysis.

2.2.10 Glycosaminoglycans content

The quantification of sulfated glycosaminoglycans (sGAGs) was performed using the 1,9-dimethylmethylene blue (DMMB) assay adapted from Barbosa et al. [77]. Briefly, lyophilized samples were collected from five independent preparations and digested overnight with 100 μg/mL proteinase K (Sigma–Aldrich, St. Louis, MO) at 56 °C followed by DNAse treatment. Then 100 μL of digested mixture was added to 1 mL of the GAG-complexating DMMB solution, which was a 16 μg/mL DMMB (Sigma–Aldrich) in 5% ethanol solution (paper filtered) with a 0.2 M guanidine hydrochloride solution containing 0.2% formic acid and 0.2% sodium formate. The resulting sGAG-DMMB complex was precipitated from the solution and then solubilized in the decomplexating solution, which was a 50 mM sodium acetate solution buffer (pH 6.8) containing 10% 1-propanol and 4 M guanidine hydrochloride. Absorbance of the decomplexed solution of DMMB and sGAGs was measured at 656 nm. sGAG concentration was calculated by calibrating against a standard curve of chondroitin sulfate-A (Sigma–Aldrich), ranging from 0 to 70 mg/mL (0 to 7.0 μg/assayed sample). Assays were performed five times and every time in duplicate. Results were expressed in μg of GAG/mg of dried tissue.

2.2.11 Biomechanical assessment

Biomechanical characteristics of native and decellularized skin were evaluated by uniaxial tensile-stress testing. Specimens were cut into a dog-bone shape using a standardized jig with the neck of the dog-bone shape measuring 2 cm in length and 0.4 cm in width. Tensile testing was done using a KES-G1 Micro-Tensile testing set-up (Kato Tech, Kyoto, Japan), with a 5-kg load cell. Two pieces of sandpaper were then used to firmly secure the samples to the specimen holder. Samples were then stretched until breakage at a deformation rate of 0.1 cm s−1. Young's Modulus in megapascals (MPa) was derived from the engineering stress/strain curve and calculated using

the area density of the ADM. For statistical purposes, the mean and p-value of five samples from each group were evaluated and compared.

2.2.12 Immunofluorescent staining of elastic fibres

For the assessment of elastic fibers, we used immunofluorescence staining. Paraffin-embedded samples were sectioned at a thickness of 5 µm. After deparaffinization and rehydration, the non-specific antibody binding sites were blocked with 5% BSA in PBS. For staining we used polyclonal rabbit Anti-Elastin primary antibody (Abcam, ab21610), 1:100 in 2% BSA in PBS and secondary Rhodamine Red™-X (RRX) AffiniPure goat anti-rabbit IgG (H+L) antibody (#111-295-144, Jackson Immunoresearch Laboratories, West Grove, PA, USA), 1:1000 in 2% goat serum in PBS. Images were collected by the systematic uniform random sampling of tissue sections, using the 20x dry objective of a Zeiss AxioObserver Z1 confocal microscope fitted with a CSU-X1 spinning disc (Yokogawa Electric) and AxioVision 4.8 (Zeiss). To quantify the elastin area fraction, confocal images were analyzed using the program ImageJ 1.50i (National Institutes of Health, USA). Images were converted to an RGB stack format and the scale was adjusted to micrometres, using a scale bar of the images, then the threshold was set to exclude background and saturated pixel intensities. Immunolabelled areas were automatically detected and the area fraction was calculated for elastin. For final quantification, the area fraction for 15 fields of view per sample were averaged over triplicate independently prepared samples.

2.2.13 Cytocompatibility

Cell adherence to the surface of ADMs was determined qualitatively through staining actin filaments with cytopainter Phalloidin 647-iFluor reagent (Abcam, ab176759), and viability was

assessed using a Live/Dead toxicity assay (Molecular Probes®, Invitrogen, Carlsbad, CA). Cells used in this study include mouse dermal fibroblast and human foreskin dermal fibroblast. The high-glucose DMED culture medium supplemented with 10% FBS was added to each ADM and incubated in a 37oC, CO2-regulated incubator for 24 h before cell seeding. For cell attachment and viability tests, 15 × 103 and 10 × 103 cells were seeded onto the top surface of each ADM, respectively, and were maintained in culture. Cell culture was stopped at 24 h post-seeding, and phalloidin staining or Live/Dead staining was performed. For the cell attachment test, after 24 h of culture, the ECM scaffolds were fixed with 4% paraformaldehyde, stained with cytopainter Phalloidin 647-iFluor reagent (Abcam, ab176759) for f-actin to visualize cells, and counterstained with the nuclear dye DAPI. For the viability test, after 24 h, the scaffolds containing cells were washed three times with 1× phosphate-buffered saline (PBS), pH 7.0, and incubated with a mixture of ethidium homodimer and calcein-AM according to the manufacturer's instructions. After 30 min, the scaffolds were washed three times with 1× PBS and visualized using a Zeiss AxioObserver Z1 confocal microscope fitted with a CSU-X1 spinning disc (Yokogawa Electric) and AxioVision 4.8 (Zeiss), and images were analyzed by Zen software.

2.2.14 Subcutaneous implantation of ADMs and biocompatibility study

Four female BALB/c mice per each treatment group were anesthetized using isoflurane and aseptically prepared for surgical subcutaneous engraftment of ADMs. Briefly, bilateral 1 cm incisions were created on the mouse dorsum followed by minimal dissections under the panniculus carnosus. ADMs (8mm in diameter) or freshly excised C57/B6 mouse skin, were placed onto dorsal pockets. Each had two implants from the same treatment group, one at left and the other in right dorsal sides; a C57/B6 fresh skin sample acted as a control and three decellularized dermal

matrices as treatment groups. All the skin incisions were closed with 5/0 vicryl sutures. They were implanted for 1, 2, 4, and 8 weeks into each mouse. All mice remained healthy, with no overt signs of inflammation over the experimental period. At proper time points, recipient mice were euthanized, and the implants along with upper skin and surrounding connective tissue were removed (Fig. 2.4). The size of the implanted ADM was measured using a ruler and then processed for routine H&E histologic examination.

2.2.15 Recall antigen and T cell proliferation assays

Spleens from ADM-matched BALB/c mice were harvested and prepared by removing fat and mesentery. Splenocytes were isolated using a 40-μm cell strainer (Fisherbrand; Fisher Scientific UK) and the back end of a plunger from a 10-mL syringe as previously described [78]. In all cases, ≥95% of cells remained viable (data not shown). Splenocytes were also isolated from C57/B6 mice spleens for the two-way mixed lymphocyte reaction (MLR) controls. After isolating the splenocytes from pre-sensitize mice and labeling them with carboxy-fluorescein diacetate succinimidyl ester (CFSE), each group was cocultured with 8-mm punch biopsies of native or decellularized skin from a corresponding group for 4 days.

To ensure that only viable cells were evaluated, 7AAD (Live/Dead) exclusion dye was used as a selection marker. Only 7AAD negative cells were gated for final analysis. Any adherent cells were detached by gently washing the tissue with medium. Cells were incubated with monoclonal antibodies for Anti-Mouse CD3 APC (ebioscience), Anti-Mouse CD4 PerCP-Cyanine5.5 (BD Biosciences), Anti-Mouse CD8a PE (ebioscience), or an equivalent isotype-matched negative control antibody. Samples were processed (minimum 30,000 live-events per sample) using a BD FACS machine (BD Biosciences). Data was acquired and analyzed using BD

CellQuest Pro software (version 4.0.1 for Mac; BD Biosciences). The gating strategy excluded debris to ensure positive gating of a lymphocyte population on the forward scatter – side scatter dot plot. Out of the live cells, CD3+, CD4+, and CD8+ cells were shown in a dot plot against CFSE, and the percentage of proliferated cells was measured on a histogram, expressed here as the proliferation index (i.e., the proportion of cells that have proliferated in response to antigen).

2.2.16 Transplantation procedure

BALB/c mice were anesthetized and hair from their backs was removed using clippers and a depilatory cream. Full-thickness wounds, including the panniculus carnosus, were created on the back of the mice using a 6-mm-in-diameter punch device in two different sites on the back of the recipient mice (Fig. 2.6A). Four female BALB/c mice per each treatment group were used, and each mouse received either two ADMs (prepared using the same method) or control skin grafts (fresh allogeneic skin). Allogeneic skin was harvested from donor C57/B6 mice. Skin grafts and ADMs (8-mm diameter) were engrafted on the 6-mm wound bed and sutured at 90° intervals using 7-0 prolene sutures (12, 3, 6 and 9 o'clock). The intervening gaps were then addressed using simple interrupted sutures with 8-0 nylon sutures (6-8 sutures) (Fig. 2.6A). Immediately following surgery, OPSITE dressing (Smith & Nephew) was sprayed onto the graft site and covered by Vaseline-impregnated gauze. Tegaderm film was applied over the graft site and then secured by a 2-cm width Co-flex bandage.

2.2.17 Statistical analysis.

Data are means ± SEM of three or more independent set of experiments. The statistical differences of mean values among ADMs and control normal skin were tested with one-way

ANOVA. Post-hoc comparisons were done using Bonferroni correction for multiple comparisons. P-values < 0.05 were considered statistically significant.

2.3 Results:

2.3.1 Assessment of decellularization

We compared freshly isolated mouse dorsal skin with site-matched decellularized skin matrix variants, namely, Triton, NLS, and LatB. Histological examinations are shown in figure 2.1A. Successful decellularization was defined as the absence of nuclei in H&E staining, with relative preservation of dermis structure. To qualitatively assess the extent of preservation of collagen fibres during decellularization, we used Masson trichrome staining (Fig. 2.1B). Both staining methods revealed that dermal and epidermal cells (nuclei included) were completely removed by all decellularization treatments, while the basic dermal architecture of collagen bundles were preserved.

Representative scanning electron micrographs of the surfaces of both sides of ADMs and their cross-sections are shown in figure 2.1C. SEM micrographs showed morphological and structural differences between the hypodermal and epidermal sides of ADMs. In brief, a network of collagen, reticular fibres, and connective tissue with varying diameters were observed on the hypodermal sides. Even though all three ADMs showed a relatively smooth epidermal-surface, resembling sheets of tightly compacted materials, they exhibited different surface topography. Cross-sectional micrographs of the materials displayed fibrous architecture with variable porosity, and interestingly, the cross section of the NLS-ADM has a distinct structural pattern resembling the normal skin (Fig. 2-1 C). Figures 2-1 D, E show the residual DNA contents before and after the decellularization with three methods. The residual DNA content, which represents the

remaining cell debris, is not detectable in ADMs. In last step of our decellularization methods we used Benzonase treatment and these results showed that our methods were adequate for eliminating the residual DNA cell content. Similar findings were observed with western blot for detection of actin protein as an abundant intracellular protein. The amount of actin in ADMs was undetectable compared with that of untreated skin (Fig. 2-1 F).

2.3.2 Collagen and sGAG content

The collagen and sulfated GAG content of the normal skin and decellularized scaffolds were assessed quantitatively. Collagen content, indicated by quantification of hydroxyproline, was equally preserved in all three methods of decellularization (Fig. 2.2A). In contrast, decellularization with NLS significantly reduced sulfated GAG while other decellularization methods did not significantly change the GAG content (Fig. 2.2B).

2.3.3 Tensile strength

Tensile strength, as a measure of engineered stress, was determined for all ADMs as well as mouse skin as a control. Performance-wise, LatB decellularized skin was most comparable with normal skin (Fig. 2.2C). Further, the tensile modulus of NLS and Triton ADMs were significantly higher than that of both LatB-ADM and normal skin ($P < 0 .05$) (Fig. 2.2D).

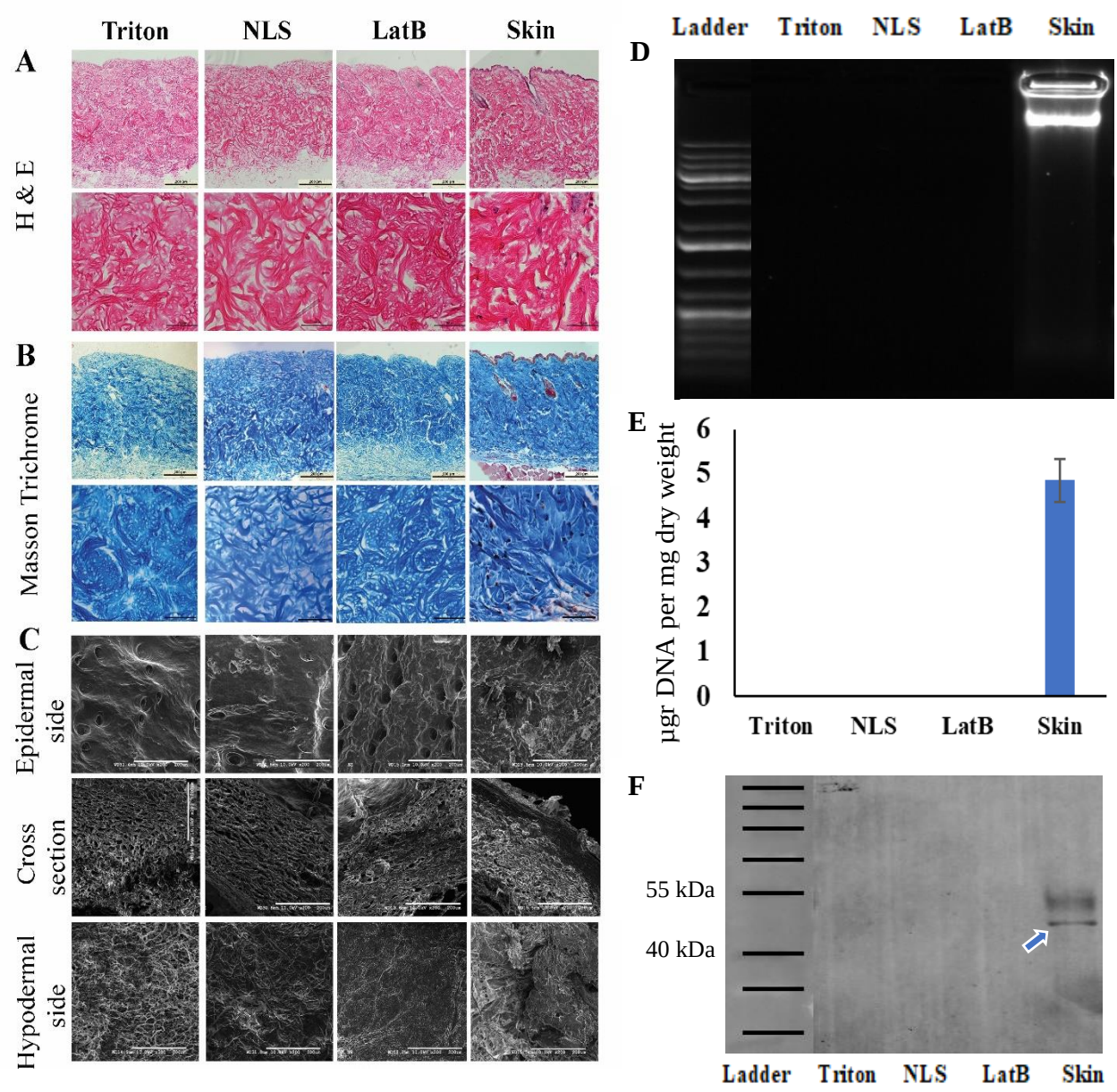

Figure 2.1. Histological analysis of native and decellularized dermis tissue. A) Hematoxylin and eosin staining of normal skin and ADMs demonstrate absence of the nuclear staining material, showing removal of cells after decellularization but preservation of the architecture of the decellularized ECM (scale bars in top and lower rows = 200 µm and 50 µm, respectively). B) Masson trichrome staining shows presence of collagen in ADMs (scale bars in top and lower rows = 200 µm and 50 µm, respectively). C) Scanning electron micrographs of the two surfaces and cross-section of the skin and ADMs samples from different treatments show their ultrastructure (scale bars = 200 µm). D, E) Residual DNA contents before and after the decellularization with three methods. F) Western blot for detection of actin protein. Arrow indicates the band corresponding to b-actin.

2.3.4 Immunofluorescent staining of elastic fibres

In order to evaluate non-collagenous proteins of ECM in decellularized matrix, elastin staining was performed. The elastic network, elastin, is in part responsible for natural skin tension and elasticity. The elastic fibres are much finer than its collagen fibres. The role of elastin fibres is to restore the collagen network to its normal condition after deformation [79]. As shown in Figure 2.2E, elastin fibres appeared fragmented and significantly less abundant in the Triton- and NLS-ADMs (12.98± 0.42 and 11.89± 0.66) than those of the LatB method and normal skin (19.20± 0.93 and 19.35± 1.00), respectively ($P < 0 .05$).

2.3.5 Cytocompatibility of ADMs

To investigate the cellular response to these scaffolds in vitro, ADMs were seeded with mouse dermal fibroblast and human fibroblasts. All cell types cultured for 24h on ADM surfaces prepared with 3 different decellularization methods, were viable as indicated by green (live cells) staining (Fig. 2.3A). There was no difference between the three materials with respect to fibroblast adherence after 24h in culture (Fi. 2.7-Sup. Fig. 1). The morphologic appearance of the fibroblasts and their density on the surface of ADMs are indicative of fibroblasts' adherence to the surface of the matrix. Differences in fibroblast morphology correspond with the observation of differences in surface topology made evident by SEM (Fig. 2.1C). To investigate the infiltration of fibroblasts into the dermal matrices, fibroblasts were kept in culture on matrices for 1 month. As shown in Figure 2.3B, all three types of ADMs were able to foster the in vitro culture of fibroblasts and allow their infiltration into the ECMs after one month of being in culture

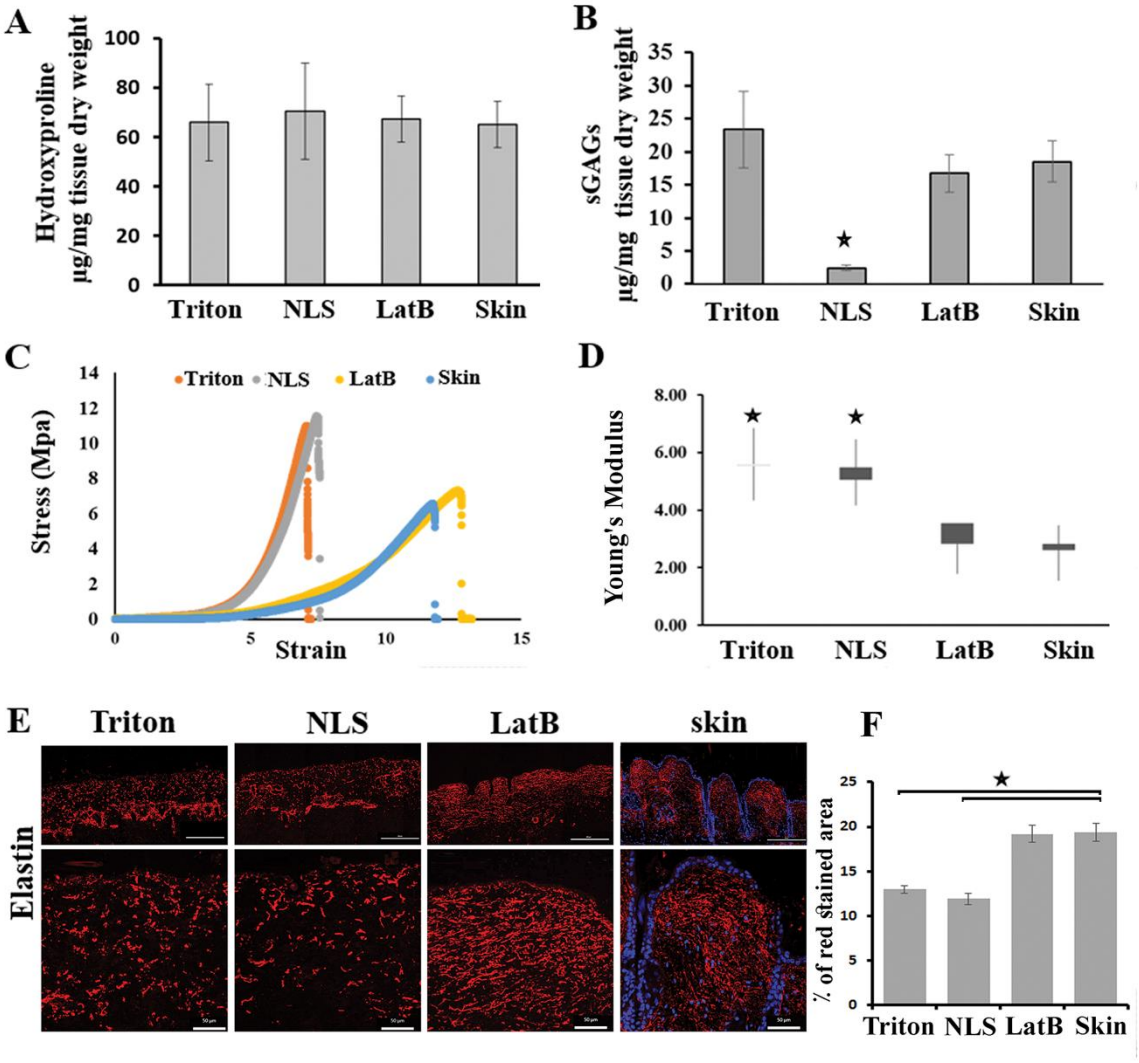

Figure 2.2. Characterization of ADMs. Samples were collected from five independent preparation for following experiments. A) Hydroxyproline contents were used as a measure of total collagen content of native and decellularized skin. B) Effects of decellularization on tissue sGAG content was significantly lower in the NLS-ADM when compared to controls (*, $P < 0.05$). C) Tensile stress-strain relationships of ADMs and normal skin. LatB decellularized skin was most comparable with normal skin. D) The tensile modulus of NLS and Triton ADMs were significantly higher than that of both LatB-ADMs and normal skin (*, $P < 0$ .05). E, F) Elastin immunofluorescent staining (scale bars in top and lower rows = 200 µm and 50 µm, respectively) and quantification. The area fraction for 15 fields of view per sample were averaged over triplicate independently prepared samples for quantification.

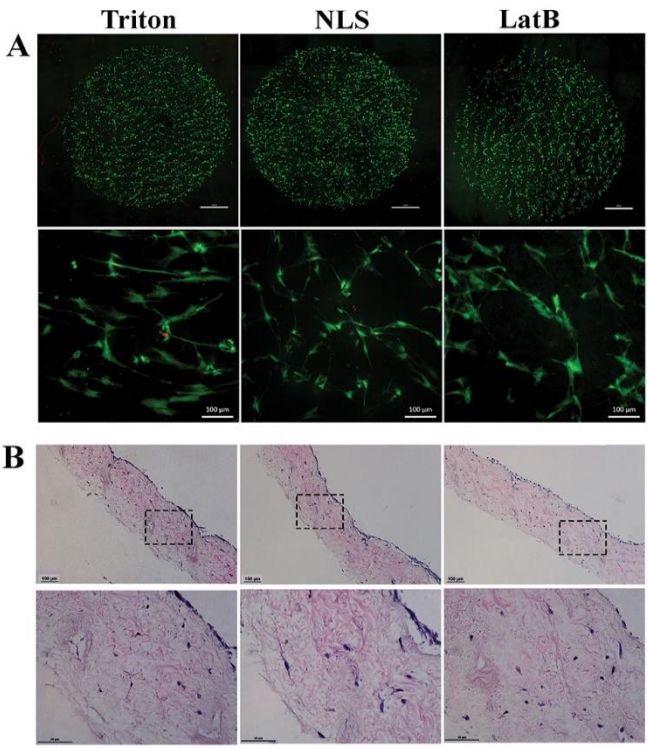

Figure 2.3. Cytocompatibility of ADMs. A) Cells were grown on the different ADMs for one day and stained with calcein and ethidium homodimer. Live cells appear green and dead cells appear red. Top row shows lower magnification (Scale bars = 1 mm) and lower row higher magnification (Scale bars = 100 µm). B) ADMs seeded with mouse fibroblasts, after four weeks in culture. The infiltration of cultured cells at epithelial surface into dermal matrix is detectable in all ADMs (scale bars in top and lower rows = 100 µm and 50 µm, respectively).

2.3.6 Biocompatibility study

Both fresh and decellularized dermal samples derived from C57/B6 mice were implanted subcutaneously on the dorsum of BALB/c mice to evaluate both immunogenicity and cell infiltration in a secondary in vivo model (Fig 2.4). After 1, 2, 4 and 8 weeks, recipient mice were euthanized, and the implants were removed, along with upper skin and surrounding connective tissue, and processed for routine H&E histologic examination (Fig. 2.4A and B). As expected, allogeneic skin presented signs of immune cell infiltrate, indicative of acute rejection by the host, as early as 1 week (Fig. 2.4A.h), with notable degradation and infiltrating immune cells within the implants at week 8 (Fig. 2.4B.l). In contrast, none of the ADMs (regardless of the decellularization method) prompted any significant immune response. In fact, there were no noticeable differences in gross morphology of ADM implants at any given time. Histology revealed that host cells migrated into all ADMs after the first week of implantation (Fig. 2.4A. e,f,g). Over the 8 weeks of follow-up, there was no evidence of ADM rejection by the recipient mouse (Fig. 2.4B).

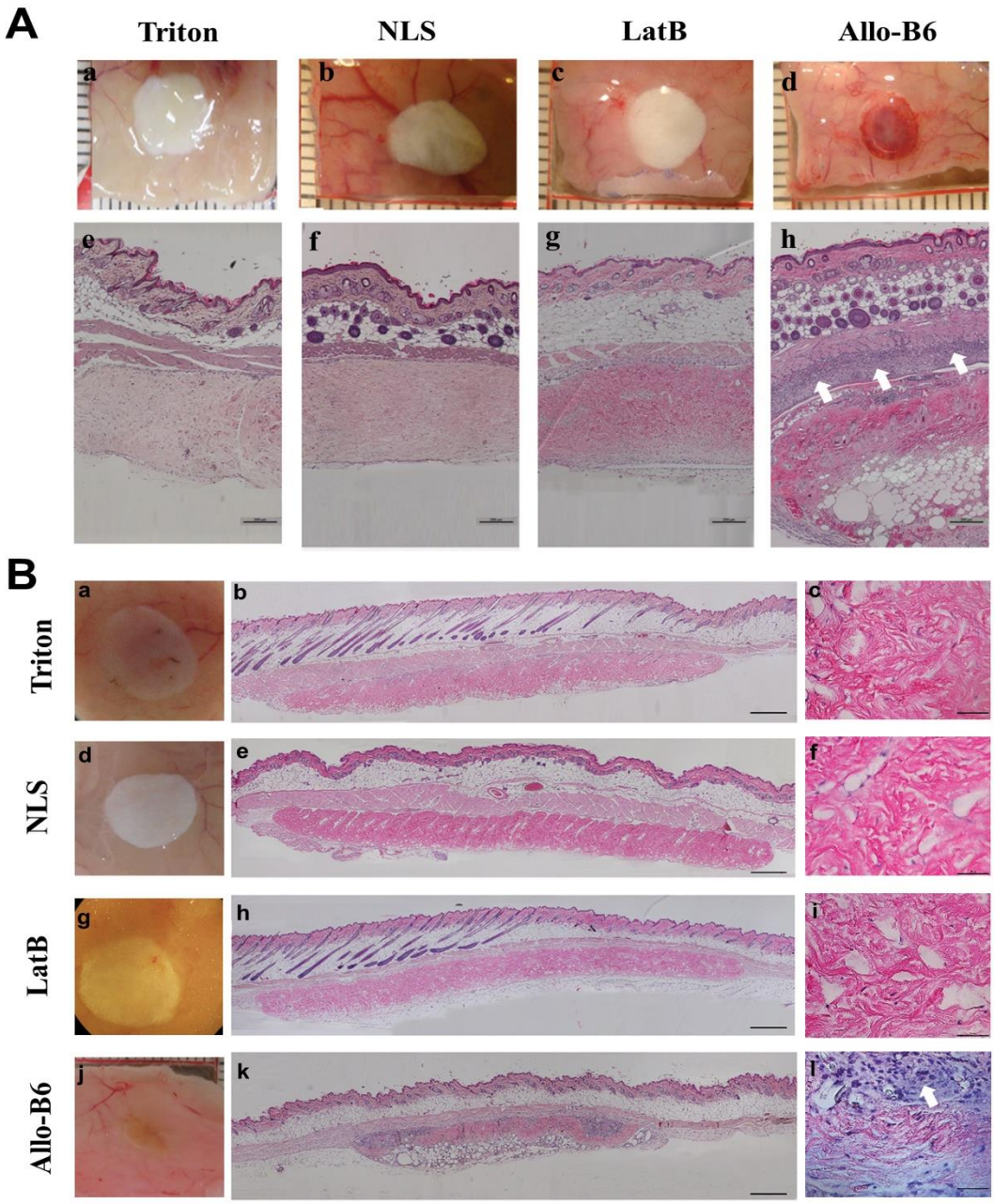

Figure 2.4. Biocompatibility study of both fresh allo-skin and decellularized dermal samples derived from C57/B6 mice implanted subcutaneously on the dorsum of BALB/c mice after (A) one week and (B) 8 weeks. Dissected ADMs after subcutaneous implantation with the overlying skin at week 1 (A-a,b,c,d) and week 8 (B- a,d,g,j). Allogeneic skin presented signs of immune cell infiltrate at week 1 (A-h), with notable degradation and infiltrating immune cells within the implants at week 8 (B-k,l). Scale bar in A. e-h = 100µm, B. b, e, h, k = 500µm, B. c, f, I, l = 50µm.

2.3.7 Assessment of T cell proliferative response to decellularized scaffolds *in vitro*

When pre-sensitized BALB/c splenocytes were stained with CFSE and cocultured with any type of B6 decellularized dermal scaffolds (acting as a recall antigen), the BALB/c T-cell proliferation rate was not significantly different from that of the unstimulated BALB/c splenocytes (data not shown). The stimulation of BALB/c splenocytes by coculturing with allogeneic, fresh B6 skin tissue or B6 splenocytes (mixed lymphocyte reaction), however, resulted in a robust BALB/c CD3+ T-cell proliferation (8.1 ± 1.33% for B6 skin coculture and 25.4 ± 1.94% for MLR, respectively. $P < 0.05$). Further analysis revealed that both CD4+ and CD8+ population of CD3+ cells showed increased proliferation in response to fresh B6 skin tissue or B6 splenocytes and not to ADMs (Fig. 2.5).

2.3.8 Biofunctionality of ADM transplantation

Macroscopically, 1 week after transplantation, ADM appeared to be engrafted in surrounding host tissue, and the migration of host cells into implanted ADM was detectable. Epithelialization was observed at the wound edges of the grafted ADM (Fig. 2.6B). Two weeks after implanting, vascularization was detectable in the margin of implants, as its colour changed to a pinkish skin colour (Fig. 2.6B). Three weeks after transplantation (Fig. 2.6C), histology results show complete recellularization and reepithelialisation. Newly formed vessels originating from wound bed penetrated upward through the ADM. The collagenous structure of the ADMs was preserved. At week 4, this reepithelialisation effectively protected the ADMs implant such that neither bacterial infection nor desiccation of the implanted ADMs was seen (Fig. 2.8- Sup. Fig. 2). There were no signs of rejection in all ADMs after transplantation at any time points tested.

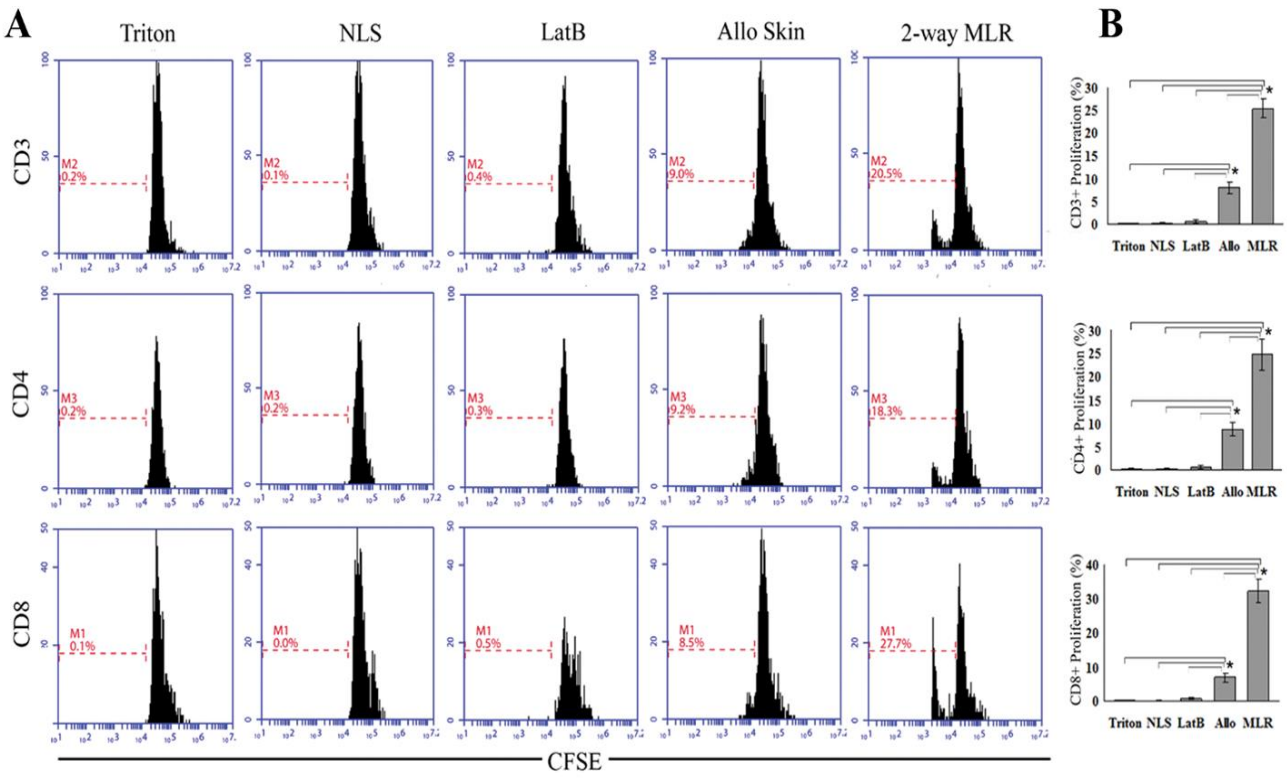

Figure 2.5. Recall antigenic T-cell (CD3, CD4 and CD8) proliferation assay by flowcytometry analysis using CFSE dye. (A) Co-culture experiments using CFSE-stained splenocytes with ADMs, allogenic B6 mouse skin and allogenic lymphocyte with a 1:1 ratio of stimulator (unstained B6 mouse splenocytes) to responder (stained Balb/C splenocytes). The percentage of proliferated CD3+, CD4+ and CD8+ cells were measured at day 3 (D3) culture and expressed as the proliferation index (i.e., the proportion of cells that have proliferated in response to the antigenic stimulus). (B) Summary of proliferation index for all samples. n = 5 samples in each group. Statistical significance indicated by asterisks, *$P < 0.05$.

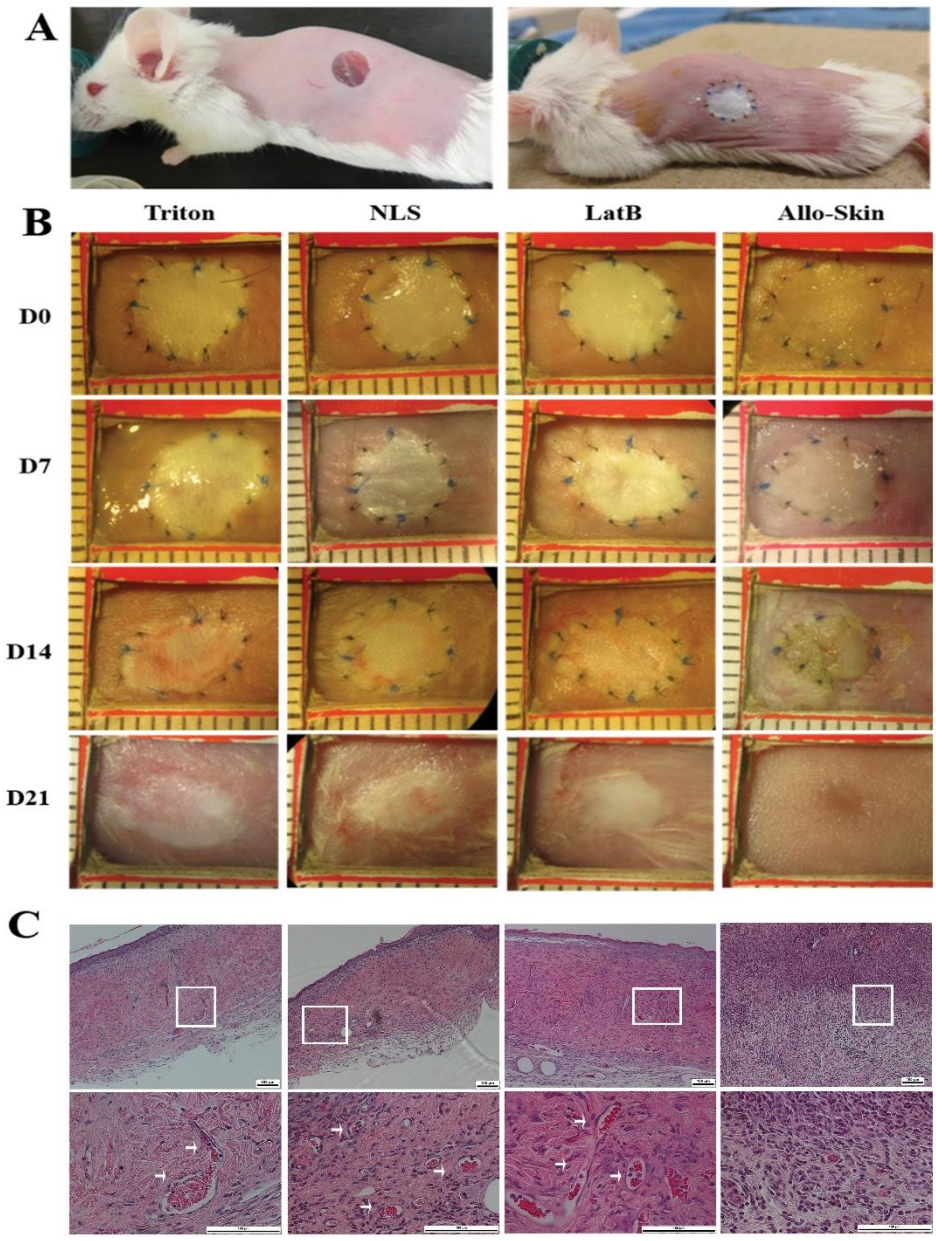

Figure 2.6. Assessment of biofunctionality of ADM in full-thickness skin wound transplantation. A) Full-thickness wounds, including the panniculus carnosus, were created on two different sites on the back of the recipient mice, and allogenic skin grafts (from B6 mice) and ADMs were engrafted on the wound bed and sutured. B) Gross images of engrafted ADMs at 1, 2 and 3 weeks after transplantation. In week 3, allogenic skin showed rejection of graft while ADMs are engrafted in host tissue without any sign of rejection. C) Three weeks after transplantation, histology results showed complete recellularization and reepithelialisation. Newly formed vessels were detectable (arrows) through the ADMs. Normal skin graft show high cellularity at the wound site (scale bars in top and lower rows = 100 µm).

2.4 Discussion

In this study, we have introduced a detergent-free method for preparing ADMs and compared it with two commonly used detergent-based decellularization methods of ADM preparation. This comparison was based on effectiveness of decellularization while maintaining the structure and functional composition of ECM components. Recalling that the advantage of an ADM over an engineered matrix in the preparation is the inclusion of cell-secreted molecules that are resident in normal skin, the best decellularization processes should thus prevent their damage and removal. Despite the variety of reported decellularization methods, there is a lack of evidence to support the use of one method over another in consideration of design characteristics. In our study, we sought to explore and evaluate the biofunctionality of three decellularization methods, in parallel, both in vitro and in vivo. In the interest of clinical applicability, we sought to further compare differently decellularized ADMs as skin substitutes in the treatment of full-thickness wounds.

The detergent-free method that we used, namely the LatB method, has been reported before for decellularization of skeletal muscle, and it is based on decellularization without using detergent and proteolytic enzymes [75]. However, in this study we used Dispase II, a neutral protease, to remove the epidermis and improve the efficiency of the decellularization process, as our preliminary results showed inefficient decellularization without using this enzyme. This method utilizes actin filament disruption by treatment with LatB, cell lysis by osmotic shock by exposure to high ionic strength salt solution, and benzonase treatment to remove residual DNA from skin.

Based on H&E and Mason trichrome staining, there was no detectable nucleus staining in ADMs prepared with the three methods, confirming complete decellularization, and the overall structure of the ECM was maintained when compared with the normal skin (Fig. 1). As evidenced

by Hydroxyproline assay, these methods did not remove collagen—the most abundant ECM structural component (Fig. 2.2A). Studies using Triton X-100 have shown mixed results from complete to inefficient cell removal and from safe to harsh on ECM molecules [80]. This discrepancy was mainly related to the tissue being decellularized and such details of protocol as Triton concentration, incubation time, agitation, and the other methods with which it was combined.

Our results showed that the decellularization method using NLS significantly removed sGAGs from the skin while Triton and LatB methods did not show any reduction when compared to normal skin (Fig. 2.2B). Previous studies have shown that most detergents cause at least some degree of removal of GAG from the scaffolds [81]. GAGs are negatively charged hydrophilic molecules, so they are capable of absorbing and retaining a large amount of water within the matrix. This feature affects the mechanical and viscoelastic behaviour of the tissue matrix [82]. Retention of sGAGs content in ADM thus has a significant impact on its function.

Biomechanical analysis of the ADMs confirmed the mechanical integrity of the ADM prepared with LatB method, since there was no difference between the normal skin and ADM, while detergent-based methods showed different stress-strain patterns and tensile modulus (Fig. 2.2C, D). Further, elastin staining showed that the LatB method has a similar staining pattern to normal skin compared with methods that use Triton or NLS (Fig. 2.2E). Elastin is a durable and insoluble protein with minimal turnover. It gives recoil and resistance to tissue such as blood vessel, lung, and skin and induces cell activities like cell migration and proliferation, matrix synthesis, and protease production [83–85]. The biomechanical properties of elastin allow skin to bear tensile stress, especially at the mobile parts of the body such as joints. Even though at the beginning of wound healing and upon injury, elastin fragments are generated and released into the

ECM to induce biological responses in cells as active ligands (elastokines) [86], later on the deposition of elastin in the dermis is aberrant and has only been detected a few months after the initial wound-healing stages [87]. Moreover, disrupted elastic fibres lead to the reduced elasticity of the mature scar. Also, the presence of elastin in a skin substitute has been shown to reduce wound contraction and improve dermal regeneration [88]. Regarding the mechanical and signalling properties of elastin during wound healing, it is obvious that the restoration of an intact elastic fibre is critical to regain functional skin after injury [83].

In this study, we provided a comparison of ADMs prepared in parallel with different methods of decellularization. Each method was associated with distinct changes to structure and composition of the resulting material. Although our assessment of post-transplanted scaffolds showed overall acceptable results for all ADMs and no-single method greatly outperformed the functionality of another, our findings indicated that a detergent-free LatB method was minimally disruptive to native ECM and was the only method that achieved effective decellularization of skin while preserving sGAGs and elastin content of the tissue as well as its biomechanical property, when compared to detergent methods.

A limitation of the present study is that a full-thickness skin wound model was created on the backs of the mice and that location is not the proper place to show the importance of having elastic skin substitute because it is not the best body site in terms of enduring tensile stress. It would be appropriate to create skin wounds in the areas like joints, which bear tensile stress. However, this is not feasible in a small rodent model. Although removal of all cell material without affecting ECM components may be fundamentally impossible, it seems apparent that methods that remove most of the cellular components are preferred. There is a variation in definition of decellularization across different studies. Some have reported a lack of positive staining for

cellular antigens such as MHC-1 and MHC-2 [89–91], and others consider the dsDNA content of decellularized tissue as compared with the native one, which they suggest should not exceed 200 base pairs in length and 50 ng per mg of dry weight of the material [92]. These criteria may depend more on tissue type and may not be proper for all decellularized bioscaffolds. Overall, our results emphasize the importance of the decellularization methods for producing ADMs and the design criteria forevaluating efficacy of these methods. We strongly recommend using controlled, parallel preparation and analysis of ADMs in vitro and in vivo to ascertain biofunctional outcomes.

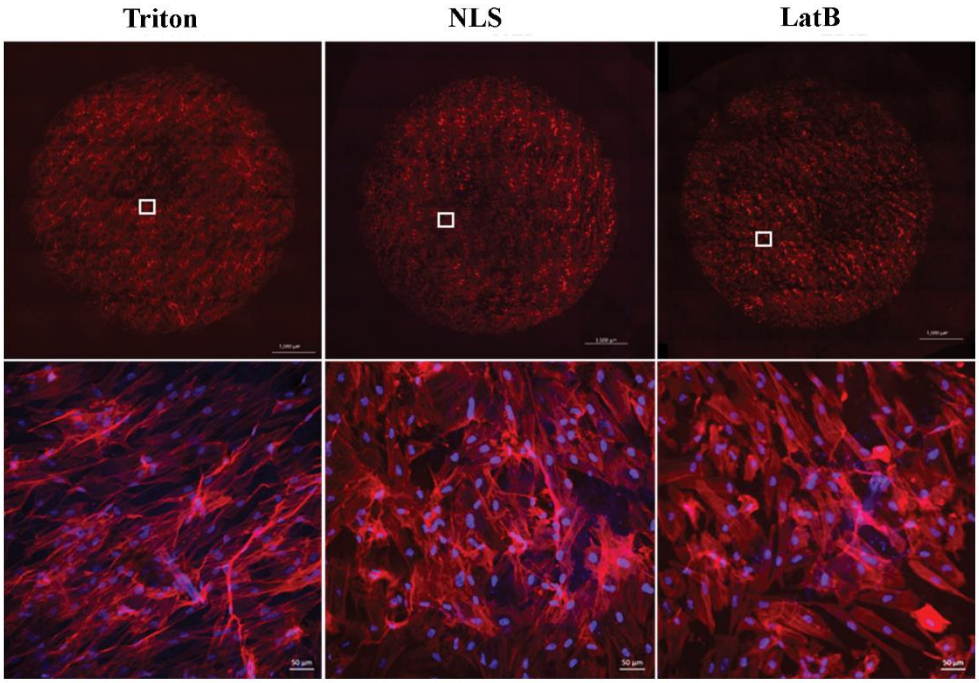

Figure 2.7. (Supplementary Figure 1). Day-1 cell attachment test. Confocal microscopy of passaged human dermal fibroblasts stained for phalloidin and counterstained with the nuclear stain DAPI, cultured on different acellular dermal matrix. Upper panel at low magnification (scale bar=1mm) and lower at high magnification (scale bar=50µm).

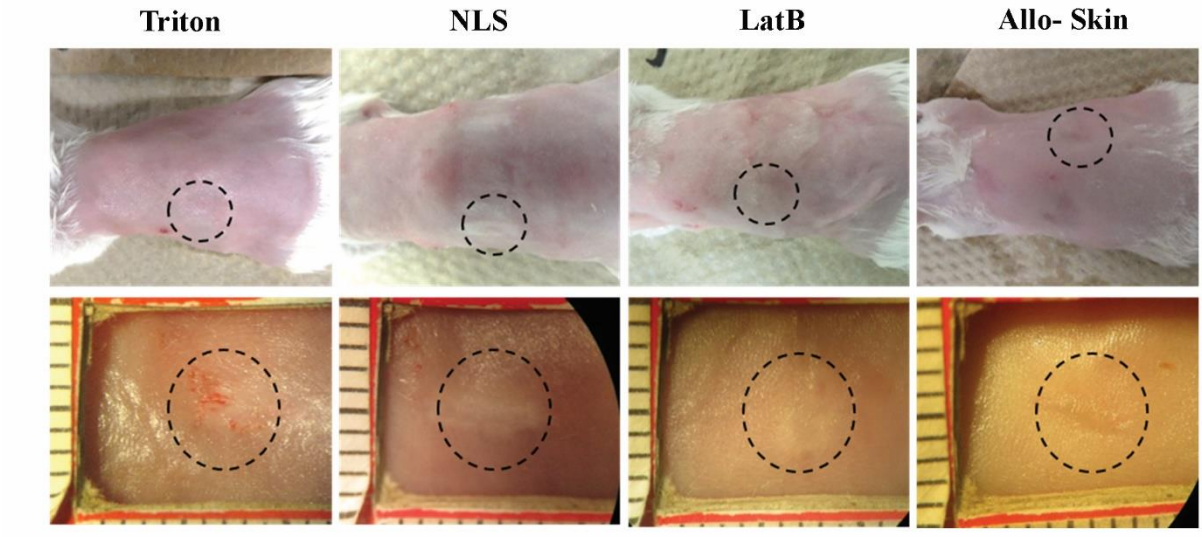

Figure 2.8. (Supplementary Figure 2). Four weeks after transplantation, all ADMs show complete integration of grafts and reepithelialisation effectively covered the ADMs transplants. Dotted line circles show original transplant sites

Chapter 3: Acellular Dermal Matrix Revitalized with Allogeneic Dermal Fibroblasts as a Biological Wound Coverage: Do We Need Fibroblasts? [1]

3.1 Introduction

The ideal treatment for wounds should stimulate regeneration with the complete restoration of original tissue, rather than repair that leads to scar formation and the absence of some cellular elements in the defected area. Although regeneration is an optimal outcome for wound healing, it is mainly found in embryonic development and not in adult tissue [2].

Currently, only autologous full-thickness skin grafts and free flaps can restore normal architecture and functions of skin. However, these methods are not applicable in large wounds and in areas with low vascularity. Also, it causes morbidity of donor sites. These limitations necessitate the production of skin substitutes [3]. One of the tissue-engineered products developed to substitute the defected skin is the acellular dermal matrix (ADM).

ADM has been used as a temporary or permanent wound covering for partial- and full-thickness wounds [5] [6] [7] [8]. ADM, ideally, is non-immunogenic and mechanically similar to skin. Because of the better preserved physiological structures of the dermis in ADM, it offers an ideal template for the growth of angiogenic cells and the promotion of vascularization [9] **.**

ADM acts as a scaffold as well as a source of growth and chemotactic factors, but to induce tissue regeneration, the presence of living cells capable of remodeling the extracellular matrix and restoring normal tissue function is necessary [29]. It has been shown that primary dermal fibroblasts synthesize essential extracellular matrix components and secrete key growth factors and cytokines that are important for wound healing [10] [44] [11]. Fibroblasts used in skin substitutes are allogeneic or autologous. Regardless of the source of fibroblasts used in skin

[1] A version of this chapter has been prepared for submission. *Ali Farrokhi,MSc, MohammadReza Rahavi,MSc, Mohammadreza Pakyari, MD, Victoria McCann, BSc, Reza Jalili, MD/PhD, Gregor Reid[2], PhD, and Aziz Ghahary, PhD* (Aug 2016).

substitutes, the improved outcome of grafting has been supported in several experimental and clinical studies in treatments of burn and chronic wounds [39] [40] [41] [43].

To have a ready-to-use skin substitute harbouring live fibroblasts, there are several advantages in using allogeneic fibroblasts over autologous ones, including reduced morbidity in patient donor sites and avoiding of a delay in treatment because of the time needed for autologous cell isolation and culture [38]. Also, the production of allogeneic cells is less expensive than the autologous cells [20]. However, the viability and immunogenicity of such cells after transplantation into an immunocompetent host have been controversial, and the usefulness of the seeded fibroblasts is still unclear, questioning whether we need to repopulate ADMs with allogeneic fibroblasts or we should use only autologous fibroblasts [51] [52] [93] [53] [54] [55].

In most experimental and clinical studies, the aspect of immunogenicity of these cells has not been studied in detail and a limitation in techniques to follow cells after transplantation may partly contribute to the conflicting reports of allogeneic fibroblasts' fate. To address these limitations, we used *in vivo* bioluminescent imaging (BLI) for assessing engraftment, survival, and migration of these cells following transplantation in an allogeneic host. Studies show that an immunologic response to an allogeneic skin graft requires T-cell activation and proliferation. Thus, to prevent acute rejection, suppression of infiltrated immune cells at early time points of engraftment is necessary [12]. Indoleamine 2,3-dioxygenase (IDO) is an enzyme that metabolizes the tryptophan in the environment. The deficiency of this essential amino acid and its toxic metabolites induce T-cell anergy and apoptosis [13] [59]. IDO-expressing cells exhibit strong immunosuppressive activity in vitro and in vivo [74] [94] [95].

As such, we hypothesized that the application of an IDO-expressing allogeneic dermal fibroblast populated within an ADM might be sufficient to create an immune-privileged area within the wound to protect fibroblasts from rejection and help the graft to restore its function by synthesizing extracellular matrix components and growth factors by these cells.

3.2 Materials and methods:

3.2.1 Ethics statement

All methods and procedures, as well as the use of animals and tissue specimens derived from animals, have been approved by Animal Ethics Committees of the University of British Columbia.

3.2.2 Mice

Male C57/B6 mice (Jackson Lab, USA) aged 3 to 4 months were used as skin donors and female Wild-type BALB/cJ, Rag-1-deficient BALB/cJ (RAG1−/−), interferon-γ (IFN-γ)–deficient BALB/cJ (IFN−/−), and common γ chain–deficient NOD-scid (NSG) mice were obtained from The Jackson Laboratory (Jackson Lab, USA) with those aged 2 to 3 months as recipients of ADMs grafts and fibroblast cell injection.

Mice were bred and maintained under specific pathogen-free conditions in accredited animal facilities at the University of British Columbia.

3.2.3 Decellularization methods

In this study, we used the detergent-free method based on our previous publication for decellularization of skin, which was utilizing Latrunculin B treatment followed by hyper- and hypotonic solutions incubation.

Briefly, after shaving the hair and application of hair removal cream followed by scrubbing with povidone-iodine solution (Triadine, H&P Industries Inc., Franklin, WI, USA), full-thickness skin was removed from the backs of donor C57/B6 mice. The panniculus carnosus and hypodermis tissues were removed manually by using a surgical blade and then washed three times with phosphate buffered saline (PBS).

After washing with PBS, the remaining part of the skin tissue was treated with 2u/ml Dispase II (gibco) in DMEM media for 1 hour in an incubator. After removing epidermis and washing three times with PBS, skin samples were incubated in 50 nM latrunculin B (Sigma-Aldrich) in high-glucose DMEM (DMEM; Gibco) for 2 hours at 37 °C to depolymerize actin filaments. Then samples were washed with distilled water twice for 15 minutes and subsequently were incubated in 0.6 mol/L potassium chloride (Sigma-Aldrich) for 90 minutes. Samples were washed with distilled water twice for 15 minutes and followed by 1.0 mol/L potassium iodide (Sigma-Aldrich) for 90 minutes. Following the high ionic solution incubations, skin samples were washed in distilled water overnight, and then the potassium chloride and potassium iodide incubations and overnight distilled water incubation were repeated. All steps were performed at room temperature with continuous shaking.

For eliminating residual RNA and DNA, ADMs were treated with 50u per ml Benzonase® Nuclease (Santa Cruz, sc-202391) for 12 hours and then washed with PBS for another 12 hours. All solutions used for ADM preparation were filter-sterilized and all

procedures were performed aseptically. Sodium azide (0.02% w/v) was present in all solutions except the last PBS washing step to prevent microbial growth.

3.2.4 Histological examinations

For histological evaluation of the harvested grafts, conventional H&E staining was done on 5 µm thickness paraffin sections.

3.2.5 Dermal fibroblast attachment and viability on ADMs scaffolds.

Cells were used in this study include mouse dermal fibroblasts and transgenic continuous IDO-expressing fibroblasts. Cells were seeded onto each of the ADMs in a density of 50x103 and were maintained in culture. Cell adherence and viability was assessed 24 hours after seeding the cells on ADM, using a Live/Dead toxicity assay (Molecular Probes®, Invitrogen, Carlsbad, CA) followed by visualization by confocal microscopy. To perform the assay, the scaffolds containing the cells were washed three times with 1× phosphate-buffered saline (PBS), pH 7.0, and incubated with a mixture of ethidium homodimer and calcein-AM according to the manufacturer's instructions. After 30 minutes the scaffolds were washed three times with 1× PBS and visualized using a Zeiss AxioObserver Z1 confocal microscope fitted with a CSU-X1 spinning disc (Yokogawa Electric) and AxioVision 4.8 (Zeiss)) and images were analyzed by Zen software.

In parallel to this, the amount of lactate dehydrogenase (LDH) in cell culture medium was used to monitor cell viability during three weeks of in vitro cell culture. This enzyme is a cytoplasmic enzyme released by dead cells, but not healthy cells. Twenty-four hours after seeding the cells and every two days after that, supernatant of cultured cells was collected and LDH amount measured by Pierce™ LDH Cytotoxicity Assay Kit (Cat:88953-Thermofisher),

according to the manufacturer's instructions. To determine the number of dead cells based on the OD value measured for LDH content and to determine the optimum number of cells to ensure LDH signal is within the linear range, we prepared a serial dilution of cells (0-20,000 cells/100µL media) in two sets of triplicate wells in a 96-well tissue culture plate and then lysed them by using a lysis buffer.

3.2.6 T Cell proliferation assays: Evaluation of suppression

The purpose of this assay is to determine whether allogeneic fibroblasts and IDO-expressing fibroblasts can suppress T-cell proliferation in a Jurkat cell line, an immortalized line of T lymphocyte, and in two-way mixed lymphocyte reaction (MLR). To perform this assay, 5×104 regular fibroblasts and IDO- expressing fibroblasts were cultured for three days on the hypodermal side of the ADM in 48-well plates in 10% FBS DMEM high-glucose media and then co-cultured with splenocytes of MLR or Jurkat cells for four days.

Splenocytes isolated from BALB/c mice spleens as previously described [65] stained with carboxy-fluorescein diacetate succinimidyl ester (CFSE) and used as a responder cells were mixed with splenocytes isolated from rat spleens, which were used as a stimulator. For co-culture with fibroblast, 1×105 responder and 5×104 stimulator cells were added to fibroblasts cultured on ADM and incubated at 37 °C in the presence of 5% CO2. The final co-culture volume per well was 400 µl, 200 µl of 10% FBS RPMI media for MLR cells and 200 µl fibroblast culture medium.

The following experimental groups were used as controls: (i) Balb/c splenocytes unstained for CFSE to check background fluorescence; (ii) CFSE-stained Balb/c splenocytes without mixing with rat splenocytes as a unstimulated negative control; (iii) two-way MLR

without co-culture with fibroblasts to ensure that Balb/c splenocytes were proliferating in response to rat antigens; and (iv) fibroblasts cultured in plate and not ADM co-cultured with two-way MLR to ensure that the effect of fibroblasts is not modified by culturing them on ADM.

Any adherent cells were detached by gently washing the tissue with medium. Cells were incubated with monoclonal antibodies for Anti-Mouse CD3 APC (ebioscience) or an equivalent isotype-matched negative control antibody. Samples were processed (minimum 30,000 live-events per sample) using a BD Acuri machine (BD Biosciences). Data was acquired and analyzed using BD Accuri 6 software (BD Biosciences). The gating strategy excluded debris to ensure positive gating of a lymphocyte population on the forward scatter-side scatter dot plot. Out of the live cells, CD3+ cells were shown in a dot plot against CFSE, and the percentage of proliferated cells was measured on a histogram, expressed here as the proliferation index (i.e., the proportion of cells that have proliferated in response to antigen).

For co-culturing fibroblasts with Jurkat cells, 1×105 CFSE-Stained jurkat cells were added to fibroblasts cultured on ADM and incubated at 37 °C in the presence of 5% CO2. After four days, the proliferative index of Jurkat cells was measured by doing flow cytometry based on CFSE staining.

3.2.7 Transplantation procedure

Transplantation of ADM and recellularized ADM was performed as described previously [96]. Briefly, after induction of anesthesia and removing hair from the back skin of recipient Balb/c mice, full-thickness excisional wounds, including the panniculus carnosus, were created in two different sites on the back of the recipient mice using a 6-mm-in-diameter punch device. In order to minimize the involvement of the contractile subcutaneous panniculus carnosus

muscle of murine skin in our wound-healing model and make it more similar to the one in humans, silicone splints with 14-mm outer and 10-mm inner diameters were placed around the perimeter of the wounds and were sutured in place to the skin. Four female BALB/c mice per each treatment group were used, and each mouse received either two ADMs, or two fibroblasts—recellularized ADMs or IDO-expressing fibroblast ADMs. Grafts (8-mm diameter) were sutured on the surrounding tissue of a 6-mm diameter wound bed (Fig. 3.3A). Immediately following surgery, OPSITE dressing (Smith & Nephew) was sprayed onto the graft site and covered by Vaseline-impregnated gauze. Tegaderm film was applied over the graft site and then secured by a 2-cm width Co-flex bandage.

3.2.8 *In vivo* depletion

To explore the role of each subset of immune cells in graft rejection, they were depleted by administering 200 μg of depleting antibody i.p. every three days beginning three days prior to cell transplantation as indicated: CD8 T cells with anti-CD8α (clone 2.43, BioXCell), CD4 T cells with anti-CD4 (clone GK1.5, BioXCell), gamma delta (γδ) T cells with anti- Vγ2 TCR (clone UC3-10A6, BioXCell), with the exception of NK-cell depletion, which were done using 200 μg of rabbit anti mouse-asialo GM1 (CL8955, Cedarlane), 24 hours before cell injection and 50 μg every three days after cell injection. Cellular depletions of CD8 T cells, CD4 T cells, and NK cells were confirmed by flow cytometry of PBMC every time before injecting new dose of antibodies (Fig. 3.7A).

3.2.9 Bioluminescence imaging (BLI)

To track the fibroblasts in vivo by BLI, a self-inactivating (SIN) lentiviral vector carrying a double fusion (DF) reporter gene of click beetle red (CBR) luciferase and enhanced green

fluorescent protein (eGFP) driven by a constitutive ubiquitin promoter (pUB) (Fig. 3.4A.a), was transduced into fibroblasts (C57/B6 mouse strain), when cells were in passage 5 as described previously [20]. After transduction, fibroblasts robustly expressed eGFP (Fig. 3.4A.b-e).

Transduced fibroblasts were transplanted by intradermal injection into the lateral side of dorsal skin of recipient mice, 1×105 per spot (Fig. 3.4B), and the first BLI was performed 6 hours after transplantation, followed by next-day imaging. After day 1, BLI was performed every other day. The BLI protocol involved intraperitoneal administration of the d-Luciferin reporter probe with 3mg of luciferin in 200 µL of PBS, followed by mild anesthesia using isofluoren, and imaged 10 minutes later using the Spectral Instrument In Vivo Imaging System. Experiments contained 3 to 5 animals per group.

3.2.10 Isolation of infiltrating immune cells to the site of cell injection in skin.

Mice were euthanized and 12 mm in diameter circle from skin at the site of cell injection were harvested and then minced using blade. To get single cell isolation, tissue samples were digested by Liberase ™ enzyme blend (Sigma-Aldrich) at 37°C for 45 minutes in Hank's Balanced Salt Solution and 250 rpm shaking. Digestion was stopped by adding RPMI media supplemented with 10% FBS and passed through 40µ pore size cell strainer and washed with same media.

3.2.11 Flow cytometry

The following fluorochrome-tagged antibodies were purchased from BD Pharmingen,: lymphocyte panel: APC-Cy(tm)7 -CD3, PE-Cy(tm)7- CD19, BV605- CD45, V500- CD4, V450- CD8a, PE- CD69, PE-CF594- CD49b, BV650- CD335 (NKp46), 7AAD as a dead cell exclusion dye, and myeloid panel: FITC-Gr-1, PE-Cy™7- CD11b, PerCP-Cy™5.5- Ly-6C,

APC-Cy™7- Ly-6G, BV711- F4/80, and DAPI as a dead cell exclusion dye. Flowcytometry was performed on an LSR Fortessa flow cytometer (BD Biosciences), and data were analyzed using FlowJo software (Tree Star Inc.).

3.3 Results:

3.3.1 Cytocompatibility of ADM

To investigate the attachment and viability of cells after seeding them on ADM, fibroblasts were cultured for 24 hours on ADM surfaces and a Live/Dead assay was performed. The viable and dead cells were shown as green and red, respectively (Fig. 3.1A). Fibroblasts adhered to ADM upon seeding and stay viable within the first 24 hours. LDH assay on collected supernatant of in vitro cultured fibroblasts on ADM for three weeks revealed minimal cell death in the period of cell culture indicating supportive effect of ADM on fibroblasts growth (Fig. 3.1B).

3.3.2 Proliferation of T cells cocultured with recellularized ADM with IDO-expressing fibroblasts was suppressed *in vitro.*

To evaluate the T-cell suppressive property of IDO- expressing fibroblasts repopulated within ADM, these cells and control fibroblasts on ADM were cocultured with two-way mixed lymphocyte reaction (MLR) and Jurkat cell line in different experimental sets. In the MLR reaction, CFSE stained splenocytes used as responder cells were mixed with rat splenocytes, which were used as stimulators.

The result of two- way MLR reaction in the presence of fibroblast-ADM, 41.4 ±5.04% of CD3+ cells were in proliferative stage. However, in the presence of IDO-Fibroblast-ADM, there was significantly reduced number of proliferating cells (3.31 ± 2.4% (p<0.05). On the other hand, as a result of T-cell suppression by IDO expression, more T cells underwent anergy

as evidenced by 45.07±4.52 % dead cells in CD3+ T-cell population in IDO-Fibroblast-ADM coculture group in compare to 7.12±0.98% in fibroblast-ADM group (Fig. 3.2A).

The suppression property of IDO-Fibroblast-ADM was confirmed in coculture of these cells with Jurkat cell line (Fig. 3.2B).

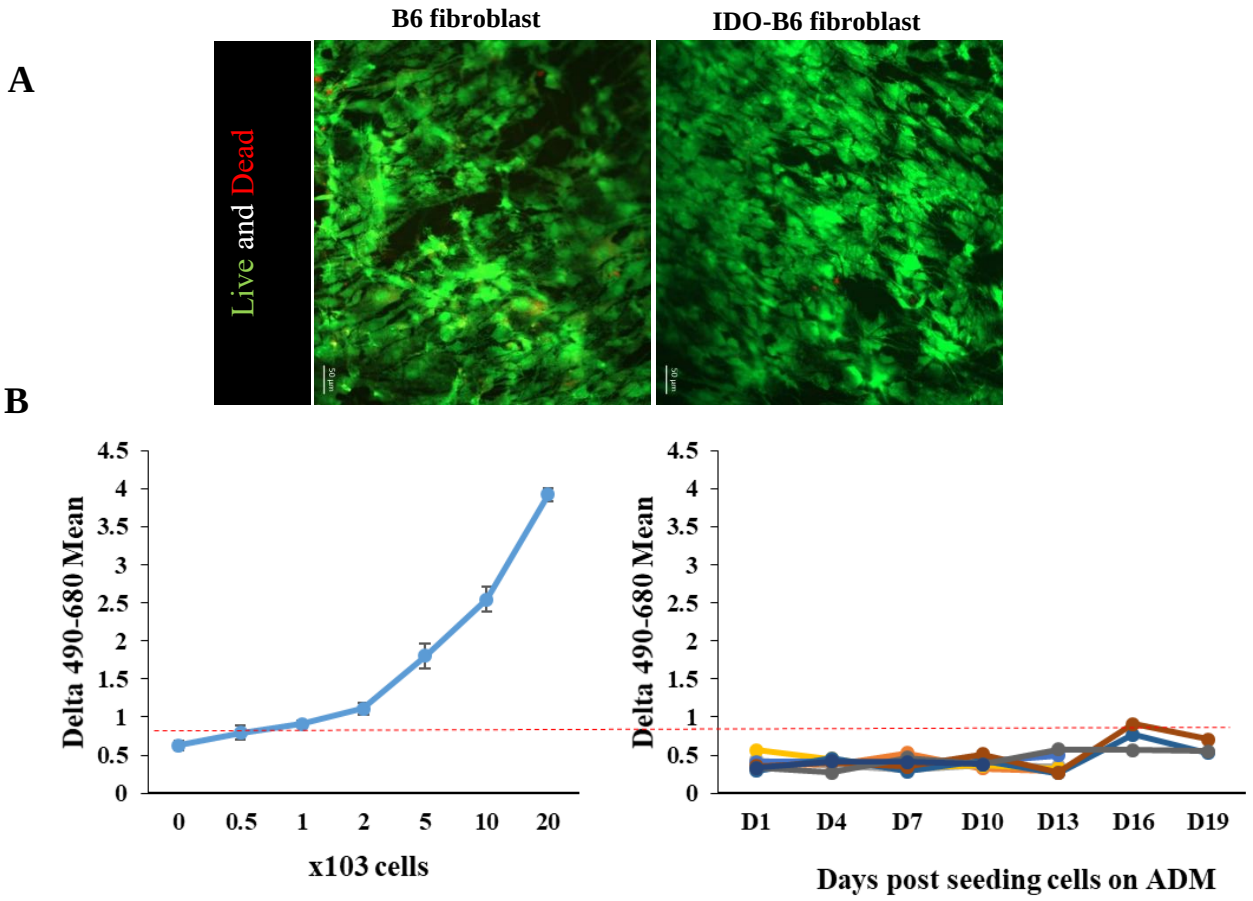

Figure 3.1. Cytocompatibility of ADMs. **A)** fibroblast and IDO- expressing fibroblasts were seeded on the ADM for one day and stained with calcein and ethidium homodimer. Live cells appear green and dead cells appear red (Scale bars = 100 µm). **B)** fibroblasts cultured on ADM for thee weeks and every three days culture media collected and analyzed by LDH assay to monitor dead cells quantity. Left panel shows a manually lysed serial dilution of cells as a control and right panned shows the collected media from fibroblast and IDO- expressing fibroblasts cultured on ADM.

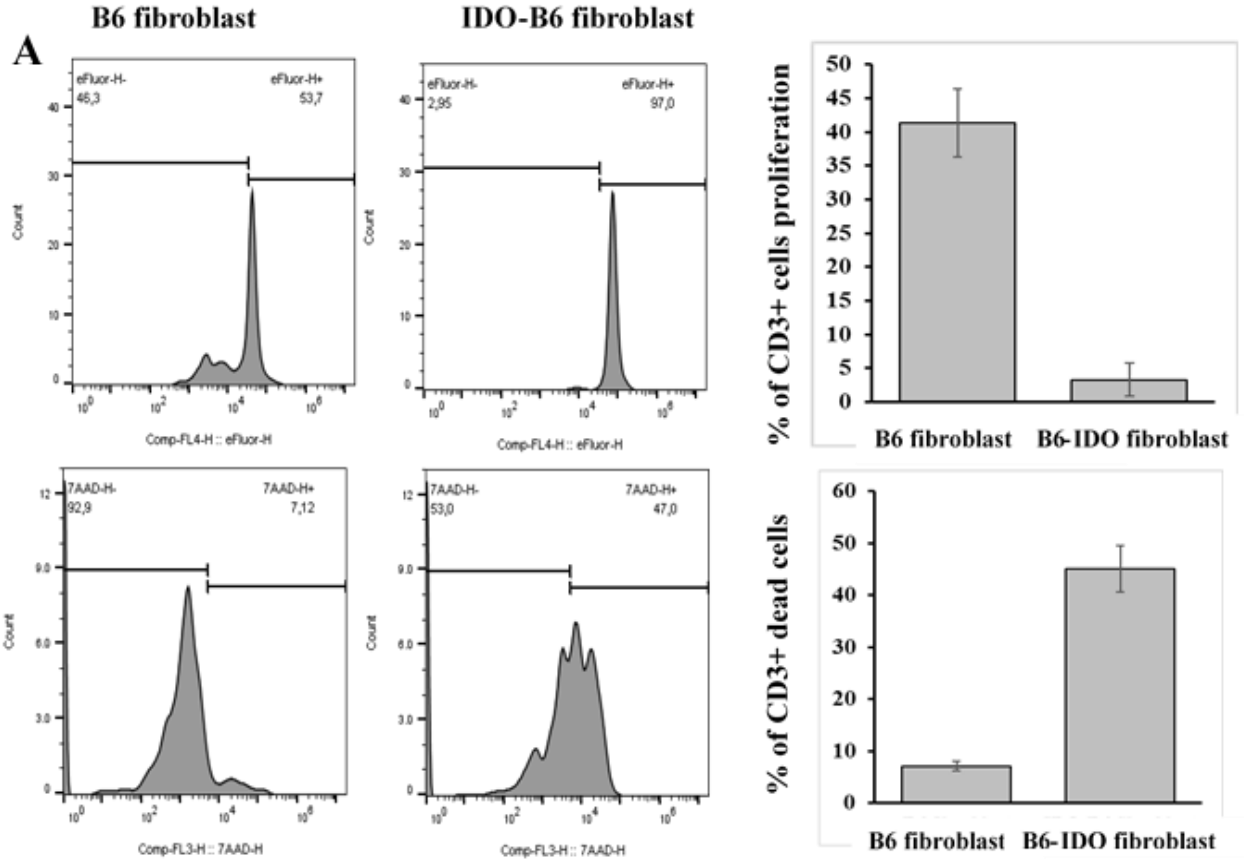

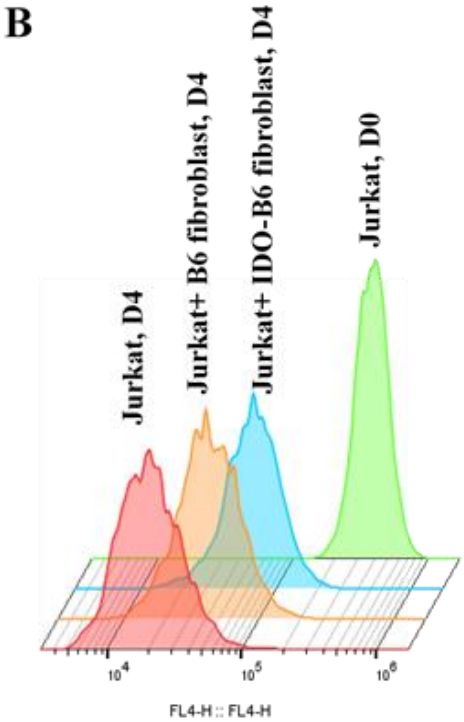

Figure 3.2. Evaluation of suppressive activity of IDO on T-Cell Proliferation. Co-culture of recellularized ADM (dermal fibroblast from C57/B6 mouse or IDO-expressing fibroblasts) with 2-way MLR (A) and Jurkat T-cell line (B). **A)** Top row shows suppressive effect of IDO on CD3+ cells and Second row represent anergy induction in CD3+ T cells. **B)** IDO-expressing fibroblasts can suppress cell proliferation in a Jurkat cell line.

3.3.3 Allogeneic dermal substitute did not promote the wound healing.

Three weeks after transplantation (Fig. 3.3A), gross images of grafted recellularized ADM showed engraftment in surrounding host tissue, and histology results confirmed complete reepithelialisation and the presence of cells inside the grafts. In terms of time required for healing and the quality of the healed wound, there was no difference between experimental groups. Investigating the type of infiltrated cells with various florescent labeling techniques (data not shown) and flowcytometry against H2kb-MHCI antigen (Fig. 3.3B) showed absence of transplanted allogeneic fibroblasts within engrafted ADM. Evaluating the fate of cells a week after transplantation, showed that small number of IDO-Fibroblasts could survive within grafted tissue but it was not consistent through multiple repeats of experiments.

Immune florescent staining of graft for immune cell infiltration at week three after transplantation revealed the presence of pan-leukocyte marker, CD45+ cells (Fig. 3.3C).

The absence of transplanted cells led us to investigate the following hypotheses: (i) Cells are dying because of lack of oxygen and nutrients due to delay in vascularization of grafted ADM; (ii) Cells are dying because of cell senescence and short life-span after transplantation; (iii) Cells are migrating from ADM graft to other parts; and (iv) Cells are immune rejected.

To address these hypotheses, we performed a series of experiments by making dual reporter Luciferase-EGFP fibroblasts and IDO-expressing fibroblasts (Fig. 3.4A.a-e.). Then cells were intra-hypo-dermally injected (Fig. 3.4B) in various strains of immune deficient and antigen depleted mice and followed by in vivo BLI in different time points post-transplantation.

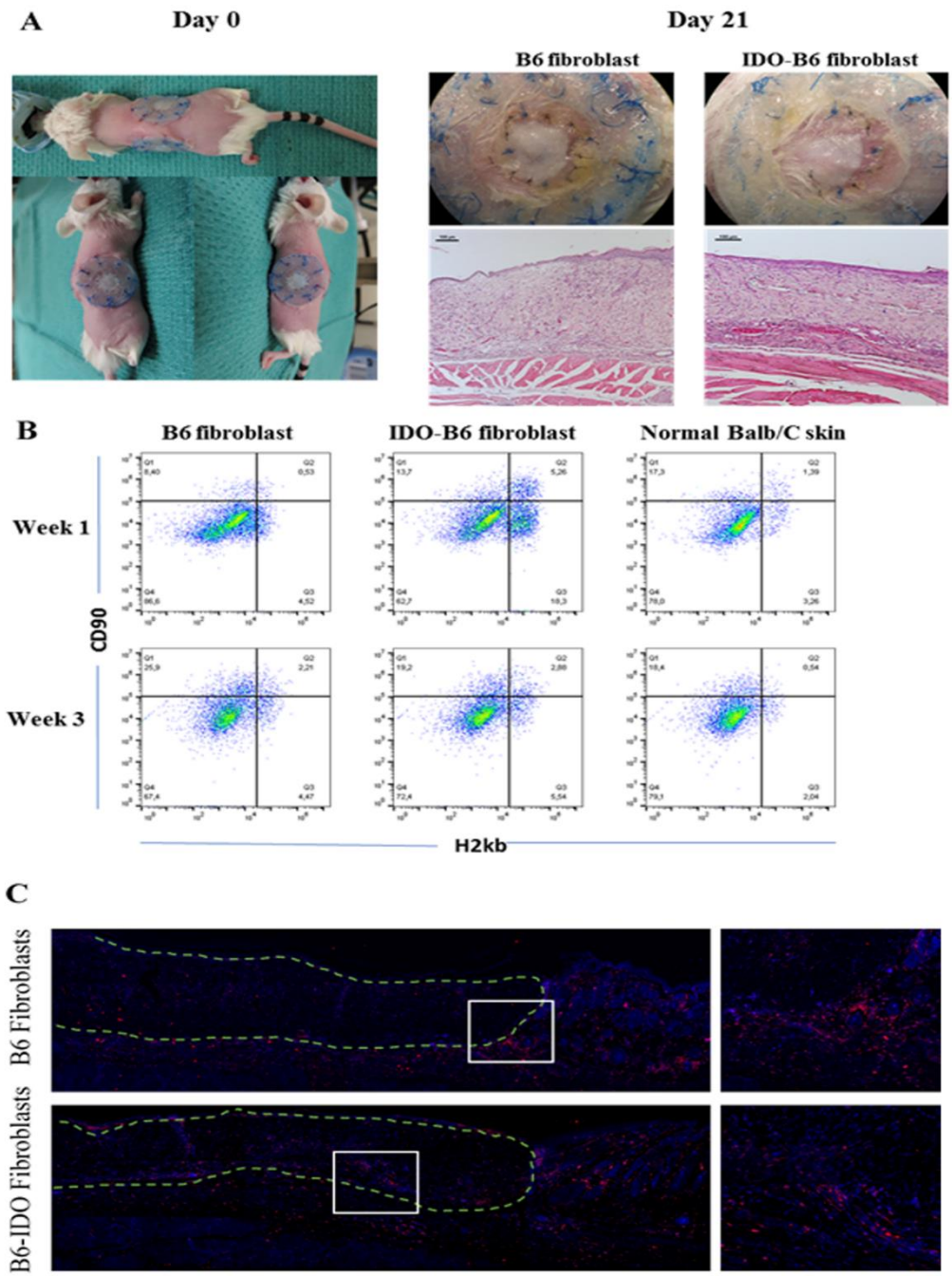

Figure 3.3. Evaluating the outcome of recellularized ADM transplantation on wound healing. **A)** gross images of the wound showed engraftment of ADM in surrounding host tissue, and histology results confirmed complete reepithelialisation and the presence of cells inside the grafts. **B)** flowcytometry of infiltrated cells to graft region against H2kb-MHCI antigen showed absence of transplanted allogeneic fibroblasts within engrafted ADM three weeks after transplantation. **C)** At week three, Immune florescent staining of the graft revealed the presence of pan-leukocyte marker, CD45+ immune cells.

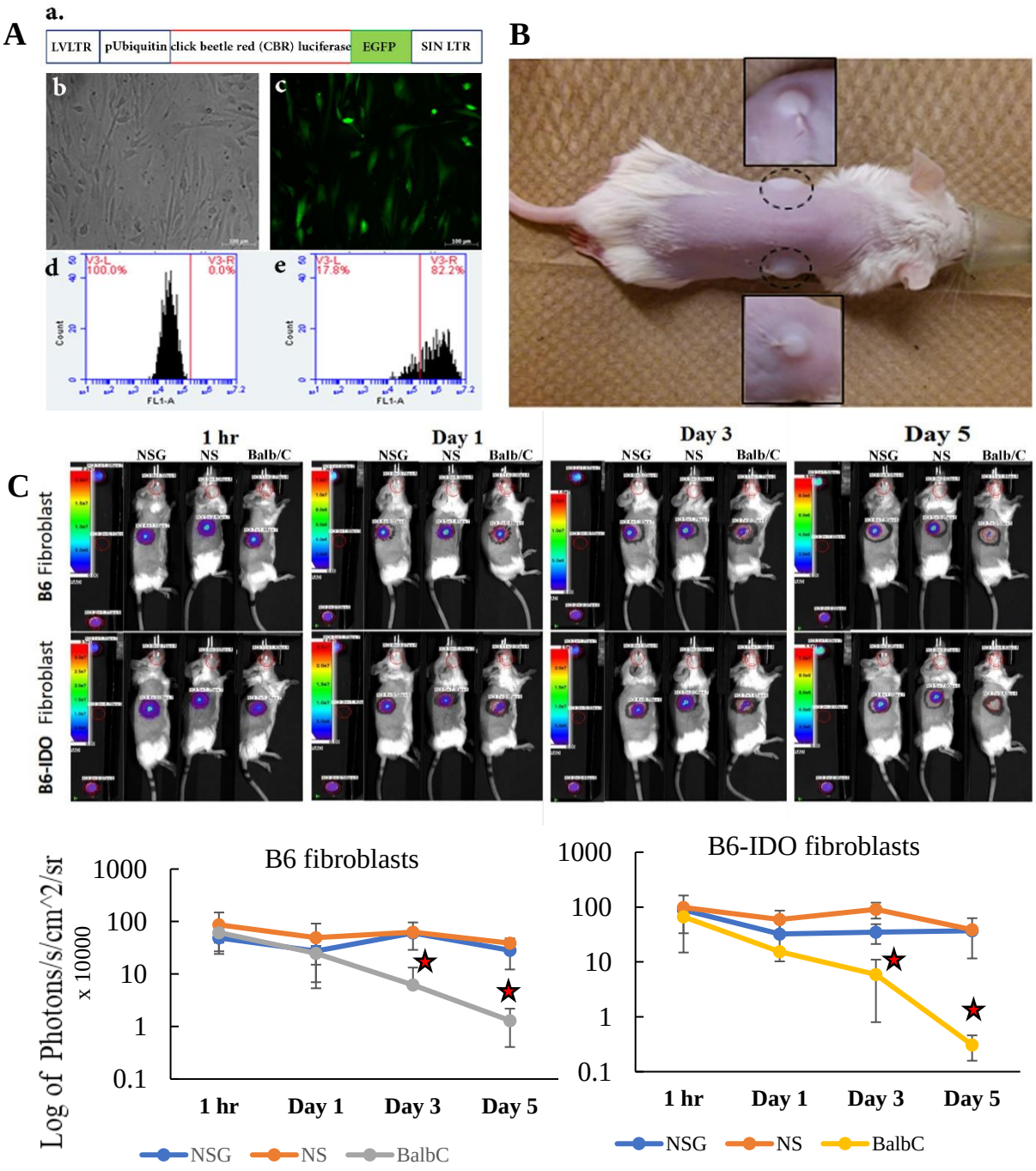

Figure 3.4. Tracking transplanted cells by *in vivo* BLI. A) dual reporter Luciferase-EGFP vector were used to transduce fibroblasts and IDO-expressing fibroblasts. B) Then cells were intra-hypo-dermally injected in to mouse skin. C) Cells were injected in to Balbc as an allogeneic and into NSG and NS as immune deficient mice, then followed by BLI at different time point. After 3 days significant reduction of luciferin signal was detected in wt-BalbC mouse but not in NSG and NS mice, $p<0.05$, and by Day 5 both cell types were rejected in wt-BalbC mice.

3.3.4 Transplanted allogeneic fibroblasts were rejected due to immunologic response.

To investigate the possible reasons for not being able to detect the transplanted cells within grafts, luciferase positive normal and IDO-expressing fibroblasts were injected intra-hypo-dermally into wild type Balbc as an allogeneic recipient and into immune deficient mice of NSG and NS, then followed by BLI. Intra-hypo-dermal injection of cells eliminates the role of delay in angiogenesis and lack of oxygen and nutrition to cells because dermis is well vascularized tissue and BLI enabled us to follow the cell fate and migration to other part of the body. Results showed that within three to five days after transplantation, cells were detectable in immune deficient NSG and NS mice but not in Balbc mice, which was an indication of immune rejection (Fig. 3.4C).

3.3.5 Natural killer T cells and g/d T cells were not involved in immune rejection of fibroblasts.

To address the question of whether the rapid rejection of transplanted fibroblasts observed in allogeneic mice is caused by innate immune cells with the capability of lysing cells, we examined the possible role of natural killer T cells and γδ T cells.

To determine if NKT cells were responsible for allogeneic reaction, we performed transplantation utilizing Ja18 knockout (Ja18-/-) and CD1d knockout (CD1d-/-) mice. Gamma/delta T cells involvement in this allogeneic reaction was investigated by transplanting cells in g/d T cell depleted mice. In all three mice models, cells were rejected in similar time to wt-Balbc recipients with no delay in rejection (Fig. 3.5).

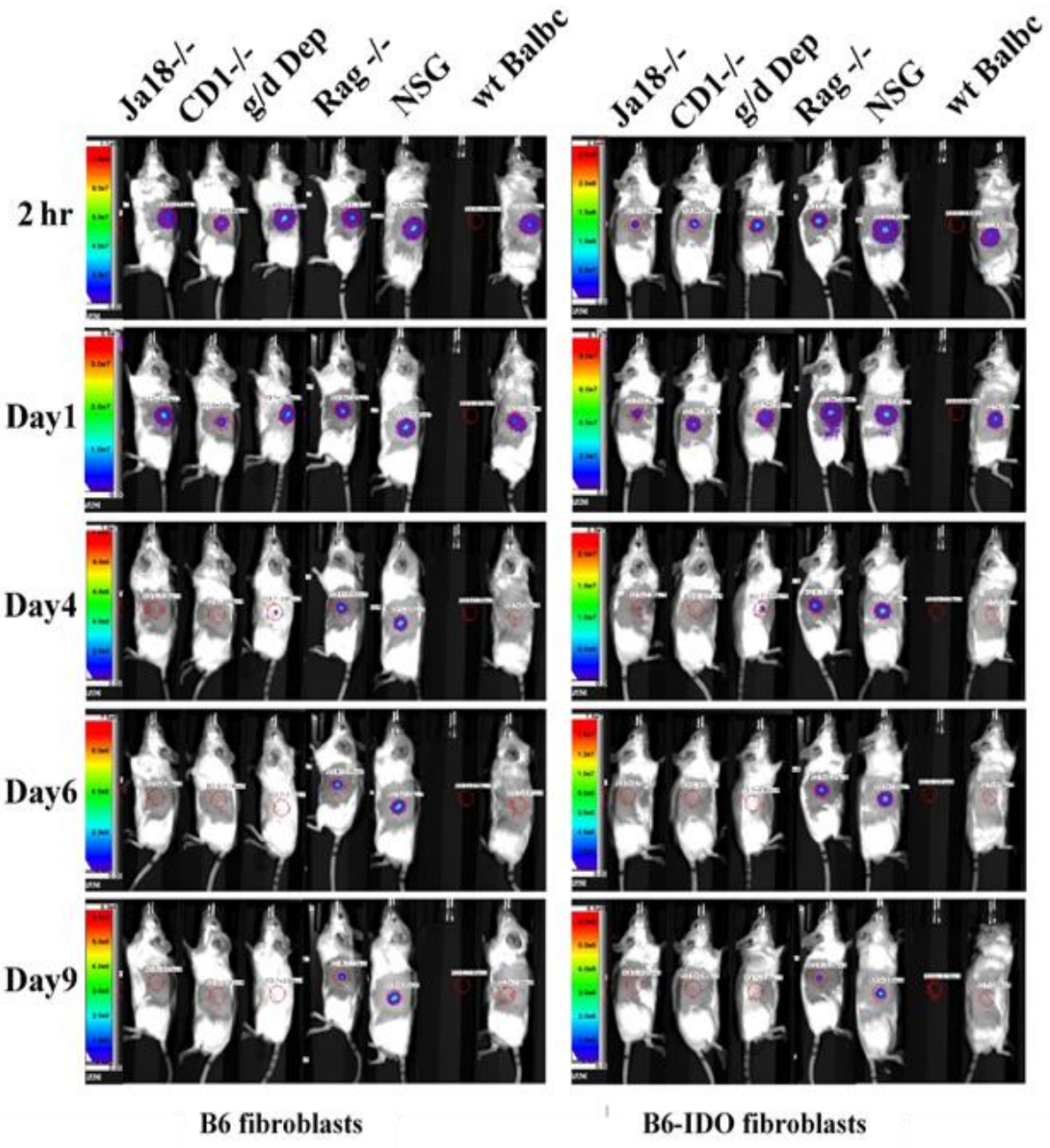

Figure 3.5. In vivo bioluminescent imaging (BLI) of transplanted fibroblasts in NKT and γδ T cell deficient mice. Representative BLI images of mice following intra-hypo-dermal transplantation of fibroblasts show a decrease in BLI signal in allogeneic (Balb/c), NKT cell deficient (Ja18-/- and CD1d-/-) and γδ T cell depleted mice, as opposed to immune deficient (NSG and Rag-/-) mice, reaching to background levels between post-transplant Days 4 and 6. Color scale bar values are in photons/sec/cm 2/steridian (p/s/cm 2 /sr).

3.3.6 Depletion of natural killer (NK) cells delayed immune rejection of fibroblasts.

To evaluate the role of NK cells in mediating fibroblasts rejection, we depleted NK cells from wt-Balbc mice by injecting anti-asialo-GM1 (ASGM-1) and cells were transplanted hypodermally. Delayed rejection of cells in the ASGM-1 treatment group was observed compared to the control group, indicating that removing NK cells increases fibroblasts' survival in wt-Balbc mice but it cannot prevent rejection (Fig. 3.6 A,B). *In vitro* co- culture of NK cell line with fibroblasts and IDO-expressing fibroblasts showed cytotoxicity of NK cells within 14-24 hrs, $p<0.05$ (Fig. 3.6 C). These results suggest that NK cells are capable of targeting fibroblasts, but they are not major cell types that target the fibroblasts *in vivo*. NK depletion of the Rag-/- mice did not alter the survival of transplanted cells. This finding confirms that NK-mediated response is not the major contributor in the allogeneic rejection of fibroblasts.

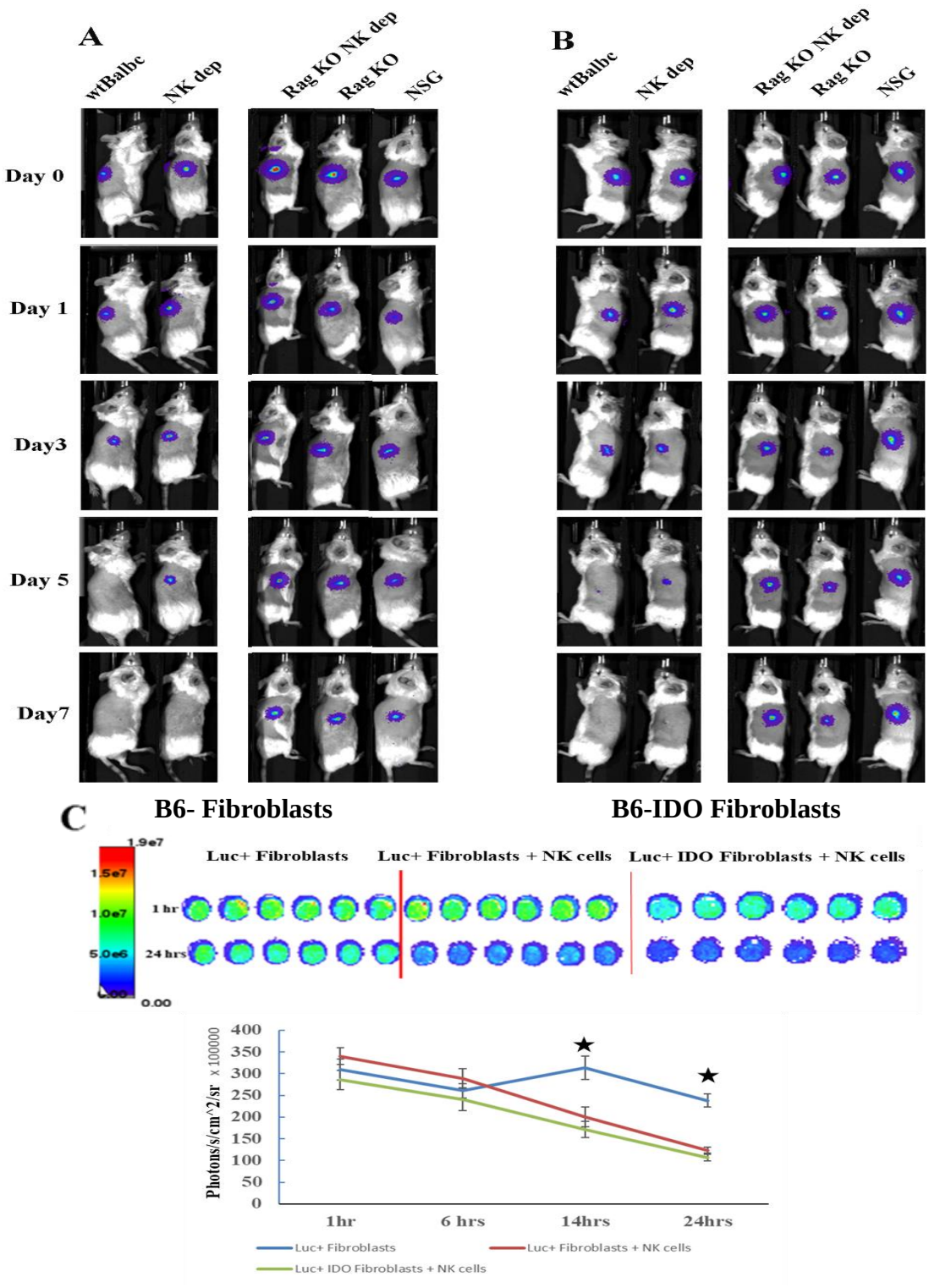

Figure 3.6. A,B) Depletion of Natural Killer Cells delayed immune rejection of fibroblasts but could not prevent rejection. Depletion of NK cells in Rag-/- mice did not change the pattern of cell rejection/survival. C) *In vitro* co- culture of natural killer cell line with fibroblasts and IDO-expressing fibroblasts showed cytotoxicity of NK cells within 14-24 hrs, $p<0.05$.

3.3.7 Simultaneous depletion but no single depletion of CD4+ and CD8+ cells could prevent rejection of fibroblasts.

In an attempt to assess T cell roles in rejection of fibroblasts, we tested the depletion of T cells using mAb towards the CD4 and CD8 cell surface molecules in cell transplanted mice. BALB/c mice were injected with anti-CD4, anti-CD8, or a combination of both starting three days before cell transplantation and followed by injection every three days. The depletion efficiency of each, or combination of antibodies were monitored by flow cytometry on 50 µl of peripheral blood samples every three days before injecting a new dose of antibodies (Fig. 3.7A).

The results showed that when mice were injected with a combination of anti-CD4 and anti-CD8, rejection of cells was prevented (Fig. 3.7B) but single depletion of CD4+ and CD8+ cells was not effective. However, single depletion of CD4+ cells showed a delay in rejection (Fig. 3.7C)

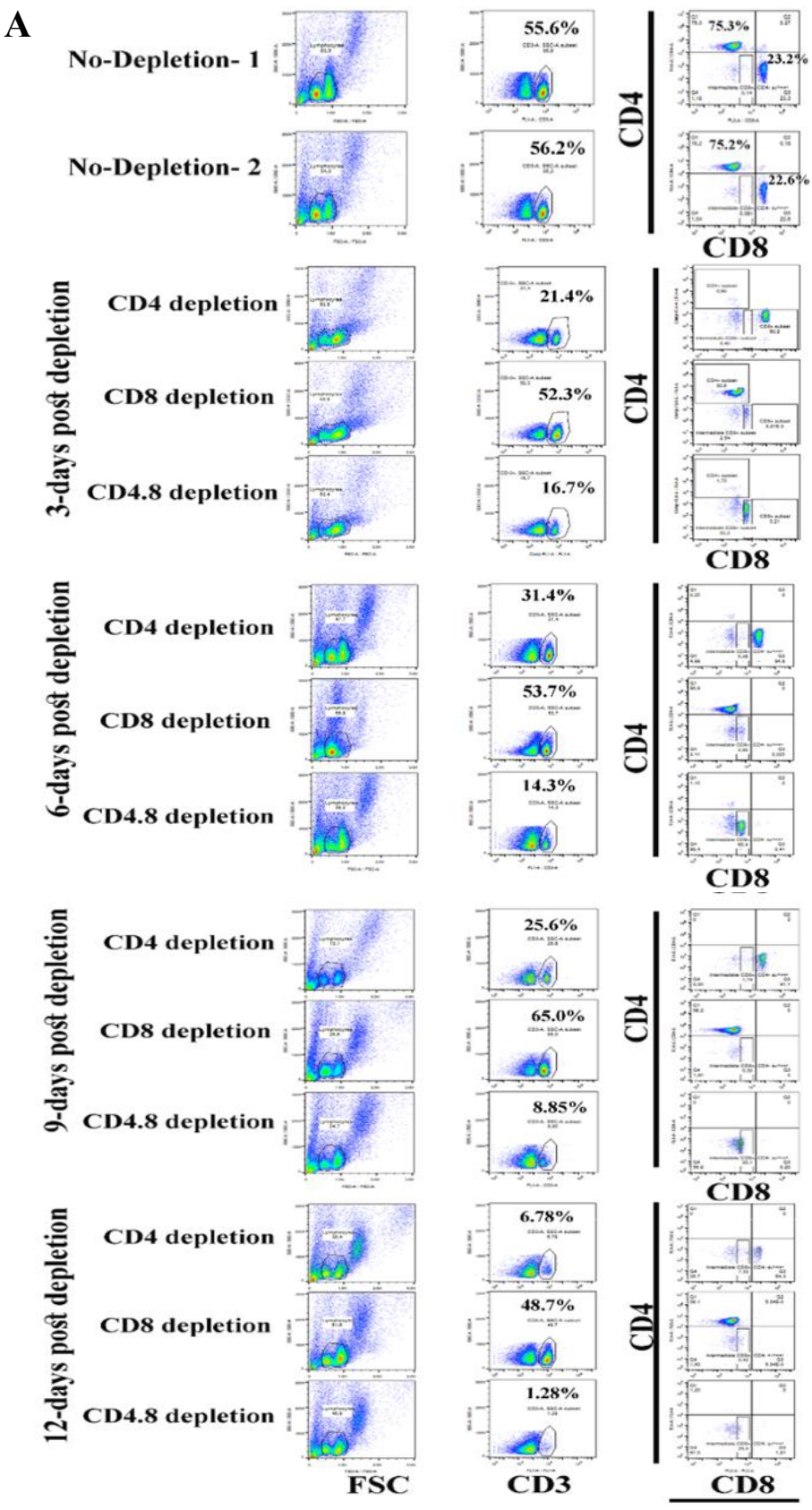
A
No-Depletion- 1
No-Depletion- 2
3-days post depletion
6-days post depletion
9-days post depletion
12-days post depletion
CD4 depletion
CD8 depletion
CD4.8 depletion
55.6%
56.2%
21.4%
52.3%
16.7%
31.4%
53.7%
14.3%
25.6%
65.0%
8.85%
6.78%
48.7%
1.28%
75.3%
23.2%
75.2%
22.6%
CD4
CD8
FSC
CD3

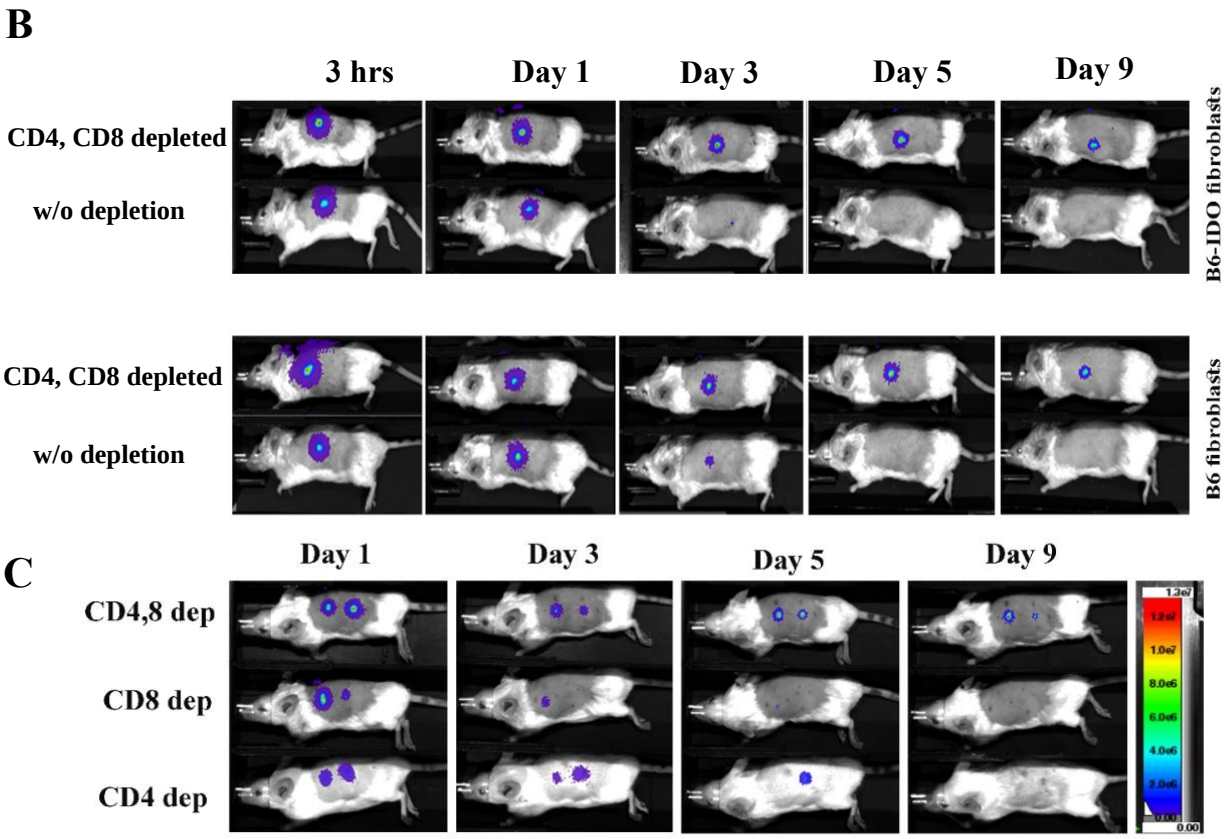

Figure 3.7. Double depletion of CD4+ and CD8+ cells prevent immune rejection of fibroblasts. A) evaluation of CD3+, CD4+ and CD8+ cells presence in peripheral blood after single and double depletion of CD4+ and CD8+ cells. B) In CD4+ and CD8+ double depleted mice, BLI shows a pattern of transplanted fibroblasts survival, however there is a decease amount of signal by day 9. C) CD4+ cells depletion delay rejection but cannot prevent it.

3.3.8 Skin samples from cell injected spots in compare to PBS injected skin harbor a greater number of myeloid cell but not cytotoxic CD8+ cells.

To test which type of immune cells are infiltrating to the site of cell injection at the time of rejection, we isolated cells from harvested tissues and analyzed them by flowcytometry in two set of panels; one for lymphocytes and the other for myeloid derived immune cells. For lymphocyte panel, first we gated single viable CD45+ cell (7AAD-) then we considered CD19-CD3+ CD4+CD69+ cells as activated CD4+ cells, CD19-CD3+ CD8+CD69+ cells as activated CD8+ cells and CD3- CD49b+ CD335+ cells as NK cells (Fig. 3.9).

For myeloid panel, first we gated single viable CD45+ cell (DAPI-) then we considered CD11b+Gr-1+ cells as monocytes, CD11b+F4/80+ cells as macrophages, Gr-1+ Ly6G+ as neutrophils and Gr-1+ Ly6c+ as other type of monocytes.

We found that a large number of host myeloid cells infiltrated allogeneic cell transplanted spots, mainly macrophages and neutrophils (Fig. 3.8B,C). Interestingly, there was not notable amount of activated CD8+ cells. However, activated CD4+ T cells were detectable (Fig. 3.9B).

Infiltration of NK cells (CD3-CD49b+CD335+) in allogeneic cell injected samples was higher than PBS injected samples (Fig. 3.9B).

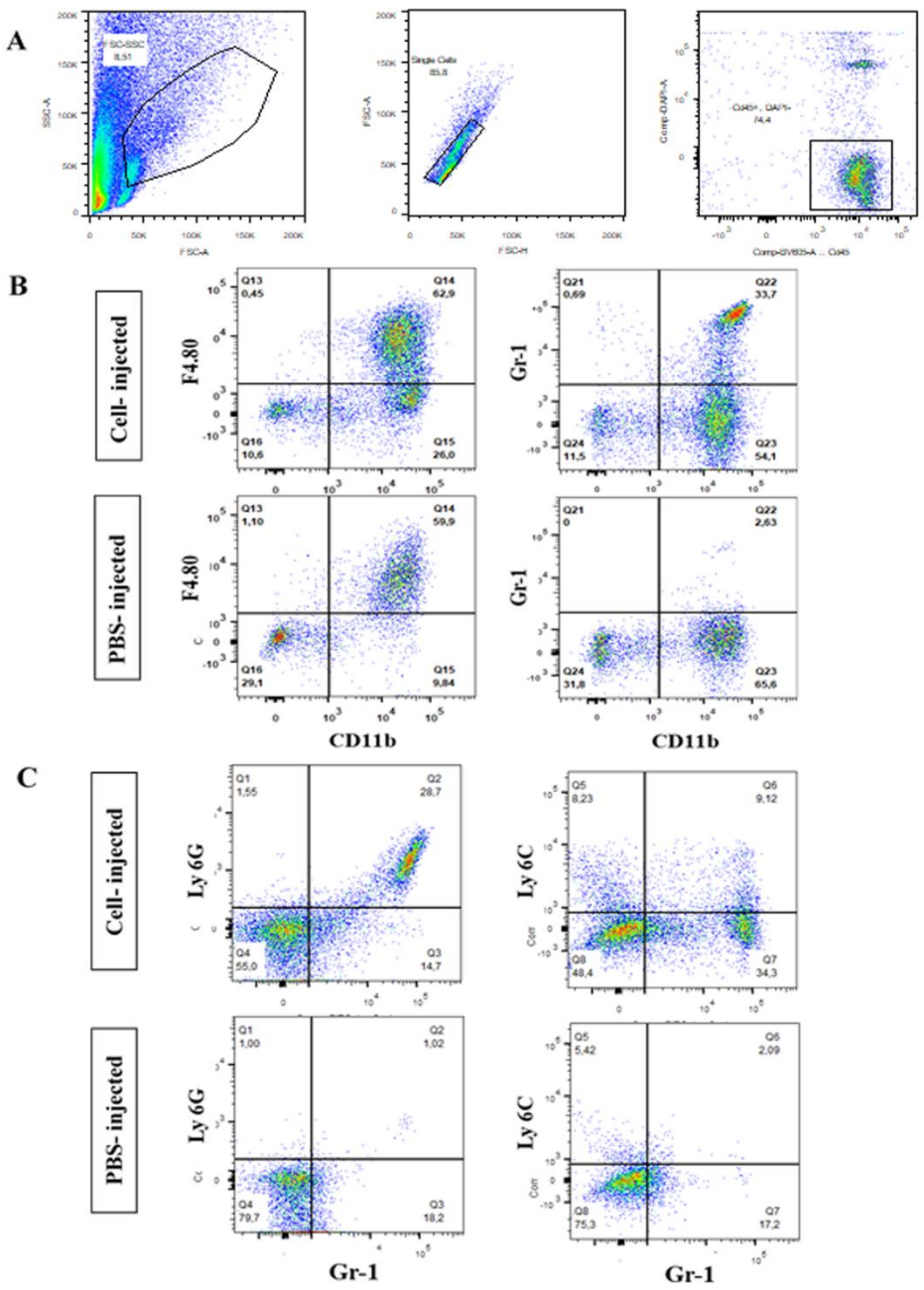

Figure 3.8. Analysis of myeloid cell infiltration after fibroblast transplantation in skin of immunocompetent recipients. Panel A represents gating strategy based on CD45+ live cells. Panel B compares macrophage (CD11b+ F4/80+) and monocyte (CD11b+ Gr-1+) population of infiltrating immune cells in cell vs PBS injected skin. Panel C shows in cell injected skin, majority of infiltrating monocytes are neutrophils while there is no neutrophil detectable in PBS injected samples.

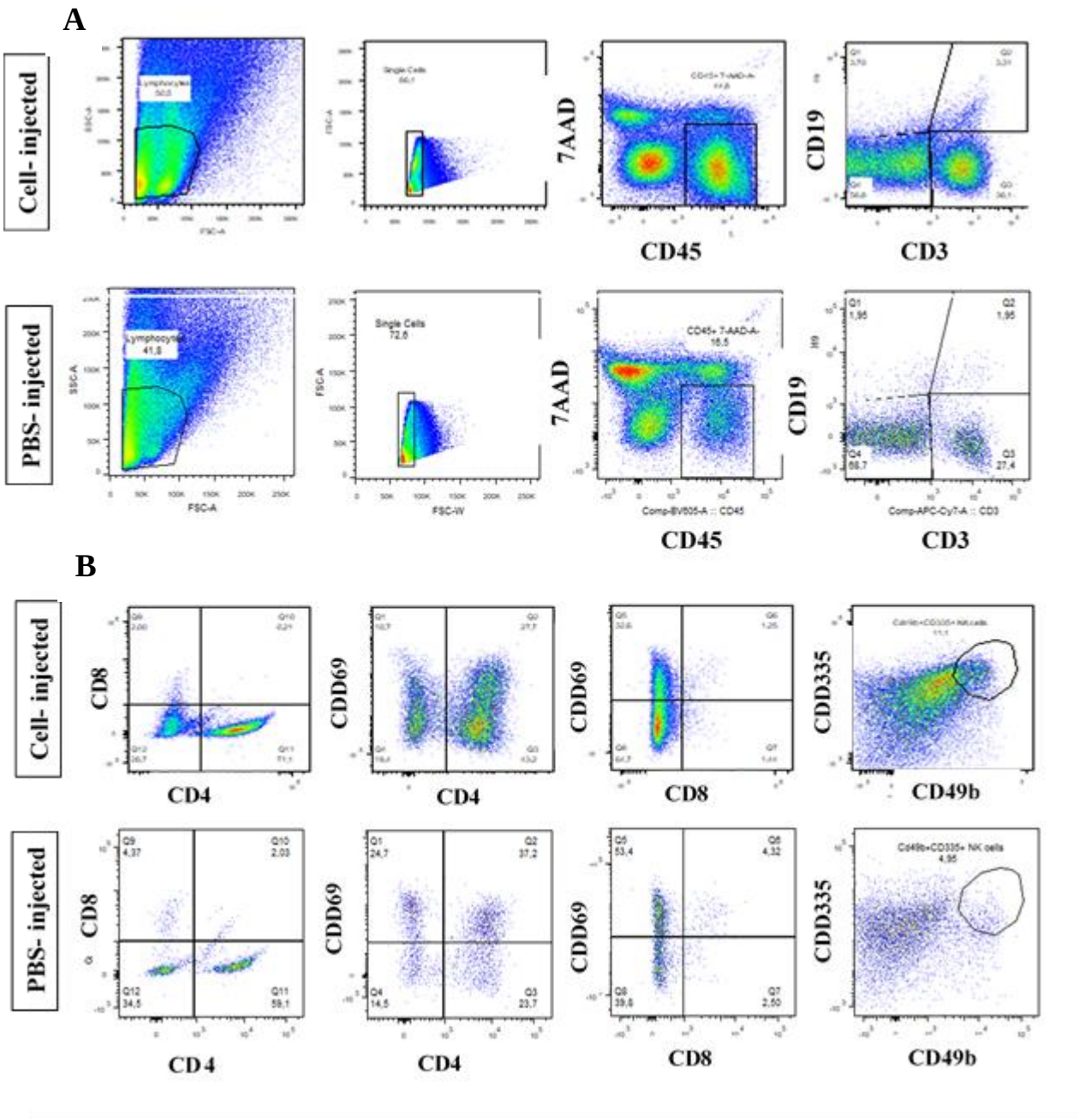

Figure 3.9. Analysis of T cell and NK cell infiltration after fibroblast transplantation in skin of immunocompetent recipients. Panel A represents gating strategy based on CD45+ live cells and then CD19-CD3+ and CD3- populations. Panel B compares activated T cells (CD11b+ F4/80+) and NK cells (CD3-CD49b+CD335+) population of infiltrating immune cells in cell vs PBS injected skin.

3.4 Discussion:

Since the development of the first human skin substitute in the early 1980s by Bell et al. [37], reconstruction of different types of skin equivalents by using fibroblasts as a major cell type involved in wound healing and skin regeneration [30] in combination with ECM components has been reported. However, the viability, immune response, and overall usefulness of transplanted cells into an immunocompetent host have been controversial [50] [43] [39] [40] [41] [54] [97]. In this study, we have shown that application of allogeneic fibroblasts populated within the ADM was not effective in promoting wound healing in comparison to ADM alone. Further analysis of grafted tissue revealed no sign of transplanted cells after three weeks. These findings set the stage in investigating the fate of transplanted cells. To achieve this, we did intra-hypo-dermal injection of fibroblasts to enable us to bypass any possible conflict of delay in vascularization of the grafts for survival of cells. By using BLI, we could follow up possible cell migration to surrounding tissues and study cell viability over the course of the transplantation study. Transplantation of cells into different strains of immune-deficient and antigen-depleted mice helped us to identify specific immune cell types involved in alloreaction against transplanted cells.

The findings provided evidence that immune rejection of transplanted fibroblasts happens when BLI labelled cells were intra-hypo-dermally injected in allogeneic host, wt-Balbc mice, while cells were not rejected in NSG and NS mice. Acute rejection of cells in allogeneic hosts raised the hypothesis for innate immune cells' involvement. To investigate which subsets of immune cells are responsible for this alloreaction, we did transplantation in Ja18 knockout (Ja18-/-) and CD1d knockout (CD1d-/-) mice for evaluation of NKT cells' role and gamma/delta T cells depletion by using antibody for evaluation of gamma/delta T cells' role. These results eliminated the possible roles of these innate immune cells. Natural killer (NK) cells as a type of innate immune

cells with capability of killing target cells were the other type of the cells that we looked at their effect on transplanted cells. We showed that depletion of NK cells in recipient mice could delay, but not prevent, the rejection of cells. The rejection of allogeneic cells by NK cells via missing self recognition has been reported in other studies as well [98] [99]. A polyclonal Ab specific to asialo GM1 (ASGM1) has been commonly used to deplete NK cells in vivo. However, there are some reports regarding the off-target effect of anti-ASGM1 on a subpopulation of NKT, CD8+ T, and γδ T cells, macrophages, eosinophils, and basophils under specific experimental conditions [100]. Since we have assessed the effect of NKT, CD8+ T, and γδ T cells in our study, we did not conclude that the observed delay in cell rejection in anti-ASGM1 treated mice is dependent on the lethal off-target effect of anti-ASGM1 on these cell types.

Transplantation of cells in Rag -/- mice revealed specific patterns in cell survival. The number of cells decreased significantly during the time course of experiment in comparison to NSG mice, but a proportion of injected cells could survive and be protected from immune rejection. The initial rejection and following survival means that the rejection of cells at the beginning is Rag independent, but later it becomes Rag dependent. Simultaneous depletion of CD4+ and CD8+ cells prevented rejection in similar pattern to Rag mice but surprisingly no single depletion of CD4+ and CD8+ cells could prevent rejection of fibroblasts, however CD4+ cells depletion showed the delay in rejection.

This part of our results was not conclusive for us to identify T-cell mediated alloresponse as an exclusive mechanism of rejection. This is because we were anticipating to see CD8+ cytotoxic T-cell depletion to be effective in preventing rejection. Also, the initial loss of cells in Rag and double depleted mice was in agreement with the non-T-cell mediated response. A similar mechanism has been reported in other studies as well [101] [102]. On the other hand, prevention

from complete rejection in Rag -/- and CD4/CD8 double depleted mice was supporting T-cell alloresponse to transplanted fibroblasts.

In this study, we showed that despite of our anticipation regarding the immune protecting effect of IDO expression by fibroblasts, it could not prevent fibroblasts rejection in our experimental condition. There are several possible explanations for this. This could be because of strong immune response generated in the first days of acute rejection by innate immune cells such as NK cells and monocytes, which overcome the immunoregulatory effect of tryptophan depravation or its metabolites. The depletion of tryptophan by local IDO expression could not be enough due to an insufficient level of IDO produced by fibroblasts, a continuous supply of tryptophan in the environment, which makes supply of tryptophan faster than degradation rate, or tryptophan deprivation alone may not be sufficient to prevent cytotoxic T cell infiltration [95].

Similar results have been reported by Yang *et al.*, which show that even though high expression of IDO and Treg marker, Foxp3, is detectable in the graft region during acute rejection of an islet cell transplantation model, this cannot counterbalance the alloimmune response [103]. In the clinical study of patient with kidney transplantation, Brandacher et al. has shown that renal tubuli express IDO during acute kidney transplantation rejection in vivo and this overexpression not only could not prevent rejection but also IDO metabolism evaluation could be used as a monitoring tools for allograft rejection [104].

In conclusion, our data indicate clear immune response to allogeneic fibroblasts with both innate and T-cell response on targeting cells. As in the field of regenerative medicine application of skin substitutes that harbor live cells continues to grow, it becomes more important that the host immune response to allogeneic cells and following complications be characterized and new strategies may need to be planned to prevent immune rejection of transplanted cells.

Chapter 4: General Discussion, Conclusion and Suggestions for Future Work

4.1 General discussion and conclusion

In this study, we had two objectives. First one was developing a detergent-free method for decellularizing skin and comparing it with two commonly used detergent-based methods of ADM preparation. The premise was to avoid the deleterious effects of detergents on ECM components, thereby maintaining ECM molecules, including cell secreted factors, as intact as possible. The results of our study showed that each decellularization method was associated with distinct structure and composition differences between the resulting ADM.

In this study, we tried to provide head-to-head comparison of the extracellular matrix scaffold materials produced with different methods of decellularization. I*n vivo* assessments of wounds based on reepithelialization, angiogenesis, infiltration of host cells, lack of alloreactivity to materials, wound contraction, and gross appearance of grafted ADMs showed that there is no superior matrix in our study and the ability to cover full thickness wounds in mouse model was equivalent among the ADMs prepared with different methods (Figure 2.6, Chapter 2). However, only the detergent-free method achieved effective decellularization of skin while preserving sulfated glycosaminoglycans (sGAGs) and elastin content of the tissue as well as its biomechanical property, when compared with detergent-based methods (Figure 2.2, Chapter 2).

Our results emphasize the importance of the decellularization protocol for producing skin ECM scaffolds and suggest considering both *in vitro* and *in vivo* outcomes for evaluating the ADM quality.

The second objective of my research was to evaluate the functional outcome of adding allogeneic fibroblasts to ADM to produce a live skin substitute for transplantation on full thickness wounds in a mouse model. One of our aims was to study the therapeutic application of IDO-expressing fibroblasts to create immune privilege for prevention of allogeneic fibroblasts rejection after transplantation of our skin substitute.

The potential benefit of including fibroblasts in skin substitute has been addressed in several experimental and clinical studies but the longevity and immunogenicity of allogeneic cells after transplantation into an immunocompetent host have been controversial. This results in the question of whether the potential benefits of allogeneic fibroblasts within ADM outweighs the consequences of the rejection associated with these immunogenic cells, or if only autologous fibroblasts should be utilized [51] [52] [93] [53] [54] [55]. One of the reasons for this debate is that in most experimental and clinical studies the aspect of immunogenicity of these cells has not been studied in detail and evaluation was limited to the outcome of transplantation in the overall wound-healing process. Also, limitations in techniques to follow the ultimate fate of allogeneic fibroblasts after transplantation may partly contribute to the conflicting reports. Commonly used techniques such as immunohistochemical (IHC) staining, fluorescent visualization, and DNA polymerase chain reaction are end point methods that allow us to study the fate of transplanted cells only after the animal has been euthanized and so require including a large number of animals to study at multiple time points. Also, migration of cells from transplanted sites to other parts or tissues might not be noticed unless numerous samples from different tissues were used [105].

To address these limitations, we used *in vivo* bioluminescent imaging (BLI) for assessing engraftment, survival, and migration of these cells following transplantation in an allogeneic host (Figure 3.4, Chapter 3). Bioluminescence is a natural biological process. When cells were modified

to express an enzyme known as luciferase, visible light is produced in the presence of a substrate (luciferin) and oxygen. Some luciferases such as firefly luciferase (Fluc) require other cofactors such as ATP and Mg2+ whereas sea pansy Renilla reniformis luciferase (Rluc) and the marine copepod Gaussia princeps luciferase (Gluc) do not. In animal studies, bioluminescence light transmitted through the tissues is detectable by charge coupled device (CCD) cameras with sensitive detectors [106] [107]. An important advantage of BLI in transplantation studies is that luciferase is expressed in only metabolically active, living cells, which enables real-time assessment of transplanted cells. In the present study, by using BLI, we demonstrated the alloresponse pattern to intradermally injected allogeneic mouse fibroblasts in immunocompetent, immunocompromised, and specific antigen depleted mice.

Transplanted cells were rejected in wtBalbc mice but not in NSG and NS mice (Figure 3.4, Chapter 3). They were also rejected in Ja18-/- and CD1d-/- mice and in γδ T cells depleted mice, ruling out the possible involvement of NKT cells and γδ T cells in allogeneic response (Figure 3.5, Chapter 3). Transplanted cells were rejected in NK depleted mice as well. However, upon NK depletion we could observe a delay in the rejection, indicating that NK cells are involved in rejecting allogenic fibroblasts, but they are not the main player (Figure 3.6, Chapter 3). NK cells are lymphocytes with cytotoxic activity and can target the cells without previous sensitization. Based on the missing-self model of target cell recognition, NK cells can attack cells that do not express at all or sufficient levels of host major histocompatibility complex (MHC) class I molecules [108,109]. It has been shown that NK cells are alloreactive and can reject both bone marrow cells and solid grafts allotransplants. NK cells are generally considered as innate

immune response cells; however they can acquire features such as Ag-specific response, clonal expansion, and memory features similar to the ones in adaptive immune response [98]. NK cells alloreactivity to both human and mouse embryonic stem cells (ESC) [99], to allogeneic hematopoietic stem cells (HSC) [110], mesenchymal stem cells [111] have been studied. The rejection of fibroblasts by NK cells has not been reported before, and it is not clear to us that the rejection pattern in our study is due to direct cytotoxic activity of NK cells or if it is a combinatorial effect with cytokines and other cell types.

Transplantation of cells in Rag -/- mice showed that the number of cells decreases within 10 days after transplantation and it is less than the cells in NSG mice. However, a proportion of injected cells could survive and be protected from immune rejection. Also, transplanted cells in double CD4 and CD8 depleted mice show the similar rejection/survival pattern to that of Rag -/- mice (Figure 3.7, Chapter 3). These results together are indicative of T cell alloresponse. However, single depletion of CD4 or CD8 did not led to protection of the fibroblasts from rejection. This finding is unexpected given the predicted prevention of rejection following depletion of cyotoxic CD8+ cells. The complexity of the rejection observed in this model is further demonstrated by the initial decrease in transplanted cell number in both Rag-/- and CD4 CD8 double depleted mice, suggestive of a pattern of innate immune or Rag -/ - independent rejection. These results were not conclusive for us to identify T-cell mediated alloresponse as an exclusive mechanism of rejection.

The non-T-cell mediated immune response to mesenchymal stem cell and allogeneic cells has been reported by other investigators as well [101] [102]. Overall, we hypothesize two possible mechanisms for immune response to allogeneic fibroblasts. The first one is the two-phase rejection model, which initially is mediated in the first week after transplantation by NK cells, monocytes and neutrophils followed by a T-cell mediated response in the second week. The second model is

based on only innate immune response. The observed results for the role of Rag-dependent and CD4+ and C8+ cells mediated response could be explained by the role of CD4+ Th cells in activation of macrophages in inflamed sites [112], the presence of a population of CD4+/C8+ monocytes/macrophages with a cytotoxic phenotype at inflammatory sites [113], and CD8+ dendritic cells that can produce interleukin-12 and stimulate inflammatory responses [114].

In this study, IDO expression by fibroblasts could not prevent allogeneic fibroblasts rejection. There are animal experimental studies and in vitro evidence for an immunoregulatory role of IDO as well as mechanistic studies from a range of murine models for transplantation that imply the possibility of IDO induction as a clinically desirable approach for immunosuppression [13][74] [115][95]. Also, over-expressing IDO donor grafts has been studied in some experimental models. Beutelspacher et al. have shown that vector-mediated overexpression of exogenous IDO in cornea allograft extends survival of the graft. However, their results showed that following allograft corneal transplantation there is a significant up-regulation of endogenous IDO mRNA in recipient corneas compared with syngeneic controls, with the highest amount at the time of rejection [116]. A similar results were obtained in an islet transplantation study in which Alexander et al. showed that transplantation of IDO-expressing islets from a non-obese diabetic (NOD) mouse into a NOD/severe combined immunodeficiency (SCID) recipient mice, after adoptive transfer of NOD diabetogenic splenocytes T cells, prolongs islet graft survival [117]. On the other hand, there are some other studies that challenge the possible immunoregulatory role of IDO in allograft transplantation. Yang et al. have shown that even though high expression of IDO and the Treg marker Foxp3 is detectable in the graft region during acute rejection of an islet cell transplantation model, this failed to counterbalance the alloimmune response [103]. In the clinical study of patients with kidney transplantation, Brandacher et al. have shown that renal tubuli

express IDO during acute kidney transplantation rejection in vivo and this overexpression not only could not prevent rejection but also that IDO metabolism evaluation could be used as a monitoring tools for allograft rejection [104].

As the literature review shows, the exact role of IDO in solid organ transplantation remains unclear, and even we cannot make a conclusion about a beneficial or detrimental role of IDO in the process of allograft rejection. In the context of our study, which is a model of allogeneic cell transplantation, IDO expression failed to protect fibroblasts from rejection. This could be because of a strong innate immune response by NK cells and monocytes at the first inflammatory stage that may overcomes the immunoregulatory effect of tryptophan depravation or its metabolites. Because of a continuous supply of tryptophan and an insufficient level of IDO produced by fibroblasts in the local environment, the depletion of tryptophan by local IDO expression may not be adequate to full suppress the T cell mediated immune response. Also, tryptophan deprivation alone may not be sufficient to prevent cytotoxic T cell infiltration and therefore, allograft rejection [95].

In summary, in this research we demonstrate that

1) ADM significantly enhanced the wound-healing process within three weeks, but there was no more improvement when we recellularized it with fibroblasts.

2) Our data indicate a clear immune response to allogeneic fibroblasts with both innate and T-cell response on targeting cells.

3) Although it has been reported by other researchers that IDO-expressing fibroblasts exhibit strong immunosuppressive activity in vitro and in vivo, we documented rejection of these cells in our study, suggesting that the application of these cells in wound sites requires further improvements.

In conclusion, two findings of this thesis are reported here for the first time. First, in Chapter 2 we showed that detergent-free decellularization of skin produce ADM with preserved structure and biomechanical property, which makes it an excellent choice for transplantation. As a second new finding of this study, as presented in Chapter 3, we documented immune response against allogeneic fibroblasts transplantation mediated mostly by innate immune cells rather than T cells, which provides new insights to development of a new clinical strategy to overcome immune response to allogeneic fibroblasts.

4.2 Suggestions for future work

Although this study shows detergent-free ADM significantly enhanced the wound-healing process and challenged the need for adding allogeneic fibroblasts to the wound, we acknowledge that further studies are required. Following are my suggestions for improving the application of allogeneic fibroblasts along with ADM to accelerate wound healing.

1. Regarding comparison of a detergent-free ADM with detergent-based methods, we could not see a significant difference upon transplantation in our wound model. Thus, the main advantage of our detergent-free ADM was its biomechanical property; having an animal wound model with which we can test elasticity of the wound region after ADM transplantation would show its significance over other ADMs.

2. The wound model used in this study is best categorized as an acute wound model. The cellular response and capacity of the host to repopulate the ADM may be considerably different from a chronic wound. It remains possible that the potential benefit

of allogeneic fibroblasts within the ADM would be demonstrated in a more "challenging" wound model.

3. Although in our study adding allogeneic fibroblasts to an ADM did not improve the wound healing process, we acknowledge that further studies are required to prevent immune rejection of fibroblasts first and then see how it can have a positive outcome upon transplantation.

4. As a possible treatment to prevent immune rejection of fibroblasts, we suggest using local anti-inflammatory treatments or local antibody depletion of monocytes to prevent infiltration of monocytes/macrophages to the site of transplantation.

5. As IDO expression by fibroblasts could not prevent fibroblast rejection in our experimental condition. This means that the overexpression of IDO needs further improvement. We recommend study of IDO interaction with innate immune cells such as monocytes and macrophages and increasing the IDO expression level per cell by using new vectors with a stronger promoter to enhance the IDO-to-tryptophan ratio *in vivo.*

References:

[1] Demidova-Rice TN, Hamblin MR, Herman IM. Acute and impaired wound healing: pathophysiology and current methods for drug delivery, part 1: normal and chronic wounds: biology, causes, and approaches to care. Adv Skin Wound Care 2012;25:304–14. doi:10.1097/01.ASW.0000416006.55218.d0.

[2] Price A. The Wound-Healing Process. Pract Adv Periodontal Surg 2008:13–22. doi:10.1002/9780470376416.ch3.

[3] Boyce ST. Design principles for composition and performance of cultured skin substitutes. Burns 2001;27:523–33. doi:10.1016/S0305-4179(01)00019-5.

[4] Badylak SF, Freytes DO, Gilbert TW. Extracellular matrix as a biological scaffold material: Structure and function. Acta Biomater 2009;5:1–13. doi:10.1016/j.actbio.2008.09.013.

[5] Wainwright DJ. Use of an acellular allograft dermal matrix (AlloDerm) in the management of full-thickness burns. Burns 1995;21:243–8. doi:10.1016/0305-4179(95)93866-I.

[6] Xiao S-C, Ben D-F, Yang J, Tang H-T, Wang G-Q, Yang Y, et al. Transplantation of Composite Skin Containing Keratinocytes Cultured on a Fibroblast-conditioned Acellular Dermal Matrix. Ann Burns Fire Disasters 2005;18:194–6.

[7] Altman AM, Matthias N, Yan Y, Song Y-H, Bai X, Chiu ES, et al. Dermal matrix as a carrier for in vivo delivery of human adipose-derived stem cells. Biomaterials 2008;29:1431–42. doi:10.1016/j.biomaterials.2007.11.026.

[8] Bannasch H, Stark GB, Knam F, Horch RE, Föhn M. Decellularized dermis in

combination with cultivated keratinocytes in a short- and long-term animal experimental investigation. J Eur Acad Dermatology Venereol 2008;22:41–9. doi:10.1111/j.1468-3083.2007.02326.x.

[9] Takami Y, Yamaguchi R, Ono S, Hyakusoku H. Clinical application and histological properties of autologous tissue-engineered skin equivalents using an acellular dermal matrix. J Nippon Med Sch 2014;81:356–63. doi:10.1272/jnms.81.356.

[10] Lamme EN, Van Leeuwen RTJ, Jonker A, Van Marle J, Middelkoop E. Living skin substitutes: Survival and function of fibroblasts seeded in a dermal substitute in experimental wounds. J Invest Dermatol 1998;111:989–95. doi:10.1046/j.1523-1747.1998.00459.x.

[11] Erdag G, Sheridan RL. Fibroblasts improve performance of cultured composite skin substitutes on athymic mice. Burns 2004;30:322–8. doi:10.1016/j.burns.2003.12.007.

[12] Benichou G, Yamada Y, Yun S-H, Lin C, Fray M, Tocco G. Immune recognition and rejection of allogeneic skin grafts. Immunotherapy 2011;3:757–70. doi:10.2217/imt.11.2.

[13] Munn DH, Zhou M, Attwood JT, Bondarev I, Conway SJ, Marshall B, et al. Prevention of allogeneic fetal rejection by tryptophan catabolism. Science 1998;281:1191–3. doi:10.1126/science.281.5380.1191.

[14] Forouzandeh F, Jalili RB, Hartwell R V., Allan SE, Boyce S, Supp D, et al. Local expression of indoleamine 2,3-dioxygenase suppresses T-cell-mediated rejection of an engineered bilayer skin substitute. Wound Repair Regen 2010;18:614–23. doi:10.1111/j.1524-475X.2010.00635.x.

[15] Suh H, Hong JP. One Stage Allogenic Acellular Dermal Matrices (ADM) and Split-Thickness Skin Graft with Negative Pressure Wound Therapy 2013.

[16] Park JY, Lee TG, Kim JY. Acellular Dermal Matrix to Treat Full Thickness Skin Defects : Follow-Up Subjective and Objective Skin Quality Assessments 2014;15:14–21.

[17] Gattazzo F, Urciuolo A, Bonaldo P. Extracellular matrix: A dynamic microenvironment for stem cell niche. Biochim Biophys Acta - Gen Subj 2014;1840:2506–19. doi:10.1016/j.bbagen.2014.01.010.

[18] Brizzi MF, Tarone G, Defilippi P. Extracellular matrix, integrins, and growth factors as tailors of the stem cell niche. Curr Opin Cell Biol 2012;24:645–51. doi:10.1016/j.ceb.2012.07.001.

[19] Cheng CW, Solorio LD, Alsberg E. Decellularized tissue and cell-derived extracellular matrices as scaffolds for orthopaedic tissue engineering. Biotechnol Adv 2014;32:462–84. doi:10.1016/j.biotechadv.2013.12.012.

[20] MacNeil S. Progress and opportunities for tissue-engineered skin. Nature 2007;445:874–80. doi:10.1038/nature05664.

[21] Liyanage SH, Purohit GS, Frye JNR, Giordano P. Anterior abdominal wall reconstruction with a Permacol implant. J Plast Reconstr Aesthetic Surg 2006;59:553–5. doi:10.1016/j.bjps.2005.06.008.

[22] Govindaraj S, Cohen M, Genden EM, Costantino PD, Urken ML. The use of acellular dermis in the prevention of Frey's syndrome. Laryngoscope 2001;111:1993–8. doi:10.1097/00005537-200111000-00024.

[23] Kirschner RE, Cabiling DS, Slemp AE, Siddiqi F, LaRossa DD, Losee JE. Repair of oronasal fistulae with acellular dermal matrices. Plast Reconstr Surg 2006;118:1431–40. doi:10.1097/01.prs.0000239612.35581.c3.

[24] Rhee PH, Friedman CD, Ridge JA, Kusiak J. The use of processed allograft dermal matrix

for intraoral resurfacing: an alternative to split-thickness skin grafts. Arch Otolaryngol Head Neck Surg 1998;124:1201–4.

[25] Rohrich RJ, Reagan BJ, Adams WPJ, Kenkel JM, Beran SJ. Early results of vermilion lip augmentation using acellular allogeneic dermis: an adjunct in facial rejuvenation. Plast Reconstr Surg 2000;105:408–9.

[26] MacAdam S a., Lennox P a. Acellular dermal matrices: Use in reconstructive and aesthetic breast surgery. Can J Plast Surg 2012;20:75–90.

[27] Stacey DH. Use of an acellular regenerative tissue matrix over chronic wounds. Eplasty 2013;13:e61.

[28] Harding K, Kirsner R, Lee D, Mulder G, Serena T. International Consensus. Acellular matrices for the treatment of wounds. London Wounds Int 2010:1–15.

[29] Olender E, Uhrynowska-Tyszkiewicz I, Kaminski A. Revitalization of biostatic tissue allografts: New perspectives in tissue transplantology. Transplant. Proc., vol. 43, 2011, p. 3137–41. doi:10.1016/j.transproceed.2011.08.069.

[30] Nolte SV, Xu W, Rennekampff HO, Rodemann HP. Diversity of fibroblasts - A review on implications for skin tissue engineering. Cells Tissues Organs 2008;187:165–76. doi:10.1159/000111805.

[31] Chang HY, Chi J-TJ, Dudoit S, Bondre C, van de Rijn M, Botstein D, et al. Diversity, topographic differentiation, and positional memory in human fibroblasts. Proc Natl Acad Sci 2002;99:12877–82. doi:10.1073/pnas.162488599.

[32] Driskell RR, Watt FM. Understanding fibroblast heterogeneity in the skin. Trends Cell Biol 2015;25:92–9. doi:10.1016/j.tcb.2014.10.001.

[33] Sorrell JM, Caplan AI. Fibroblast heterogeneity: more than skin deep. J Cell Sci

2004;117:667–75. doi:10.1242/jcs.01005.

[34] Driskell RR, Lichtenberger BM, Hoste E, Kretzschmar K, Simons BD, Charalambous M, et al. Distinct fibroblast lineages determine dermal architecture in skin development and repair. Nature 2013;504:277–81. doi:10.1038/nature12783.

[35] Ambler C a, Watt FM. Adult epidermal Notch activity induces dermal accumulation of T cells and neural crest derivatives through upregulation of jagged 1. Development 2010;137:3569–79. doi:10.1242/dev.050310.

[36] Rinkevich Y, Lindau P, Ueno H, Longaker MT, Weissman IL. Germ-layer and lineage-restricted stem/progenitors regenerate the mouse digit tip. Nature 2011;476:409–13. doi:10.1038/nature10346.

[37] Eugene Bell , H . Paul Ehrlich DJ. B and TN. Living Tissue Formed in vitro and Accepted as Skin-Equivalent Tissue of Full Thickness. Science (80-) 1981;211:1052–4.

[38] Bello YM, Falabella a F, Eaglstein WH. Tissue-engineered skin. Current status in wound healing. Am J Clin Dermatol 2001;2:305–13. doi:11721649.

[39] Boyce ST, Simpson PS, Rieman MT, Warner PM, Yakuboff KP, Bailey JK, et al. Randomized , Paired-Site Comparison of Autologous Engineered Skin Substitutes and Split-Thickness Skin Graft for Closure of Extensive , Full-Thickness Burns 2011:1–10. doi:10.1097/BCR.0000000000000401.

[40] Pajardi G, Rapisarda V, Somalvico F, Scotti A, Russo G Lo, Ciancio F, et al. Skin substitutes based on allogenic fibroblasts or keratinocytes for chronic wounds not responding to conventional therapy: A retrospective observational study. Int Wound J 2016;13:44–52. doi:10.1111/iwj.12223.

[41] Marston WA, Sabolinski ML, Parsons NB, Kirsner RS. Comparative effectiveness of a

bilayered living cellular construct and a porcine collagen wound dressing in the treatment of venous leg ulcers. Wound Repair Regen 2014;22:334–40. doi:10.1111/wrr.12156.

[42] Coulomb B, Friteau L, Baruch J, Guilbaud J, Chretien-Marquet B, Glicenstein J, et al. Advantage of the Presence of Living Dermal Fibroblasts within in Vitro Reconstructed Skin for Grafting in Humans. Plast Reconstr Surg 1998;101:1891. doi:10.1097/00006534-199806000-00018.

[43] Kuroyanagi Y, Yamada N, Yamashita R, Uchinuma E. Tissue-engineered product: Allogeneic cultured dermal substitute composed of spongy collagen with fibroblasts. Artif Organs 2001;25:180–6. doi:10.1046/j.1525-1594.2001.025003180.x.

[44] Bennett NT, Schultz GS. Growth-Factors and Wound-Healing - Biochemical-Properties of Growth-Factors and Their Receptors. Am J Surg 1993;165:728–37. doi:Doi 10.1016/S0002-9610(05)80797-4.

[45] Trompezinski S, Berthier-Vergnes O, Denis A, Schmitt D, Viac J. Comparative expression of vascular endothelial growth factor family members, VEGF-B, -C and -D, by normal human keratinocytes and fibroblasts. Exp Dermatol 2004;13:98–105. doi:10.1111/j.0906-6705.2004.00137.x.

[46] Spiekstra SW, Breetveld M, Rustemeyer T, Scheper RJ, Gibbs S. Wound-healing factors secreted by epidermal keratinocytes and dermal fibroblasts in skin substitutes. Wound Repair Regen 2007;15:708–17. doi:10.1111/j.1524-475X.2007.00280.x.

[47] Maarof M, Law JX, Chowdhury SR, Khairoji KA, Saim A Bin, Idrus RBH. Secretion of wound healing mediators by single and bi-layer skin substitutes. Cytotechnology 2016;68:1–12. doi:10.1007/s10616-015-9940-3.

[48] Okamoto E, Kitano Y. Expression of basement membrane components in skin

equivalents--influence of dermal fibroblasts. J Dermatol Sci 1993;5:81–8.

[49] Krejci NC, Cuono CB, Langdon RC MJ. In vitro reconstitution of skin: fibroblasts facilitate keratinocyte growth and differentiation on acellular reticular dermis. 1991. doi:10.1111/1523-1747.ep12491522.

[50] Cedidi CC, Wilkens L, Berger A, Ingianni G. Influence of human fibroblasts on development and quality of multilayered composite grafts in athymic nude mice. Eur J Med Res 2007;12:541–55.

[51] Sher S, Hull B, Rosen S, Church D, Friedman L, Bell E. Acceptanceof allogeneic fibroblasts in skin equivalent transplants..pdf 1983.

[52] Otto WR, Nanchahal J, Lu QL, Boddy N, Dover R. Survival of allogeneic cells in cultured organotypic skin grafts. Plast Reconstr Surg 1995;96:166–76. doi:10.1097/00006534-199507000-00025.

[53] Lamme EN, Van Leeuwen RTJ, Mekkes JR, Middelkoop E. Allogeneic fibroblasts in dermal substitutes induce inflammation and scar formation. Wound Repair Regen 2002;10:152–60. doi:10.1046/j.1524-475X.2002.10901.x.

[54] Price RD, Das-Gupta V, Harris P a, Leigh IM, Navsaria H a. The role of allogenic fibroblasts in an acute wound healing model. Plast Reconstr Surg 2004;113:1719–29. doi:10.1097/01.PRS.0000117367.86893.CE.

[55] Morimoto N, Saso Y, Tomihata K, Taira T, Takahashi Y, Ohta M, et al. Viability and function of autologous and allogeneic fibroblasts seeded in dermal substitutes after implantation. J Surg Res 2005;125:56–67. doi:10.1016/j.jss.2004.11.012.

[56] Löb S, Königsrainer A. Role of IDO in organ transplantation: promises and difficulties. Int Rev Immunol 2009;28:185–206. doi:10.1080/08830180902989119.

[57] Hirata F, Hayaishi O. Studies on indoleamine 2,3-dioxygenase. I. Superoxide anion as substrate. J Biol Chem 1975;250:5960–6.

[58] Hayaishi O. Utilization of superoxide anion by indoleamine oxygenase-catalyzed tryptophan and indoleamine oxidation. Adv Exp Med Biol 1996;398:285–9.

[59] Munn DH, Mellor AL. Indoleamine 2,3 dioxygenase and metabolic control of immune responses. Trends Immunol 2013;34:137–43. doi:10.1016/j.it.2012.10.001.

[60] Sprent J. Antigen-Presenting Cells: Professionals and amateurs. Curr Biol 1995;5:1095–7. doi:10.1016/S0960-9822(95)00219-3.

[61] Kündig TM, Bachmann MF, Dipaolo C, Simard JJL, Battegay M, Lother H, et al. Fibroblasts as Efficient Antigen-Presenting Cells in Lymphoid Organs. Science (80-) 1995;268:1343–7.

[62] Saada JI, Pinchuk I V, Barrera C a, Adegboyega P a, Suarez G, Mifflin RC, et al. Subepithelial myofibroblasts are novel nonprofessional APCs in the human colonic mucosa. J Immunol 2006;177:5968–79. doi:10.1016/S0739-5930(08)70123-5.

[63] Gruschwitz MS, Vieth G. Up-regulation of class II major histocompatibility complex and intercellular adhesion molecule 1 expression on scleroderma fibroblasts and endothelial cells by interferon-gamma and tumor necrosis factor alpha in the early disease stage. Arthritis Rheum 1997;40:540–50.

[64] Wassenaar A, Snijders A, Abraham-Inpijn L, Kapsenberg ML, Kievits F. Antigen-presenting properties of gingival fibroblasts in chronic adult periodontitis. Clin Exp Immunol 1997;110:277–84.

[65] Curran T-A, Jalili RB, Farrokhi A, Ghahary A. IDO expressing fibroblasts promote the expansion of antigen specific regulatory T cells. Immunobiology 2014;219.

doi:10.1016/j.imbio.2013.06.008.

[66] Kalorama. Global Wound Care Markets. Kalorama Information, New York 2015;5th.

[67] Gottrup F. A specialized wound-healing center concept: Importance of a multidisciplinary department structure and surgical treatment facilities in the treatment of chronic wounds. Am J Surg 2004;187:19–20. doi:10.1016/S0002-9610(03)00303-9.

[68] Gattazzo F, Urciuolo A, Bonaldo P. Extracellular matrix: A dynamic microenvironment for stem cell niche. Biochim Biophys Acta - Gen Subj 2014;1840:2506–19. doi:10.1016/j.bbagen.2014.01.010.

[69] Takami Y, Matsuda T, Yoshitake M, Hanumadass M, Walter RJ. Dispase/detergent treated dermal matrix as a dermal substitute. Burns 1996;22:182–90. doi:10.1016/0305-4179(95)00123-9.

[70] Uygun BE, Soto-Gutierrez A, Yagi H, Izamis M-L, Guzzardi MA, Shulman C, et al. Organ reengineering through development of a transplantable recellularized liver graft using decellularized liver matrix. Nat Med 2010;16:814–20. doi:10.1038/nm.2170.

[71] Nakayama KH, Batchelder C a., Lee CI, Tarantal AF. Decellularized Rhesus Monkey Kidney as a Three-Dimensional Scaffold for Renal Tissue Engineering. Tissue Eng Part A 2010;16:2207–16. doi:10.1089/ten.tea.2009.0602.

[72] Moore M a., Samsell B, Wallis G, Triplett S, Chen S, Jones AL, et al. Decellularization of human dermis using non-denaturing anionic detergent and endonuclease: a review. Cell Tissue Bank 2015;16:249–59. doi:10.1007/s10561-014-9467-4.

[73] Ketchedjian A, Jones AL, Krueger P, Robinson E, Crouch K, Wolfinbarger L, et al. Recellularization of decellularized allograft scaffolds in ovine great vessel reconstructions. Ann Thorac Surg 2005;79:888–96. doi:10.1016/j.athoracsur.2004.09.033.

[74] Jalili RB, Rayat GR, Rajotte R V, Ghahary A. Suppression of islet allogeneic immune response by indoleamine 2,3 dioxygenase-expressing fibroblasts. J Cell Physiol 2007;213:137–43. doi:10.1002/jcp.21100.

[75] Gillies AR, Smith LR, Lieber RL, Varghese S. Method for decellularizing skeletal muscle without detergents or proteolytic enzymes. Tissue Eng Part C Methods 2011;17:383–9. doi:10.1089/ten.tec.2010.0438.

[76] Matsushima R, Nam K, Shimatsu Y, Kimura T, Fujisato T, Kishida A. Decellularized dermis-polymer complex provides a platform for soft-to-hard tissue interfaces. Mater Sci Eng C 2014;35:354–62. doi:10.1016/j.msec.2013.11.007.

[77] Barbosa I, Garcia S, Barbier-Chassefière V, Caruelle JP, Martelly I, Papy-García D. Improved and simple micro assay for sulfated glycosaminoglycans quantification in biological extracts and its use in skin and muscle tissue studies. Glycobiology 2003;13:647–53. doi:10.1093/glycob/cwg082.

[78] Fishman JM, Lowdell MW, Urbani L, Ansari T, Burns AJ, Turmaine M, et al. Immunomodulatory effect of a decellularized skeletal muscle scaffold in a discordant xenotransplantation model. Proc Natl Acad Sci U S A 2013;110:14360–5. doi:10.1073/pnas.1213228110.

[79] Sherratt MJ. Tissue elasticity and the ageing elastic fibre. Age (Omaha) 2009;31:305–25. doi:10.1007/s11357-009-9103-6.

[80] Crapo PM, Gilbert TW, Badylak SF. An overview of tissue and whole organ decellularization processes. Biomaterials 2011;32:3233–43. doi:10.1016/j.biomaterials.2011.01.057.

[81] Gilbert TW, Sellaro TL, Badylak SF. Decellularization of tissues and organs. Biomaterials

2006;27:3675–83. doi:10.1016/j.biomaterials.2006.02.014.

[82] Lovekamp JJ, Simionescu DT, Mercuri JJ, Zubiate B, Sacks MS, Vyavahare NR. Stability and function of glycosaminoglycans in porcine bioprosthetic heart valves. Biomaterials 2006;27:1507–18. doi:10.1016/j.biomaterials.2005.08.003.

[83] Almine JF, Wise SG, Weiss AS. Elastin signaling in wound repair. Birth Defects Res Part C - Embryo Today Rev 2012;96:248–57. doi:10.1002/bdrc.21016.

[84] Senior RM, Griffin GL, Mecham RP. Chemotactic responses of fibroblasts to tropoelastin and elastin-derived peptides. J Clin Invest 1982;70:614–8. doi:10.1172/JCI110654.

[85] Tajima S, Wachi H, Uemura Y, Okamoto K. Modulation by elastin peptide VGVAPG of cell proliferation and elastin expression in human skin fibroblasts. Arch Dermatol Res 1997;289:489–92. doi:10.1007/s004030050227.

[86] Duca L, Floquet N, Alix a. JP, Haye B, Debelle L. Elastin as a matrikine. Crit Rev Oncol Hematol 2004;49:235–44. doi:10.1016/j.critrevonc.2003.09.007.

[87] Raghunath M, Bächi T, Meuli M, Altermatt S, Gobet R, Bruckner-Tuderman L, et al. Fibrillin and elastin expression in skin regenerating from cultured keratinocyte autografts: morphogenesis of microfibrils begins at the dermo-epidermal junction and precedes elastic fiber formation. J Invest Dermatol 1996;106:1090–5. doi:10.1111/1523-1747.ep12339373.

[88] de Vries HJ, Middelkoop E, Mekkes JR, Dutrieux RP, Wildevuur CH, Westerhof H. Dermal regeneration in native non-cross-linked collagen sponges with different extracellular matrix molecules. Wound Repair Regen 1994;2:37–47. doi:10.1046/j.1524-475X.1994.20107.x.

[89] Moore M a, Ph D. Decellularization of Human Dermis Using MATRACELL ®

Technology : Process , Preclinical Studies , and Medical Applications Decellularization of Human Dermis Using MATRACELL ® Technology : Process , Preclinical Studies , and Medical Applications n.d.:1–16.

[90] Keane TJ, Swinehart I, Badylak SF. Methods of tissue decellularization used for preparation of biologic scaffolds and in vivo relevance. Methods 2015. doi:10.1016/j.ymeth.2015.03.005.

[91] Fishman JM, Ansari T, Sibbons P, De Coppi P, Birchall M a. Decellularized rabbit cricoarytenoid dorsalis muscle for laryngeal regeneration. Ann Otol Rhinol Laryngol 2012;121:129–38.

[92] Reing JE, Brown BN, Daly K a., Freund JM, Gilbert TW, Hsiong SX, et al. The effects of processing methods upon mechanical and biologic properties of porcine dermal extracellular matrix scaffolds. Biomaterials 2010;31:8626–33. doi:10.1016/j.biomaterials.2010.07.083.

[93] Phillips TJ, Manzoor J, Rojas A, Isaacs C, Carson P, Sabolinski M, et al. The longevity of a bilayered skin substitute after application to venous ulcers. Arch Dermatol 2002;138:1079–81.

[94] Li J, Meinhardt A, Roehrich M, Golshayan D, Dudler J, Pagnotta M, et al. Indoleamine 2 , 3-dioxygenase gene transfer prolongs cardiac allograft survival. Am J Physiol Hear Circ Physiol 2007;12:3415–23. doi:10.1152/ajpheart.00532.2007.

[95] Brandacher G, Margreiter R, Fuchs D. Clinical relevance of indoleamine 2,3-dioxygenase for alloimmunity and transplantation. Curr Opin Organ Transplant 2008;13:10–5. doi:10.1097/MOT.0b013e3282f3df26.

[96] Pakyari M, Farokhi A, Khosravi-Maharlooei M, Kilani RT, Ghahary A, Brown E. A new

method for skin grafting in murine model. Wound Repair Regen 2016;24:695–704. doi:10.1111/wrr.12445.

[97] Nanchahal J, Dover R, Otto WR. Allogeneic skin substitutes applied to burns patients 2002;28:254–7.

[98] Liu W, Xiao X, Demirci G, Madsen J, Li XC. Innate NK cells and macrophages recognize and reject allogeneic nonself in vivo via different mechanisms. J Immunol 2012;188:2703–11. doi:10.4049/jimmunol.1102997.

[99] Perez-Cunningham J, Ames E, Smith RC, Peter AK, Naidu R, Nolta J a, et al. Natural Killer Cell Subsets Differentially Reject Embryonic Stem Cells Based on Licensing. Transplantation 2014;97:992–8. doi:10.1097/TP.0000000000000063.

[100] Hideto N, Kaori M, Yohei K, Yoshiyuki M, Hajime K. NK Cell-Depleting Anti-Asialo GM1 Ab Exhibits a Lethal Off-Target Effect on Basophils In Vivo. J Immunol 2011;186:5766–71. doi:10.4049/jimmunol.1100370.

[101] Zecher D, van Rooijen N, Rothstein DM, Shlomchik WD, Lakkis FG. An innate response to allogeneic nonself mediated by monocytes. J Immunol 2009;183:7810–6. doi:10.4049/jimmunol.0902194.

[102] Griffin MD, Ryan AE, Alagesan S, Lohan P, Treacy O, Ritter T. Anti-donor immune responses elicited by allogeneic mesenchymal stem cells: what have we learned so far? Immunol Cell Biol 2013;91:40–51. doi:10.1038/icb.2012.67.

[103] Yang H, Ding R, Sharma VK, Hilaire F Saint, Lagman M, Li B. Hyperexpression of Foxp3 and IDO During Acute Rejection of Islet Allografts 2007;83:1643–7. doi:10.1097/01.tp.0000263991.74052.46.

[104] Brandacher G, Cakar F, Winkler C, Schneeberger S, Obrist P, Bo C, et al. Non-invasive

monitoring of kidney allograft rejection through IDO metabolism evaluation 2007:60–7. doi:10.1038/sj.ki.5002023.

[105] Kidd S, Spaeth E, Dembinski JL, Dietrich M, Watson K, Klopp A, et al. Direct evidence of mesenchymal stem cell tropism for tumor and wounding microenvironments using in vivo bioluminescent imaging. Stem Cells 2009;27:2614–23. doi:10.1002/stem.187.

[106] Badr CE, Tannous BA. Bioluminescence imaging: Progress and applications. Trends Biotechnol 2011;29:624–33. doi:10.1016/j.tibtech.2011.06.010.

[107] Contag CH, Bachmann MH. Advances in in vivo bioluminescence imaging of gene expression. Annu Rev Biomed Eng 2002;4:235–60. doi:10.1146/annurev.bioeng.4.111901.093336.

[108] Yokoyama WM, Kim S. How do natural killer cells find self to achieve tolerance? Immunity 2006;24:249–57. doi:10.1016/j.immuni.2006.03.006.

[109] Raulet DH. Missing self recognition and self tolerance of natural killer (NK) cells. Semin Immunol 2006;18:145–50. doi:10.1016/j.smim.2006.03.003.

[110] Charron D. Immunogenomics of hematopoietic stem cell transplantation. Pathol Biol (Paris) 2005;53:171–3. doi:10.1016/j.patbio.2004.03.006.

[111] Spaggiari GM, Capobianco A, Becchetti S, Mingari MC, Moretta L. Mesenchymal stem cell – natural killer cell interactions: evidence that activated NK cells are capable of killing MSCs, whereas MSCs can inhibit IL-2 – induced NK-cell proliferation. Blood 2006;107:1484–90. doi:10.1182/blood-2005-07-2775.Supported.

[112] Murray PJ, Wynn TA. Protective and pathogenic functions of macrophage subsets. Nat Rev Immunol 2011;11:723–37. doi:Doi 10.1038/Nri3073.

[113] Baba T, Ishizu A, Iwasaki S, Suzuki A, Tomaru U, Ikeda H, et al. CD4+/CD8+

macrophages infiltrating at inflammatory sites: a population of monocytes/macrophages with a cytotoxic phenotype. Technology 2012;107:2004–12. doi:10.1182/blood-2005-06-2345.

[114] Shortman K, Heath WR. The CD8+ dendritic cell subset. Immunol Rev 2010;234:18–31. doi:10.1111/j.0105-2896.2009.00870.x.

[115] Yu G, Fang M, Gong M, Liu L, Zhong J, Feng W, et al. Steady state dendritic cells with forced IDO expression induce skin allograft tolerance by upregulation of regulatory T cells. Transpl Immunol 2008;18:208–19. doi:10.1016/j.trim.2007.08.006.

[116] Beutelspacher SC, Pillai R, Watson MP, Tan PH, Tsang J, McClure MO, et al. Function of indoleamine 2,3-dioxygenase in corneal allograft rejection and prolongation of allograft survival by over-expression. Eur J Immunol 2006;36:690–700. doi:10.1002/eji.200535238.

[117] Alexander AM, Crawford M, Bertera S, Rudert W a, Takikawa O, Robbins PD, et al. Adoptive Transfer of Diabetogenic Splenocytes. Cloning 2002;51.